



PONTIFICIA UNIVERSIDAD CATOLICA DE CHILE

ESCUELA DE INGENIERIA

# ***IN VITRO* DIGESTIBILITY OF FOOD-GRADE EMULSIONS**

**ELIZABETH TRONCOSO AHUÉS**

Thesis submitted to the Office of Research and Graduate Studies in partial fulfillment of the requirements for the Degree of Doctor in Engineering Sciences

Advisor:

**JOSÉ MIGUEL AGUILERA RADIC**

Santiago de Chile, December, 2013

© 2013, Elizabeth Troncoso Ahués



PONTIFICIA UNIVERSIDAD CATOLICA DE CHILE  
ESCUELA DE INGENIERIA

# ***IN VITRO* DIGESTIBILITY OF FOOD-GRADE EMULSIONS**

**ELIZABETH TRONCOSO AHUÉS**

Members of the Committee:

**JOSÉ M. AGUILERA**

**EDUARDO AGOSIN**

**GEORGINA DÍAZ**

**VILBETT BRIONES**

**NOEMÍ ZARITZKY**

**CRISTIÁN VIAL**

Thesis submitted to the Office of Research and Graduate Studies in partial fulfillment of the requirements for the Degree of Doctor in Engineering Sciences

Santiago de Chile, December, 2013

*Dedicated to all people who always  
supported and encouraged me to  
complete this work*

## ACKNOWLEDGEMENTS

First and foremost I offer my sincerest gratitude to the people behind this work. I owe a special debt to Humberto, my great life partner who keeps me in balance. Thank you for being my love, my friend. He has made my life happy, exciting and fun, and without him I would have had many more stressful and worrisome moments.

I wish to express my sincere gratitude to my advisor José Miguel Aguilera, for all his support, help and constructive criticism, and for providing me with strong academic foundations.

I would like to thank all my labmates. In special, I thank Rommy for all the support with knowledge and for being a wonderful friend. It is a great pleasure to acknowledge the contribution of Debbie Meza from the Office of Research and Graduate Studies who helped bring this work to fruition.

I would like to thank the National Commission for Science and Technology (CONICYT) for my doctoral fellowship and my research stay at the University of Massachusetts - Amherst. I must mention my special acknowledgement to professor David Julian McClements for accepting me as visiting scholar at the Biopolymers and Colloids Research Laboratory in the Department of Food Science at the University of Massachusetts. I express a strong sense of gratitude to people who helped me during my stay in Amherst. Also, I have to thank Uri Lesmes and Jean Alamed at UMASS for their valuable comments and critical reading of the manuscripts.

**This research was funded by the National Commission for Science and Technology (CONICYT) project FONDECYT 1095199.**

## LIST OF CONTENTS

DEDICATORY	ii
ACKNOWLEDGEMENTS	iii
ABSTRACT	vii
RESUMEN	ix
LIST OF PAPERS	xi
<b>1. INTRODUCTION</b>	<b>1</b>
1.1. Nutrient bioavailability is affected by the food matrix	2
1.2. Lipid food structures	4
1.3. Structuring emulsion-based lipid food matrices to improve bioavailability	6
1.4. Scope and objectives of this thesis	8
1.5. Outline of the thesis	9
<b>2. FOOD MICROSTRUCTURE AND DIGESTION</b>	<b>13</b>
2.1. Introduction	13
2.2. Food structures	14
2.3. The reactor inside our bodies	15
2.4. Food structures in the mouth	16
2.5. Food structures in the stomach	16
2.6. Food structures in the intestine	17
2.7. Conclusions	21
<b>3. RHEOLOGICAL AND MICROSTRUCTURAL CHARACTERIZATION OF WPI-STABILIZED O/W EMULSIONS EXHIBITING TIME- DEPENDENT FLOW BEHAVIOR</b>	<b>23</b>
3.1. Introduction	23
3.2. Materials and methods	26
3.2.1. Materials	26
3.2.2. Emulsion formation	26

3.2.3. Rheological properties of O/W emulsions	27
3.2.4. Modeling of flow behavior of the O/W emulsions	27
3.2.5. Modeling of the time-dependent rheological behavior of the O/W emulsions	28
3.2.6. Microstructural characterization of the O/W emulsions	29
3.2.7. Statistical analysis	30
3.3. Results and discussion	30
3.3.1. Rheological behavior of WPI-stabilized O/W emulsions	30
3.3.2. Modeling of the constant shear rate test by the SK model	39
3.4. Conclusions	42
<b>4. FABRICATION, CHARACTERIZATION AND LIPASE DIGESTIBILITY OF FOOD-GRADE NANOEMULSIONS</b>	<b>46</b>
4.1. Introduction	46
4.2. Materials and methods	48
4.2.1. Raw materials	48
4.2.2. Solution preparation	49
4.2.3. Nanoemulsion preparation	50
4.2.4. Characterization of nanoemulsions properties	52
4.2.4.1. Particle size measurements	52
4.2.4.2. Particle electrical charge measurements	52
4.2.4.3. Appearance of nanoemulsions	53
4.2.4.4. Microscopic analysis	53
4.2.5. <i>In vitro</i> digestion model	54
4.2.6. Statistical analysis	55
4.3. Results and discussion	55
4.3.1. Effect of disperse phase composition and solvent evaporation on particle size	55
4.3.2. Interpretation of droplet size changes induced by the emulsification	58

process and physicochemical properties of the phases	
4.3.3. The appearance of nanoemulsions	61
4.3.4. The electrical charge on oil droplets surface in the nanoemulsions	62
4.3.5. <i>In vitro</i> digestibility of nanoemulsions	64
4.4. Conclusions	68
<b>5. INFLUENCE OF PARTICLE SIZE ON THE <i>IN VITRO</i> DIGESTIBILITY OF PROTEIN-COATED LIPID NANOPARTICLES</b>	<b>73</b>
5.1. Introduction	73
5.2. Materials and methods	75
5.2.1. Materials	75
5.2.2. Solution preparation	75
5.2.3. Nanoemulsion preparation	76
5.2.4. Characterization of nanoemulsions properties	76
5.2.4.1. Particle characteristics	76
5.2.4.2. Microstructure analysis	77
5.2.5. <i>In vitro</i> digestion model	77
5.2.6. Data analysis	79
5.3. Results and discussion	79
5.3.1. Influence of organic phase composition on particle size	79
5.3.2. Electrical characteristics of lipid nanoparticles	83
5.3.3. <i>In vitro</i> digestibility of the nanoemulsions	85
5.4. Conclusions	90
<b>6. GENERAL CONCLUSIONS AND FUTURE PROSPECTS</b>	<b>95</b>
6.1. General conclusions	95
6.2. Future prospects	97

PONTIFICIA UNIVERSIDAD CATOLICA DE CHILE  
ESCUELA DE INGENIERIA

***IN VITRO* DIGESTIBILITY OF FOOD-GRADE EMULSIONS**

Thesis submitted to the Office of Research and Graduate Studies in partial fulfillment of the requirements for the Degree of Doctor in Engineering Sciences by

**ELIZABETH TRONCOSO AHUÉS**

**ABSTRACT**

As foods rather than nutrients become a primary consideration in the search for better health and well-being, the role of food structure becomes prominent. In this scenario, a better understanding of the structural changes of lipid foods in the gastrointestinal tract and interactions taking place will allow the rational design of foods. The hypothesis of this work is that it is possible to design new emulsion-based foods by using proper techniques to control rheological and microstructural properties, and the *in vitro* lipid digestion. The overall objective of this thesis was to increase our knowledge about the impact of different factors controlling food digestion in model lipid food systems with the aim of developing product concepts that have tailor-made physical and nutritional properties. Oil-in-water (O/W) emulsions-based foods stabilized by proteins (whey protein isolate, WPI, and  $\beta$ -lactoglobulin, BLG) or non-ionic surfactants (Tween 20) were fabricated in order to characterize them and correlate their structural properties with their rheological behavior and *in vitro* lipid digestion under conditions simulating those in the small intestine. Experimental methods to determine rheological properties, micro and macrostructural properties (oil droplet diameter, droplet size distribution, electrical charge, morphology, and appearance), and *in vitro* digestibility (release of free fatty acids) were developed. Using different rheological tests that simulated shear forces present in the gastrointestinal tract, it was found that the decrease in the apparent viscosity of WPI-stabilized O/W emulsions (*diameter* < 1.0  $\mu\text{m}$ ) could be due to shear-

induced structural changes when a constant shear rate was applied. This behavior could be related to the disruption of the emulsion flocs and the rearrangement of the oil droplets promoted by the flow field. On the other hand, a combination of high-pressure homogenization and solvent (hexane) displacement techniques was used to fabricate O/W nanoemulsions stabilized by Tween 20 and BLG. The influence of particle diameter ( $< 180$  nm) on the *in vitro* digestion of lipid droplets was examined using simulated small intestine conditions. Lipid droplets with different sizes were prepared by varying the oil-to-solvent ratio in the disperse phase prior to homogenization. The fraction of free fatty acids (FFAs) released from emulsified triacylglycerols during digestion was measured by an *in vitro* model (pH-Stat titration). Nanoemulsions stabilized by non-ionic surfactant exhibited a lag-period before any FFAs were released. After the lag-period, the digestion rate increased with decreasing oil droplet diameter (increasing specific surface area). The total amount of FFAs released from the emulsions increased from 61% to 71% as the mean droplet diameter decreased from 172 nm to 60 nm. For nanoemulsions stabilized by BLG, the lipid digestion rate initially decreased with decreasing particle diameter (for *diameter* = 170-119 nm), but then it increased (for *diameter* = 118-96 nm). This dependence is contrary to the usual assumption that lipid digestion increases with increasing lipid surface area. All these results suggest that a better understanding of the microstructure and colloidal basis of emulsion-based food systems has an important effect on lipid digestion.

Members of the Doctoral Thesis Committee:

José M. Aguilera

Eduardo Agosin

Georgina Díaz

Vilbett Briones

Noemí Zaritzky

Cristián Vial

Santiago, December, 2013

PONTIFICIA UNIVERSIDAD CATOLICA DE CHILE  
ESCUELA DE INGENIERIA

**DIGESTIBILIDAD *IN VITRO* DE EMULSIONES DE GRADO ALIMENTARIO**

Tesis enviada a la Dirección de Investigación y Postgrado en cumplimiento parcial de los requisitos para el grado de Doctor en Ciencias de la Ingeniería.

**ELIZABETH TRONCOSO AHUÉS**

**RESUMEN**

Como los alimentos, más que los nutrientes, son esenciales en la búsqueda de una mejor salud y bienestar, el rol de la estructura alimentaria se hace prominente. Así, una mejor comprensión de los cambios estructurales de alimentos lipídicos en el tracto gastrointestinal, y las interacciones que toman lugar, permitirán el diseño racional de alimentos. La hipótesis de este trabajo es que es posible diseñar nuevos alimentos basados en emulsiones para controlar sus propiedades reológicas y microestructurales, y su digestión lipídica *in vitro*. El objetivo general de esta tesis fue incrementar nuestro conocimiento acerca del impacto de factores diferentes que controlan la digestión de alimentos lipídicos con el propósito de desarrollar productos con propiedades físicas y nutricionales hechas a la medida. Se fabricaron emulsiones aceite-en-agua (O/W) estabilizadas por proteínas (aislado de suero proteico, WPI, y  $\beta$ -lactoglobulina, BLG) o surfactante no iónico (Tween 20) para caracterizarlas y correlacionar sus propiedades estructurales con su conducta reológica y digestión *in vitro* bajo condiciones que simulan a las del intestino delgado. Se desarrollaron métodos experimentales para determinar propiedades reológicas, propiedades micro y macroestructurales (diámetro de gota, distribución de tamaño, carga eléctrica, morfología y apariencia), y digestibilidad *in vitro* (liberación de ácidos grasos libres). Usando tests reológicos diferentes tratando de simular fuerzas de corte presentes en el tracto gastrointestinal, se encontró que el descenso en la viscosidad aparente de emulsiones O/W estabilizadas con WPI (*diámetro*

< 1.0  $\mu\text{m}$ ) sometidas a una tasa de corte constante podría deberse a cambios estructurales inducidos por el esfuerzo de corte. Esta conducta podría deberse a la destrucción de flóculos de la emulsión y al reordenamiento de las gotas de aceite producto del campo de flujo. Por otra parte, se usó una combinación de técnicas de homogenización a presión alta y desplazamiento de solvente (hexano) para fabricar nanoemulsiones O/W estabilizadas por Tween 20 y BLG, examinando la influencia del diámetro de partícula (< 180 nm) de las nanoemulsiones en la digestión *in vitro* de lípidos. La preparación de nanoemulsiones con diferentes diámetros de partícula se realizó variando la razón aceite/solvente en la fase dispersa, previo a la homogenización. La fracción de ácidos grasos liberados se midió con un modelo *in vitro* (titración pH-Stat). Nanoemulsiones estabilizadas con surfactante no iónico exhibieron un período lag antes de la liberación de ácidos grasos y, luego de este período, la tasa de digestión se incrementó al reducir el diámetro de partícula (mayor área superficial específica). La cantidad total de ácidos grasos liberados aumentó de 61% a 71% al reducir el diámetro de partícula de 172 nm a 60 nm. Para nanoemulsiones estabilizadas con BLG, la tasa inicial de digestión descendió al reducir el diámetro de partícula de 170 nm a 118 nm, pero luego se incrementó al reducir el diámetro de 118 nm a 96 nm. Esta dependencia es contraria a la suposición usual de que la digestión de lípidos aumenta con el incremento del área superficial. Estos resultados sugieren que un mejor entendimiento de la microestructura y bases coloidales de emulsiones de grado alimentario tiene un efecto importante en la digestión de lípidos.

Miembros de la Comisión de Tesis Doctoral:

José M. Aguilera

Eduardo Agosin

Georgina Díaz

Vilbett Briones

Noemí Zaritzky

Cristián Vial

Santiago, Diciembre, 2013

## LIST OF PAPERS

This thesis is based on the following papers, referred to in the text by their respective Roman numerals (II-V).

- Chapter II:** Food microstructure and digestion. Troncoso, E. and Aguilera, J. M. Food Science and Technology Journal, 23(4), 30-33 (2009).
- Chapter III:** Rheological and microstructural characterization of WPI-stabilized O/W emulsions exhibiting time-dependent flow behavior. Bellalta, P., Troncoso, E., Zúñiga, R. N. and Aguilera, J. M. LWT-Food Science and Technology, 46(2), 375-381 (2012).
- Chapter IV:** Fabrication, characterization and lipase digestibility of food-grade nanoemulsions. Troncoso, E., Aguilera, J. M. and McClements, D. J. Food Hydrocolloids, 27(2), 355-363 (2012).
- Chapter V:** Influence of particle size on the *in vitro* digestibility of protein-coated lipid nanoparticles. Troncoso, E., Aguilera, J. M. and McClements, D. J. Journal of Colloid and Interface Science, 382(1), 110-116 (2012).

### Book chapter

This Doctoral thesis was also the substantive basis for writing the following book chapter:

Zúñiga, R. N. and Troncoso, E. (2012). Improving nutrition through the design of food matrices. In: B. Valdez (Ed.), Scientific, Health and Social Aspects of the Food Industry (pp. 295-320). Rijeka, Croatia: InTech. ISBN: 978-953-307-916-5.

### Proceedings

Parts of this work have also been presented at four international and national congresses under the following references:

Troncoso, E., Aguilera, J. M. and McClements, D. J. Lipid nanoparticles stabilized by proteins: Formation, characterization, and *in vitro* digestibility. In: Proceedings of the

16th World Congress of Food Science and Technology (IUFoST), August 13-16, Foz de Iguazú, Brasil (2012).

Troncoso, E., Aguilera, J. M. and McClements, D. J. *In vitro* digestion of edible nanoemulsions. In: Proceedings of the 25th Interamerican Congress of Chemical Engineering. 18th Chilean Congress of Chemical Engineering, November 14-17, Santiago, Chile (2011).

Troncoso, E., Aguilera, J. M. and McClements, D. J. Development of nanoemulsions by a process based on an emulsification-evaporation technique. 11th International Congress of Engineering and Food (ICEF 11), May 22-26, Athens, Greece (2011).

Bellalta, P., Troncoso, E., Zúñiga, R. N. and Aguilera, J. M. Rheological and microstructural characterization of WPI-stabilized emulsions formed by ultrasound. 11th International Congress of Engineering and Food (ICEF 11), May 22-26, Athens, Greece (2011).

## 1. INTRODUCTION

Control of digestion and the release of nutrients from the food matrix is an alternative approach to attack the obesity problem and other food-related diseases, such as cardiovascular disease, hypertension, type II diabetes mellitus, and even cancer. The concept of a food matrix points to the fact that nutrients are contained into a larger continuous medium that may be of cellular origin (i.e., fruits and vegetables) or a structure produced by processing, where nutrients interact at different length scales with the components and structures of the medium (Aguilera and Stanley, 1999). Research on human digestion has often been undertaken with a view to changing the rates of digestion and delivery sites of macronutrients that might affect satiety and thus caloric intake. Several aspects of human eating behavior and food digestion may be relevant for identifying effective measures to treat or prevent food-related diseases. Although most of people in developed and developing countries eat an unbalanced diet, an increasing part of the consumers are progressively more aware of the relationship between diet and health. Thus, the demand for functional food products that address specific health benefits is growing steadily (Palzer, 2009). The food industry is currently responding by reformulating its products, especially looking at salt, sugar and fat content with a particular emphasis on healthier fat compositions (Lundin et al., 2008). New designed foods with lower amounts of fat, controlled release of bioactives, in-body self-assembly structures or slowly digestible starches are being developed by the food industry. The structure of these products must be modified accordingly to equalize the physical (e.g., rheology) and sensory (e.g., taste, release of aromas) properties of the original food. Therefore, designed food structures are required to diminish the sensorial impacts of such product modifications.

The food industry has gathered considerable information about the composition, biochemistry, structure, and physical properties of foods. The principles of process engineering of biomaterials and the fundamental role of food structure in understanding the behavior of foods during processing are well established (Aguilera, 2005; German and Watzke, 2004). This knowledge is the basis for the food industry to formulate,

process, preserve and distribute foods. Although the total amount of a nutrient in natural and formulated foods may be obtained from composition tables, its bioavailability (i.e., the rate and extent to which a nutrient contained in a food is absorbed and become available at the site of action) depends on many factors, for instance, food microstructure, processing conditions, presence of other components, among others (Parada and Aguilera, 2007). However, there is still a lack of information about the performance of foods inside our body, which has limited the capacity of the industry to create products with tailored nutritional properties. Therefore, this thesis is an attempt to relate how the changes induced in food matrices, mainly focused on lipid food matrices like oil-in-water (O/W) emulsions, affect their physicochemical properties and nutrient bioavailability. Although food digestibility and nutrient bioavailability are subjects in vogue today, a better understanding of the relationship between food properties, digestion and absorption would help in the rational design of foods with enhanced nutritional properties.

### **1.1. Nutrient bioavailability is affected by the food matrix**

The food industry is extremely innovative in terms of new products, but is highly traditional in term of processes. For a particular food product, a limited range of unit operations have been employed for some considerable time, and the same process lines are used to make a range of different product structures. The actual challenge is to develop novel functional structures through innovative processing or new units operations. It is conceivable that enhanced nutritional properties of foods may be achieved by proper assembly of hierarchical structures from the microscopic level up to the macroscale (i.e., bottom up approach). These new fabrication techniques will require understanding and precise control of assembly processes at all scales.

Nutrient bioavailability is gaining considerable attention in food technology. While one of the ongoing concerns of the food industry has always been to produce and provide the consumer with safe food, the nutritional and caloric composition is now becoming equally important. For this reason, during the last years considerable research has been

conducted to modify food matrices, on the basis of their physicochemical properties and possible effects on food digestion. For instance, the direct effect of physical properties (e.g., microstructure, particle size and physical state) of foods has been evaluated by its influence on nutrient absorption. So, different intentional modifications could be induced by food technologists to design and fabricate foods with controlled nutrient bioavailability.

Foods can be viewed as delivery systems of macro and micronutrients to improve nutrition. Delivery systems to encapsulate, protect and deliver bioactive components are widely used by the pharmaceutical industry to carry these active agents to specific locations within the gastrointestinal tract (GIT) and release them at controlled rates. Using this knowledge the food industry, through the design of food matrices, is developing similar systems to encapsulate, protect and deliver food components. However, the effectiveness of the encapsulation process relies on the preservation of the bioavailability of the encapsulated component and the release of it in the correct portion within the GIT. As mentioned before, not much is known about the influence of food structure and its breakdown on nutrient release in the GIT. This point is of primary importance because only what is released can be bioavailable for absorption (Parada and Aguilera, 2007).

In order to produce structured foods and develop a strategy for controlled release of food nutrients at desired sites in the GIT, it is essential to understand the kinetics of food disintegration and predict its digestion and subsequent metabolism. The biochemical, physiological, and physicochemical parameters that influence these processes need to be understood. This knowledge will benefit the food-processing industry in developing proper food structures for health purposes. The possibility of predicting the release of nutrients from food matrices under simulated GIT conditions is of utmost relevance in order to be able to define relationships between the food matrix and nutrients, as well as for looking at the interaction of ingredients with the enzymes involved in the digestive process. Although *in vivo* methods provide direct data of bioavailability, ethical restrictions and complex protocols when humans are used in biological research limit

this type of studies (Parada and Aguilera, 2007). Therefore, the need for validated *in vitro* methods is urgent in order to evaluate and compare the effect of the microstructure on the amount and the rate of nutrients release in the GIT.

## **1.2. Lipid food structures**

It is usually considered that in a normal diet, some 25 to 30% of the total calories are conveniently supplied as lipid. Certain lipids are needed for good health (e.g., essential fatty acids and fat-soluble vitamins). Nevertheless, the over-consumption of some dietary lipids (e.g., cholesterol, saturated fats, and trans-fatty acids) increases the prevalence of some public health problems, including cardiovascular disease and obesity (Simopoulos, 1999). In this scenario, an improved knowledge of lipid structure could address the rational design of dietary lipids to enhance or retard lipid digestion, aspect having strong nutritional and health impact.

Lipids are a chemically heterogeneous group of compounds characterized by being insoluble in water, but soluble in organic solvents. In general, lipids are conformed by fats and oils. The basic unit of natural fats and oils is the triacylglycerol (TAG) molecule; however, others molecules, such as monoacylglycerols (MAG), diacylglycerols (DAG), and phospholipids (PL), can be dietary lipids too. The TAG molecule consists of a glycerol backbone to which are acylated three fatty acids (FA). Two FAs are at the ends of the glycerol molecule (*sn*-1 and *sn*-3 positions) pointing in one direction, while the third FA molecule in the middle (*sn*-2 position) is pointing in the opposite direction. The dietary FAs molecules that compose the TAG structure may vary in the number of carbon atoms and the presence of double bounds from saturated FA to unsaturated FA. The type and position of the FA chains on the glycerol backbone affect the structure of TAG molecule and, consequently, its bioavailability. TAGs containing short- and medium-chain FA have higher rate of FA release during lipolysis than for long-chain FA, and is faster for FA at the *sn*-1 and *sn*-3 positions than at *sn*-2 position (Fave et al., 2004). On the other hand, a typical TAG molecule can exhibit three physical states: crystal, bulk, and interface. These physical states will determine the

properties and characteristics of the physical state of the lipid phases in foods, which vary from liquid to crystalline phases. The lipid phases in most foods are usually liquid at body temperature (~37°C), but in some foods they may be either fully or partially crystalline. The crystallinity of the lipid phase may alter the ability of enzymes to digest the emulsified lipids. For example, the release rate of a lipophilic drug can be decreased with increasing crystallinity degree of lipid droplets (Olbrich et al., 2002). Hence, according to the above-mentioned aspects, the composition, structural organization and physical state of the lipid phase will control lipid digestion. In addition, lipids have the property of forming in the presence of water different self-assembled structures. These mesophase structures include monolayers, micelles, reverse micelles, bilayers, and hexagonal phases. The behavior of lipids in aqueous medium is determined by intrinsic parameters such as lipid polarity, length and branching of acylated FAs, presence of double bonds, among others (Ulrich, 2002). Mesophase structures of lipids have different sizes and configurations and for this reason, they are found many applications in food, pharmaceutical, and cosmetics industries. Nowadays, bilayer vesicles (i.e., often called liposomes) have received widespread attention because of their ability to entrap functional components. This characteristic allows use of these structures as drug-delivery vehicles for controlling the release of incorporated agents.

The lipid molecules in foods may be organized into a number of different forms, including as bulk, structural, emulsified, colloidal, or interfacial structures (McClements, 2005). However, invariably, all ingested lipids end up as an emulsion either by gastric emulsification or prior to ingestion during the manufacturing process. The structure of these emulsions is determined by the nature of the lipid phase, the aqueous phase and the interface (Lundin et al., 2008). Particularly, the properties of the interface modulate lipid digestion. The interface of emulsified lipids is determined by the physicochemical properties of the lipid droplets, such as size (which determines the interfacial area of lipid droplets), structure, and the molecular structure of the triglycerides that constitute the lipid droplet (Armand et al., 1999). Several works have investigated the impact of emulsion structure on lipid digestion. For example, it has been demonstrated that a lower

initial fat droplet size facilitates fat digestion by lipase (Armand et al., 1999). Additionally, the composition of the emulsion interface can limit the lipase activity. Interfaces composed by phospholipids limit fat digestion in the absence of bile salts because there are few possible points where lipase can access the emulsified substrate (Wickham et al., 1998).

In principle, rational design of lipid structures may be a useful tool for food processors to control lipid digestibility and bioavailability. Nevertheless, there is clearly a need for further research to establish the key physicochemical factors that impact the performance of food lipids inside the gastrointestinal tract.

### 1.3. Structuring emulsion-based lipid food matrices to improve bioavailability

Currently, much attention has been paid to the formulation of emulsion-based food systems to encapsulate, protect and/or release lipophilic constituents. A variety of emulsion-based delivery systems are available, including conventional emulsions, nanoemulsions, solid lipid particles, multiple emulsions, and multilayer emulsions (Figure 1.1). Due to their compositional and structural complexity, the structural design of these systems is still very far from being an exact science and further research is still needed to achieve a detailed understanding of the molecular characteristics, structural organization, physicochemical properties, and functional performance of these delivery systems (McClements et al., 2009).

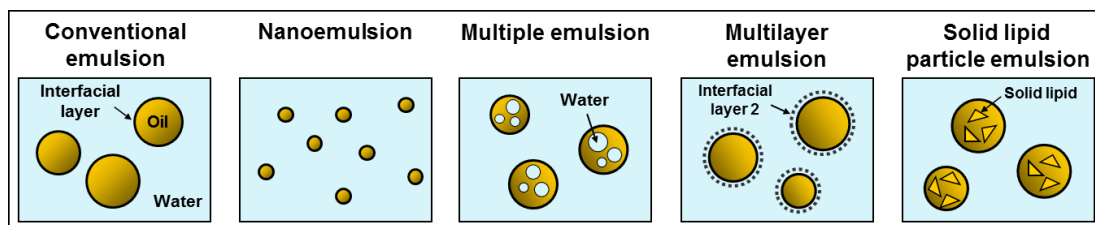


Figure 1.1. Examples of different emulsions-based delivery systems

Conventional emulsions consist of oil droplets (*diameter* ~  $\mu\text{m}$ ) dispersed in an aqueous medium, with the oil droplets being surrounded by emulsifier molecules. O/W emulsions

contain a non-polar region (the oil phase), a polar region (the aqueous phase), and an amphiphilic region (the interfacial layer). Then, within O/W emulsions it is possible to incorporate functional agents that are polar, non-polar, and amphiphilic (McClements, 2005). Nevertheless, conventional emulsions have some limitations (e.g., physical instability) that promote the development of more sophisticated structured systems. Like conventional emulsions, nanoemulsions consist of small oil droplets (*diameter* < 200 nm) dispersed within a continuous phase, with each droplet being surrounded by a protective coating of emulsifier molecules. For certain applications, nanoemulsions do have a number of advantages over conventional emulsions due to their relatively small particle size: (i) they scatter light weakly and so tend to be transparent; (ii) they have high physical stability; (iii) they have unique rheological characteristics; and, (iv) they can greatly increase the bioavailability of encapsulated lipophilic components (Mason et al., 2006). Additionally, the very small oil droplet size in nanoemulsions increases the digestion rate and the total amount of free fatty acids released during digestion in comparison with conventional emulsions (Li & McClements, 2010). This last characteristic may be of interest for the design of lipid food for humans with disorders that prevent efficient digestion or absorption of lipids (e.g., cystic fibrosis or pancreatitis) (Fave et al., 2004).

Multiple emulsions are systems in which dispersed droplets contain smaller droplets inside (Figure 1.1). Particularly, water-in-oil-in-water (W/O/W) emulsions consist of small water droplets contained within larger oil droplets that are dispersed in an aqueous continuous phase. In these systems, functional components can potentially be located in a number of different ways. Water soluble components can be incorporated into the inner or outer water phase, while oil soluble components can be incorporated into the oil phase. Potential advantages of multiple emulsions over conventional emulsions as delivery systems are: (i) functional ingredients could be trapped inside the inner water droplets and released at a controlled rate in the GIT; (ii) functional ingredients could be protected from chemical degradation; and (iii) reduction of the overall fat content of food products by loading the oil phase with water droplets (McClements et al., 2009).

The quality and functional performance of conventional O/W emulsions can be improved by the formation of multilayered interfaces using the layer-by-layer electrostatic deposition technique (Guzey & McClements, 2006). Multilayered emulsion delivery systems may have a number of advantages over conventional single-layered emulsions: (i) improved physical stability to environmental stresses; (ii) greater control over the release rate of functional agents due to the ability to manipulate the thickness and permeability of the laminated interfacial coating; and (iii) ability to trigger release of functional agents in response to specific changes of environmental conditions in the GIT, such as dilution and/or pH (McClements et al., 2009).

On the other hand, it is possible to control the physical location of a lipophilic component and to slow down molecular diffusion processes using conventional emulsions by crystallizing the lipid phase. These systems are known as solid lipid particle emulsions, which consist of emulsifier coated (partially) solid lipid particles dispersed in an aqueous continuous phase (Figure 1.1) (Videira et al., 2002). By controlling the morphology of the crystalline lipid matrix it is possible to obtain more precise control over the release kinetics of functional compounds. Additionally, both lipophilic and hydrophilic bioactives can be incorporated within the same system using solid lipid particle emulsions (McClements et al., 2009). Hence, there are a large number of different ways that can be used by food manufacturers to embed lipophilic compounds within food matrices with different degradation rates. However, the selection of a particular matrix is a matter of functional preference.

#### **1.4. Scope and objectives of this thesis**

From the above presentation it is clear that the subject of controlling lipid food structure in processed foods will increasingly attract the attention of researchers in the field and the related industries. More research will be needed on new lipid structures to regulate lipid digestion and its subsequent bioavailability. This thesis covers an untapped area of food engineering science, namely that of breakdown of food emulsions inside the gastrointestinal tract. The fundamental hypothesis of this work is that it is possible to

design new emulsion-based foods by using proper techniques to control the *in vitro* lipid digestion. Therefore, the overall objective of the present thesis was to increase our knowledge about the impact of different factors controlling food digestion in model lipid food systems with the aim of developing product concepts that have tailor-made physical and nutritional properties. In order to achieve this aim, the thesis was divided into the following specific objectives:

- Review the impact of food microstructure on digestion, analyzing the sequential degradation of food nutrients during their passage in the GIT (Chapter II).
- Study the time-dependent rheological properties of protein-stabilized O/W emulsions to establish relationships between structure and shear rate similar to those found in the GIT, and relating this information with the microstructure of the emulsions (Chapter III).
- Study the effect of the organic phase composition on the particle size distribution, electrical characteristics, microstructure, and appearance of nanoemulsions stabilized by a small molecule non-ionic surfactant (Tween 20) and, subsequently, the influence of particle size on the *in vitro* digestibility of emulsions under simulated small intestinal conditions (Chapter IV).
- Study the impact of interfacial properties on the *in vitro* digestibility of protein-coated lipid nanoparticles (Chapter V).

### **1.5. Outline of the thesis**

The central theme of this thesis is the study of *in vitro* digestibility of O/W emulsions, analyzing different factors that control their performance in the GIT. In Chapter 2, a brief review of the existing relationship between food microstructure and digestion of different macronutrients is conducted, since this is a prerequisite to make a global analysis of the subject covered in this work. Chapter 3 presents the rheological and microstructural characterization of protein-stabilized O/W emulsions and their time-dependent flow behavior, as possibly found in the GIT when this kind of structures are

digested. Chapter 4 investigates the fabrication and characterization of food-grade nanoemulsions and their digestibility by lipase. In this chapter, the influence of particle size on the *in vitro* digestion of nanoemulsions containing lipid droplets (corn oil) stabilized by a non-ionic surfactant (Tween 20) was examined using simulated small intestine conditions. In Chapter 5, the influence of particle size on the *in vitro* digestion of BLG-coated lipid nanoparticles was also examined using simulated small intestine conditions. Nanoemulsions were prepared by high-pressure homogenization and organic solvent (hexane) evaporation. The effect of the initial organic phase composition on the size, microstructure, electrical properties, and digestion of the lipid nanoparticles was evaluated.

Finally in the Chapter 6, the main findings of the previous chapters are discussed.

A summary of the contents of the Chapters II to V is schematically presented in Fig. 1.2, showing the relationship between the different chapters of this thesis.

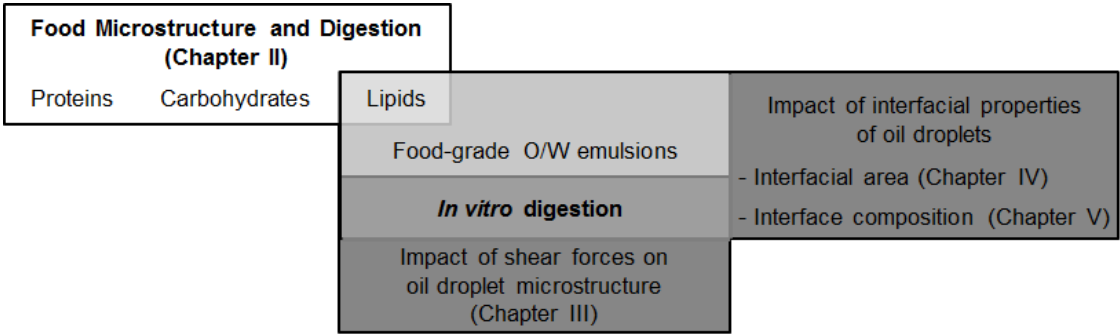


Figure 1.2. Overview of the studies comprising this thesis.

## REFERENCES

- Aguilera, J. M. (2005). Why food microstructure?. *Journal of Food Engineering*, 67(1-2), 3-11.
- Aguilera, J. M., and Stanley, D. W. (1999). *Microstructural Principles of Food Processing and Engineering*. 2<sup>nd</sup> Edition. Aspen Publishers Inc., Gaithersburg, MA.
- Armand, M., Pasquier, B., André, M., Borel, P., Senft, M., Peyrot, J., Salducci, J., Portugal, H., Jaussan, V., and Lairon, D. (1999). Digestion and absorption of 2 fat emulsions with different droplet sizes in the human digestive tract. *American Journal of Clinical Nutrition*, 70(6), 1096-1106.
- Fave, G., Coste, T., and Armand, M. (2004). Physicochemical properties of lipids: New strategies to manage fatty acid bioavailability. *Cellular and Molecular Biology*, 50(7), 815-831.
- German, J. B., and Watzke, H. J. (2004). Personalizing food for health and delight. *Comprehensive Reviews in Food Science and Food Safety*, 3(4), 145-151.
- Guzey, D., and McClements, D. J. (2006). Formation, stability and properties of multilayer emulsions for application in the food industry. *Advances in Colloid and Interface Science*, 128-130(1), 227-248.
- Li, Y., and McClements, D. J. (2010). New mathematical model for interpreting pH-Stat digestion profiles: Impact of lipid droplet characteristics on *in vitro* digestibility. *Journal of Agricultural and Food Chemistry*, 58(13), 8085-8092.
- Lundin, L., Golding, M., and Wooster T. J. (2008). Understanding food structure and function in developing foods for appetite control. *Nutrition & Dietetics*, 65(3), 79-85.
- Mason, T., Wilking, J., Meleson, K., Chang, C., and Graves, S. (2006). Nanoemulsions: Formation, structure, and physical properties. *Journal of Physics: Condensed Matter*, 18(41), 635-666.
- McClements, D. J. (2005). *Food emulsions: Principles, Practice, and Techniques*. CRC Press, Boca Raton, FL.
- McClements, D. J., Decker, E., Park, Y., and Weiss, J. (2009). Structural design principles for delivery of bioactive components in nutraceuticals and functional foods. *Critical Reviews in Food Science and Nutrition*, 49(6), 577-606.

- Olbrich, C., Kayser, O., and Muller, R. (2002). Lipase degradation of Dynasan 114 and 116 solid lipid nanoparticles (SLN) - Effect of surfactants, storage time and crystallinity. *International Journal of Pharmaceutics*, 237(1-2), 119-128.
- Palzer, S. (2009). Food structures for nutrition, health and wellness. *Trends in Food Science and Technology*, 20(5), 194-200.
- Parada, J., and Aguilera, J. M. (2007). Food microstructure affects the bioavailability of several nutrients. *Journal of Food Science*, 72(2), 21-32.
- Simopoulos, A. (1999). Essential fatty acids in health and chronic disease. *American Journal of Clinical Nutrition*, 70(3), 560-569.
- Ulrich, A. (2002). Biophysical aspects of using liposomes as delivery vehicles. *Bioscience Reports*, 22(2), 129-150.
- Videira, M., Botelho, M., Santos, A., Gouveia, L., de Lima, J., and Almeida, A. (2002). Lymphatic uptake of pulmonary delivered radiolabelled solid lipid nanoparticles. *Journal of Drug Targeting*, 10(8), 607-613.
- Wickham, M., Garrood, M., Leney, J., Wilson, P., and Fillery-Travis, A. (1998). Modification of a phospholipid stabilized emulsion interface by bile salt: Effect on pancreatic lipase activity. *Journal of Lipid Research*, 39(3), 623-632.

## 2. FOOD MICROSTRUCTURE AND DIGESTION

### 2.1. Introduction

The fundamental role of food structure in understanding the behavior of foods during processing and eating is well established (Aguilera, 2005). New interest has arisen regarding the function that food structure may play once foods are inside the body and, consequently, in our nutrition, health and well-being (Figure 2.1). Attention is further supported by the increased belief that foods and not nutrients are the fundamental unit of nutrition (Jacobs and Tapsell, 2007).

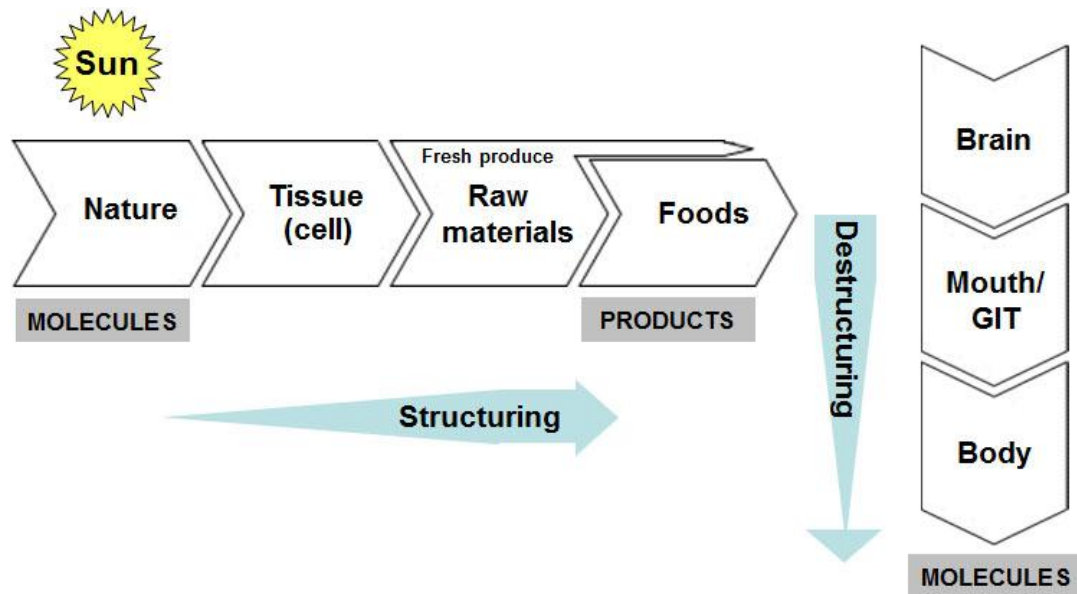


Figure 2.1. Foods we eat: from molecules to products and back to molecules. While food processing induces structure formation, digestion is basically a destructuring step.

Thus, the release of nutrients from the food matrix (the composite containing the nutrients in a food) as well as the interactions between food components and restructuring phenomena during transit in the digestive system becomes far more important than the original contents of nutrients. In this respect, Lundin et al. (2008) have recently stated that there is an emerging interest in the impact of food structure on

digestive behavior and its relationship to human nutrition, because the interactions between individual macronutrients (protein, fat and carbohydrate) control in many cases the rate of digestive processes, such as proteolysis and lipolysis, influence satiety and condition the absorption of nutrients. This chapter summarises some of the major findings presently available on the effect of food microstructure on the digestive process.

## **2.2. Food structures**

We ingest nutrients in the form of microstructures spanning in size from nanometers to a few millimeters (Aguilera and Stanley, 1999). In plant tissue, major food components such as starch, storage proteins and most lipids are contained in discrete, homogeneous packets embedded in the cellular cytoplasm. Other food molecules are hierarchically assembled into functional structures as is the case of the cellulose and pectin in plant cell walls and of collagen and the myofibrillar proteins in muscle tissues. Some key food molecules are bound or enclosed in organelles, and thus are not readily available. Moreover, during processing or cooking new structures are formed and further complex interactions, yet to be resolved, develop from the molecular level to the micron scale (see Figure 2.2). This is the chemical and structural panorama of the food we eat and digestion has to liberate and breakdown molecules to a state in which they can be absorbed, but in so doing restructuring and interactions take place complicating further our understanding of nutrient release and its bioaccessibility (Parada and Aguilera, 2007). For instance, the presence of an insoluble state (e.g., clotted milk proteins, precipitated polysaccharides or highly viscous fibre) is known to delay gastric emptying (Hoebler et al., 2002). In summary, when it comes to nutrition, health and wellbeing, the microstructure of foods within our bodies matters.

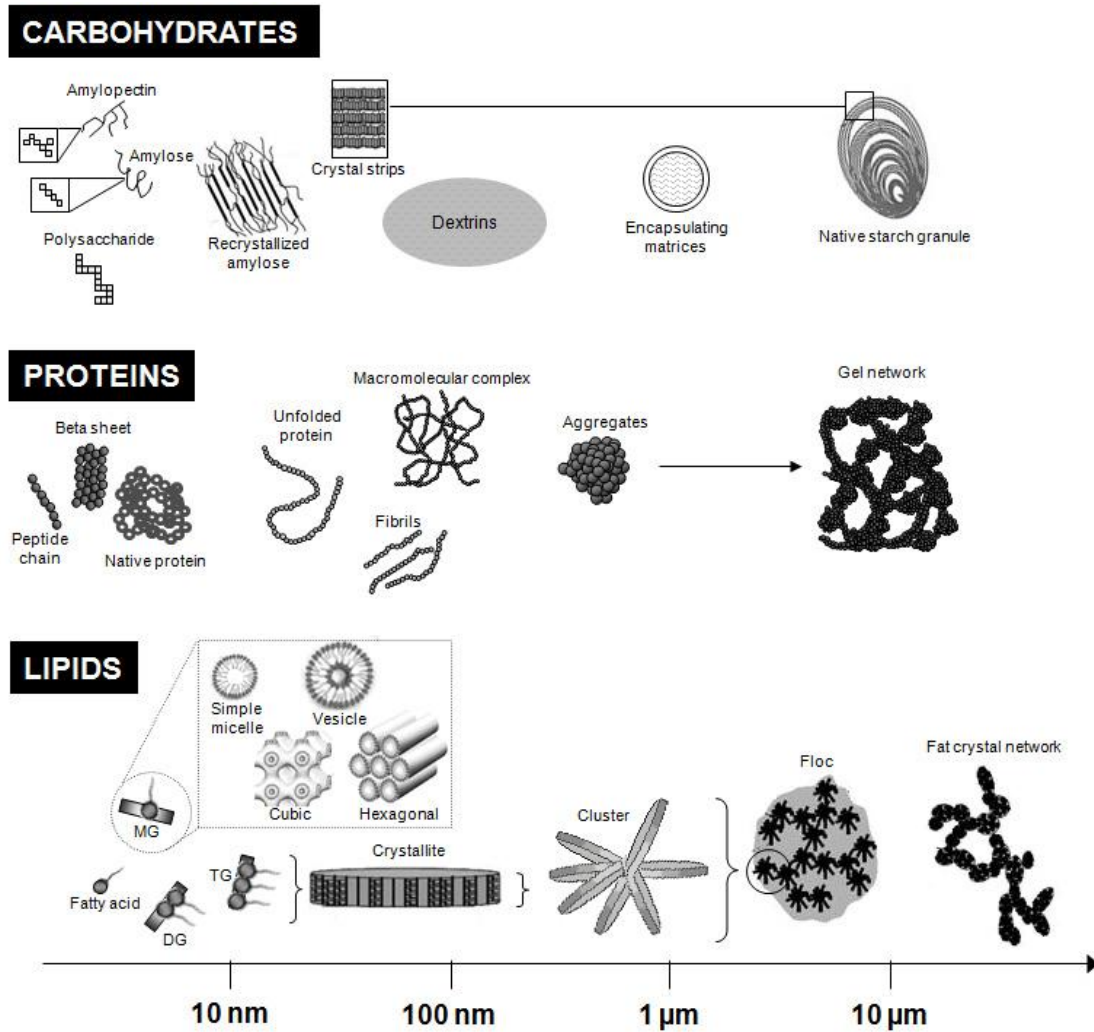


Figure 2.2. Some hierarchical structures of major food components as may be present in foods.

### 2.3. The reactor inside our bodies

The GIT is a versatile multi-compartment reactor that operates on a variable solid/liquid feed but delivers more or less standardised products. The main organs of the GIT include the mouth, the stomach and the small intestine. The GIT is connected to the vascular, lymphatic and nervous systems allowing the regulation of the digestive response, delivery of absorbed compounds to organs in the body and the regulation of food intake (Schneeman, 2002). In the GIT, the structure of foods undergoes major size reduction

facilitating the release of nutrients embedded in the food matrix so they may be subjected to enzymatic action and eventually absorbed. Mouth and stomach are the major compartments where foods are disintegrated into smaller sizes, whereas the small intestine is the major site of macromolecular breakdown and nutrient absorption. In the GIT, both mechanical forces and chemical reactions breakdown ingested food into small molecules, and the kinetics of digestion depends on the particular physicochemical characteristics of the flowing contents as well as on physiological conditions. Disintegration and dissolution are affected by the formulation and processing conditions (e.g. shear, mixing, heat) used at the manufacturing/preparation stage (Kong and Singh, 2008). Using starch as an example, equal amounts consumed in foods prepared using different added ingredients (e.g. presence of sugar) and water contents, and subject to diverse forming and heating conditions will differ in their kinetics of digestion. Before absorption in the gut, any compound of interest has to be bioaccessible, meaning that it has to be in a molecular dispersed state, colloidal form, or within a micellar system in the case of hydrophobic materials.

#### **2.4. Food structures in the mouth**

The oral step is rapid but plays an important role in reducing particle size, mixing, hydrating and lubricating the contents with saliva so that a bolus is formed and swallowed. Mastication increases the surface area of food pieces but it may be quite inefficient in breaking open some plant tissues as demonstrated by the presence of intact cells of nuts in the faeces (Ellis et al., 2004). While a small portion of starch is hydrolysed by the enzyme  $\alpha$ -amylase due to the short retention time, almost no protein or fat digestion occurs in the mouth.

#### **2.5. Food structures in the stomach**

The motility of the stomach mixes the ingested bolus with gastric juice, which contains acid and digestive enzymes (e.g. gastric lipase, pepsin and mucin), inducing further reduction of particle size, remixing and phase separation. Dietary lipid is dispersed into a

finely divided emulsion by the peristalsis of the stomach, creating a lipid-water interface where enzymatic hydrolysis by gastric lipases takes place. In healthy humans, gastric lipase leads to the hydrolysis of 10-30% of ingested TAGs, the main hydrolytic products being DAGs and free fatty acids (FFAs). It has been shown *in vitro* that some components of dietary fibre interfere with the lipid emulsification process, leading to a smaller area of “clean” interface and consequently to lower TAG lipolysis (Armand, 2007). Likewise, the nature of a preexisting adsorbed layer on fat droplets conditions hydrolysis. Proteins stabilising an emulsion may undergo conformational changes by the acidic environment of the stomach, especially if they are denatured and become aggregated, thus affecting lipolysis. The emulsion leaving the stomach contains emulsified lipids as fine droplets (i.e.  $< 0.5 \mu\text{m}$  in diameter) as well as a hydrolysed lipid fraction.

The action of pepsin on proteins results in a mixture of polypeptides, oligopeptides and some free amino acids. In any case, the efficacy of proteolysis in the stomach depends on the structural changes of individual proteins or protein assemblies, as affected by the lower pH and ionic strength. For example, casein, unlike whey proteins, coagulates in the stomach and as a result the overall gastric emptying time for casein is longer. This reduced postprandial increase in plasma amino acids compared to that of non-coagulating whey proteins, has led to the concept of “fast” and “slow” proteins (Hall et al., 2003).

## **2.6. Food structures in the intestine**

The peristaltic motor activity propels the chyme along the length of the intestine where it is exposed to pancreatic enzymes (such as pancreatic lipase, co-lipase, trypsin, chymotrypsin and carboxipeptidases) and bile salts, while mixed with phospholipids and sloughed intestinal cells. In the case of lipids, the combined action of bile and pancreatic juice brings about a marked change in the physicochemical form of the luminal lipid emulsion. Pancreatic lipase is secreted into the duodenum, and in the presence of co-lipase it hydrolyses the remaining TAGs to form MAGs and FFAs. Pancreatic lipase

(and gastric lipase as well) acts on emulsified substrates, thus, the physicochemical properties of the emulsion-water interface largely determine the extent of enzyme binding and consequent lipolysis. Finally, lipid digestion continues in the small intestine with desorption and dispersion of insoluble lipid into an absorbable form. Digested lipids are solubilised in the lumen of the intestine into at least two types of nanostructures: bile salt micelles and unilamellar vesicles. These assemblies deliver digested lipids to an aqueous-enterocyte layer where they are subsequently absorbed into the enterocyte's brush border membrane lining the surface of the small intestine (Singh and Horne, 2009). Figure 2.3 shows a scheme of the digestive process for lipid foods in the GIT.

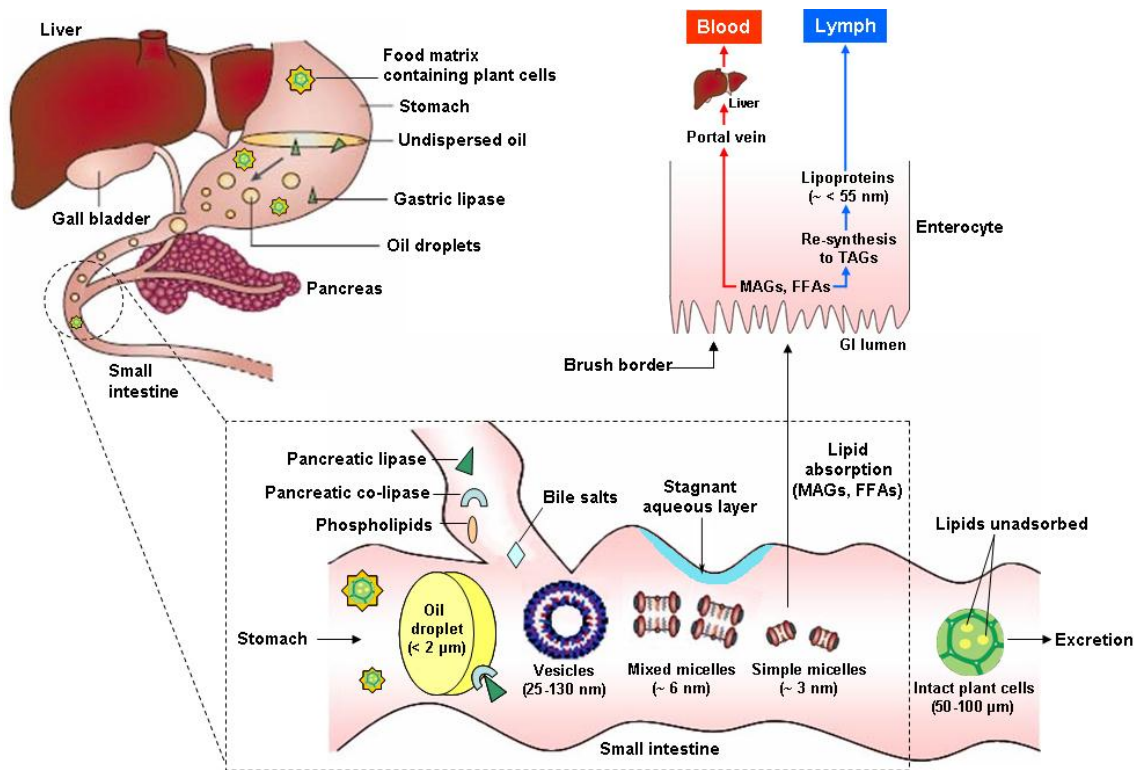


Figure 2.3. Schematic diagram of the digestive process of an oily plant food. The dynamics of digestion of fatty foods in the GIT leads to the breakdown of complex structures, which disassemble during transit or may remain intact. Adapted from Porter et al. (2007).

The final steps in the digestion of proteins take place in the intestinal lumen and are associated with small intestinal mucosal cells, which contain a number of peptidases. The collective result of the action of proteases in the GIT is to reduce the majority of dietary protein to a mixture of free amino acids, dipeptides and tripeptides, making them available to the various carrier-transporters of the brush border membrane. However, the physical and chemical state of proteins, affected by the environment of the GIT or previous processing (e.g. thermal treatment), might change the intestinal transport properties as has been shown for allergenic proteins. Harsh conditions in the GIT, interaction with lipids and the formation of larger aggregates contribute to the allergenicity of plant food proteins (Breiteneder and Mills, 2005). Thermal denaturation not only affects the physical state of proteins but also their susceptibility to the pepsin and the trypsin/chymotrypsin mixture. The presence of plant hydrocolloids (e.g. pectins) and their nonspecific interactions with some proteins reduces the accessibility of proteases to cleavage sites.

Complex carbohydrates are digested to monosaccharides, mostly glucose, galactose and fructose, prior to absorption in the small intestine. Intestinal digestion occurs through reactions mediated by pancreatic  $\alpha$ -amylases and by disaccharidases anchored to the brush border surface of the enterocytes. Enterocytes are then responsible for the complete absorption of the sugars into the body and once absorbed, galactose and fructose are mostly converted to glucose for metabolism or storage (Wright et al., 2003). The physical form of food is the major determinant of the rate of digestion of both starches and sugars. The extent of starch digestion within the small intestine is variable, depending on its physical form and a substantial amount of undigested starch enters the colon, where may be fermented by bacteria or simply appear in faeces. The degree of gelatinisation of starch granules and of recrystallisation of the released polymers is of vital importance in the breakdown to sugars because both phenomena influence the susceptibility to enzymatic degradation. In this context, a classification of starchy foods based on intrinsic factors (i.e. physical structure) has been proposed for starch digestibility in the small intestine as it may vary from a rapid digestion to indigestibility

(i.e. resistant starch) (Figure 2.4) (Lehmann and Robin, 2007). The incomplete digestion of starch is related to the matrix surrounding starch, the nature and physicochemical properties of the starch per se at the granule and molecular levels (e.g. granule size and amylose/amylopectin ratio), and the presence of other dietary components (e.g. sugar, dietary fibre and lipid). The “encapsulation” of starch granules by a protein network is an important factor in explaining the slow degradation of starch by  $\alpha$ -amylase in pasta, which may limit its accessibility due to different structural factors, such as porosity, compactness and tortuosity of the protein matrix, and structure of starch.

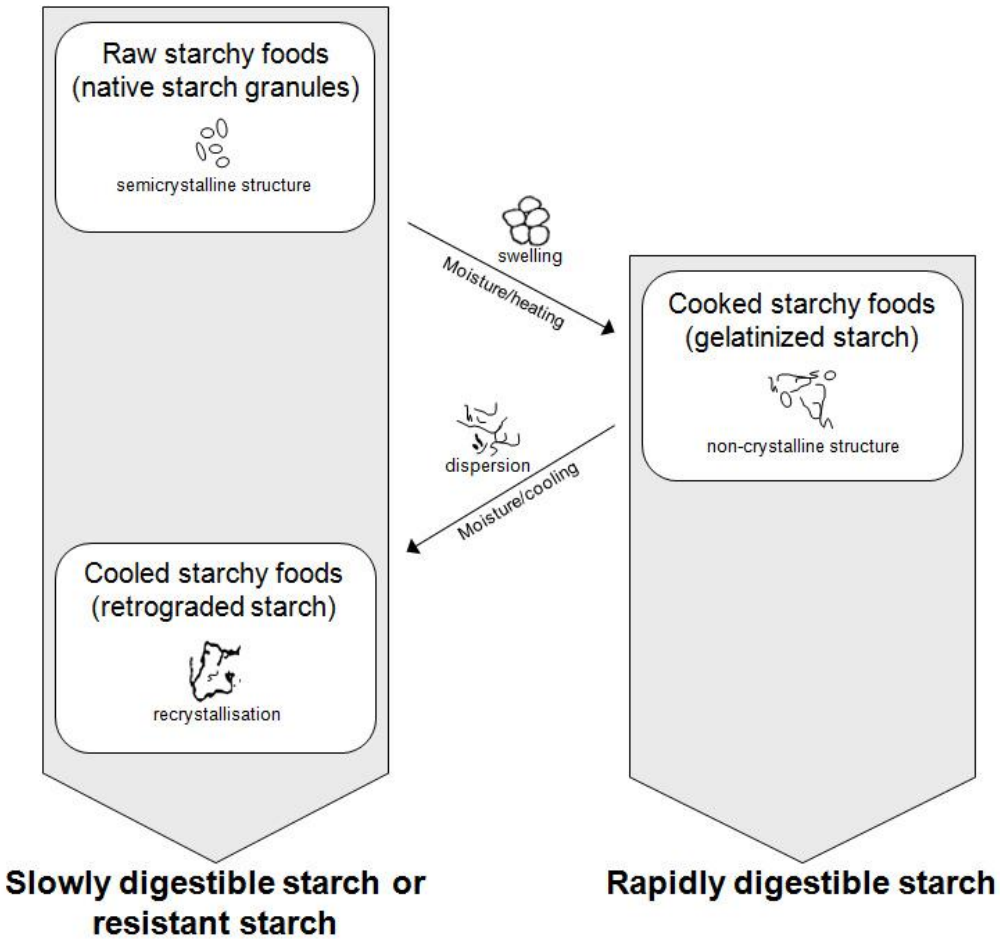


Figure 2.4. Digestibility of starch in the small intestine according to the structural changes of starch granule induced by processing.

## 2.7. Conclusions

As foods rather than nutrients become a primary consideration in the search for better health and well-being, the role of food structure becomes even more prominent. A better understanding of the structural changes in the gut and interactions taking place will allow the rational design of foods and bioactive supplements for specific conditions. This is not an easy task since we eat meals that vary in the quantity and quality of food components as well as in the type of matrices in which they are contained. Experimental apparatus that simulate the dynamics in the GIT on real foods are urgently needed to rapidly screen the effects of food microstructure and then proceed to validation by expensive in vivo human experiments.

## References

- Aguilera, J. M., and Stanley, D. W. (1999). *Microstructural Principles of Food Processing and Engineering*. 2<sup>nd</sup> ed. Aspen Publishers Inc, Gaithersburg, MD.
- Aguilera, J. M. (2005). Why food microstructure?. *Journal of Food Engineering*, 67, 3-11.
- Armand, M. (2007). Lipases and lipolysis in the human digestive tract: where do we stand?. *Current Opinion in Clinical Nutrition and Metabolic Care*, 10, 156-164.
- Breiteneder, H., and Mills, E. N. C. (2005). Plant food allergens – structural and functional aspects of allergenicity. *Biotechnology Advances*, 23, 395-399.
- Ellis, P. R., Kendall, C. W. C., Ren, Y., Parker, C., Pacy, J. F., Waldron, K. W., and Jenkins, D. J. A. (2004). Role of cell walls in the bioaccessibility of lipids in almond seeds. *American Journal of Clinical Nutrition*, 80, 604-613.
- Hall, W. L., Millward, D. J., Long, S. J., and Morgan, L. M. (2003). Casein and whey exert different effects on plasma amino acid profiles, gastrointestinal hormone secretion and appetite. *British Journal of Nutrition*, 89, 239-248.
- Hoebler, C., Lecannu, G., Belleville, C., Devaux, M. -F., Popineau, Y., and Barry, J. L. (2002). Development of an *in vitro* system simulating bucco-gastric digestion to assess the physical and chemical changes of food. *International Journal of Food Science and Nutrition*, 53, 389-402.

Jacobs, D. R., and Tapsell, L. C. (2007). Food, not nutrients, is the fundamental unit in nutrition. *Nutrition Reviews*, 65, 439-450.

Kong, F., and Singh, R. P. (2008). Disintegration of solid foods in human stomach. *Journal of Food Science*, 73(5), 67-80.

Lehmann, U., and Robin, F. (2007). Slowly digestible starch - its structure and health implications: A review. *Trends in Food Science & Technology*, 18, 346-355.

Lundin, L., Golding, M., and Wooster, T. J. (2008). Understanding food structure and function in developing food for appetite control. *Nutrition & Dietetics*, 65(3), S79-S85.

Parada, J., and Aguilera, J. M. (2007). Food microstructure affects the bioavailability of several nutrients. *Journal of Food Science*, 72, 21-32.

Porter, J. H., Trevaskis, N. L., and Charman, W. N. (2007). Lipids and lipid-based formulations: optimizing the oral delivery of lipophilic drugs. *Nature Reviews Drug Discovery*, 6, 231-248.

Schneeman, B. O. (2002). Gastrointestinal physiology and functions. *British Journal of Nutrition*, 88(2), S159-S163.

Singh, H., Ye, A., and Horne, D. (2009). Structuring food emulsions in the gastrointestinal tract to modify lipid digestion. *Progress in Lipid Research*, 48, 92-100.

Wright, E. M., Martín, M. G., and Turk, E. (2003). Intestinal absorption in health and disease-sugars. *Best Practice & Research Clinical Gastroenterology*, 17(6), 943-956.

### **3. RHEOLOGICAL AND MICROSTRUCTURAL CHARACTERIZATION OF WPI-STABILIZED O/W EMULSIONS EXHIBITING TIME-DEPENDENT FLOW BEHAVIOR**

#### **Abstract**

The rheological behavior of O/W emulsions stabilized by WPI and its relationship with their possible microstructural changes was studied. Sunflower oil-in-water emulsions (50, 55, and 60 g oil/100g) were prepared by ultrasound. Rheological properties of the emulsions were determined by: flow curve test, constant shear rate test, and hysteresis loop test. In order to evaluate microstructural changes in the emulsions induced by shear rate, droplet size and droplet size distributions were obtained using image analysis techniques. Emulsions containing 50 and 55 g oil/100g showed a Newtonian behavior, whereas emulsions with 60 g oil/100g exhibit shear thinning behavior. Under constant deformation, the emulsions presented a decrease in their apparent viscosity. The hysteresis loop test revealed that increasing oil content increases the degree of thixotropy of the emulsions. Additionally, before and after the application of the constant deformation test, droplet size distributions did not show differences, reflecting that the decrease in the apparent viscosity with time may be generated by breakdown and further deformation and/or reorganization of oil droplets flocs. In turn, experimental data obtained from the constant shear stress test was fitted using a structural kinetic model. The rate constant ( $k$ ) values showed no particular trend with oil content and shear rate, indicating that probably wall slip occurred at high shear rates and high oil contents.

#### **3.1. Introduction**

Considerable research has been carried out by food scientists to establish the physicochemical and structural basis of food properties. For many years, food science has attempted to identify relationships between food composition, structural

organization and interactions of food components, and the bulk physical and sensory properties of foods, such as texture, appearance, flavor, and shelf life (Aguilera, 2005). Thus, the principles of process engineering of biomaterials and the fundamental role of food structure in understanding the behavior of foods during processing are well established (Aguilera, 2005; German and Watzke, 2004). This knowledge is the basis for the development of novel food matrices with targeted health and nutritional benefits. In addition, although the total amount of a nutrient in natural and processed foods may be obtained from composition tables, its bioavailability depends on many factors, such as food microstructure, processing conditions, digestion conditions and presence of other components. However, there is still a lack of clarity concerning the performance of foods inside our body, which has limited the capacity of the industry to create products with tailored nutritional properties.

Particularly, emulsion-based food products have been widely studied due to their natural or commercial availability, exhibiting a wide variety of different physicochemical and organoleptic characteristics. Many natural and processed foods consist either partly or wholly as emulsions or have been in an emulsified state at some time during their production; such foods include milk, cream, butter, margarine, mayonnaise, sauce, among others (McClements, 2005). The understanding and manipulation of bulk properties of emulsion systems are of utmost importance in the food industry. Shelf life, mouth-feel and flow properties, to name a few, are to great extent determined by interactions present between the system's constituents.

Crucial for creating the desired structure is an excellent control of the bulk properties during processing of foods by the manufacturer. An important challenge for food emulsion science is therefore to understand, monitor and control the changes in colloidal interactions, rheology and microstructure during processing (Dagleish, 2006). The rheological properties of emulsions are needed to design in a more rational fashion new emulsion-based foods and also processing operations which depend on the way that foods behave when flows (e.g., flow through a pipe, stirring in a mixer, passage through a heat-exchanger, etc.). In particular, the time-dependency of the flow properties of food

emulsions is of great practical importance in pumping or mixing operations, which must be carefully controlled so that the food sample has an apparent viscosity that is suitable for the next processing operation (McClements, 2005). In this scenario, rheological measurements are frequently used by food scientists as an analytical tool to provide fundamental insights about the structural organization and interactions of the components within emulsions. For example, measurements of viscosity versus shear rate can be used to estimate the strength of the colloidal interactions between droplets of fluid emulsions (Tadros, 2004).

The chemical composition and microstructure are known to have a significant effect on the rheological properties of food products and, consequently, on the performance of various end-use applications, including food digestion. In particular, food emulsions are compositionally and structurally complex materials that exhibit a wide range of different rheological behaviors, ranging from low-viscosity fluids (such as milk and fruit juice beverages) to fairly hard solids (such as refrigerated margarine or butter), according to the structure, dimensions, and organization of the components in food emulsions. This variability in the rheological properties of food emulsions is dominated by the fact that the droplets are flocculated, and so it is important to understand the factors that determine the structure of these systems. In general, food emulsions contain droplets that can present various types of colloidal interactions acting between them (e.g., van der Waals, electrostatic, steric, hydrophobic, and depletion), which dramatically influence the rheology of food emulsions. For example, two emulsions with the same droplet concentration could have rheological properties varying from a low-viscosity Newtonian liquid to a highly viscoelastic material, depending on the nature of the colloidal interactions (McClements, 2005).

In order to deepen into the structural changes of food emulsions under shearing, as those found during gastric and intestinal digestion, rheological studies can be conducted to predict these changes. As an example, when food emulsions are subjected to shear forces induced by different processing conditions, the rate at which an emulsion changes its structural organization and the mechanism by which this process occurs depend on its

composition and microstructure, as well as on the environmental conditions it experiences (Aguilera and Stanley, 1999). Further, according to the flow conditions, reversible and irreversible structural changes can be induced in food emulsions (Bower et al., 1999). The characterization of time-dependent rheological properties of food systems requires establishing relationships between structure and flow (Abu-Jdayil, 2003). This information is particularly useful for food manufacturers who need to formulate emulsions with enhanced shelf-life or promote emulsion instability in a controlled fashion. Hence, the objective of this study was to investigate the rheological properties of O/W emulsions stabilized by WPI during controlled rheological tests as affected by the oil content and shear rate, relating this information with the microstructure of these emulsions.

## **3.2. Materials and methods**

### **3.2.1. Materials**

Whey protein isolate (BiPRO™, Davisco Foods International Inc., Le Sueur, MN, USA) was employed as the sole emulsifying agent to stabilize the O/W emulsions. A commercial brand of sunflower oil (Natura™, Córdoba, Argentina) was used as dispersed phase. Distilled water was employed in the preparation of all the formulations.

### **3.2.2. Emulsion formation**

Emulsions were prepared from a dispersed and an aqueous phase. The dispersed phase consisted of sunflower oil, whereas aqueous phase corresponded to emulsifier solutions prepared by stirring for at least 2 hours WPI powder into distilled water at 25°C, avoiding foam formation. These solutions were kept at 4°C for at least 12 h to ensure complete hydration of proteins. pH of continuous phase was measured with a digital pH-meter (pH 200, Hanna Instruments, Italy) and presented a value of  $7.0 \pm 0.1$  for all samples. To elaborate the O/W emulsions, sunflower oil was added dropwise to emulsifier solutions while mixing at 25°C using a stirring plate at 960 rpm for 1 min, forming a pre-

emulsion with different oil contents (50, 55 and 60 g oil/100g) and with a constant oil-to-protein mass ratio of 15:1. The final emulsion formation was carried out using an ultrasonic processor (Branson Sonifier 450, Branson Ultrasonics, Danbury, CT, USA) with a 19 mm stainless steel ultrasound probe used to sonicate the pre-emulsion. The ultrasound probe was adjusted 1 cm below the surface of the sample. Sonication was performed in pulsed mode (frequency: one pulse per second, pulse duration: 0.3 s) at a nominal power level of 100 W for 180 s.

### **3.2.3. Rheological properties of O/W emulsions**

All rheological tests were made in a controlled shear rate rheometer (Rheolab MC20, Physica Inc., Stuttgart, Germany). Samples were carefully poured into the rheometer cup and allowed to stand at least 10 min before shearing. Test temperature was set at  $25 \pm 0.1^\circ\text{C}$  using a thermoregulated water bath (Viscotherm VT10, Physica Inc., Stuttgart, Germany). The test geometry was a coaxial cylinder geometry conforming to DIN 53019 (bob radius: 22.5 mm; length: 67.5 mm; cup radius: 24.4 mm).

The rheological characterization of the emulsions was performed using three different tests: i) flow curve test, where the shear rate was increased linearly from 0 to 500 s<sup>-1</sup> during 60 min; ii) constant shear rate test, where the emulsions were subjected to deformation by applying different shear rates (100, 300 and 500 s<sup>-1</sup>) during 60 min; iii) hysteresis loop test, where the shear rate was increased linearly from 0 to 500 s<sup>-1</sup> during 60 min (upward ramp) and then the shear rate was decreased from 500 to 0 s<sup>-1</sup> during 60 min (downward ramp).

### **3.2.4. Modeling of flow behavior of the O/W emulsions**

Over the range of shear rates, the experimental flow curves of the emulsions were described by a Power Law model as follows:

$$\tau = K \cdot \dot{\gamma}^m \quad (3.1)$$

where  $\tau$  is the shear stress (Pa),  $K$  is the consistency index (Pa s<sup>m</sup>),  $\dot{\gamma}$  is the shear rate (s<sup>-1</sup>), and  $m$  is the flow behavior index (dimensionless). For a Newtonian emulsion  $m = 1$ , for an emulsion which exhibits shear thinning behavior  $m < 1$ , and for an emulsion which exhibits shear thickening  $m > 1$ .

### 3.2.5. Modeling of the time-dependent rheological behavior of the O/W emulsions

To understand the time-dependent behavior of the O/W emulsions, data from the constant shear rate test was fitted to a structural kinetic (SK) model. This model assumes that the change in the time-dependent rheological behavior is associated with shear-induced breakdown of the internal structure of non-food and food products (Abu-Jdayil, 2003; Cheng and Evans, 1965; Mallik et al., 2010; O'Donnell and Butler, 2002). Hence, the SK model can be expressed as an  $n$ -order kinetic equation that describes the structural breakdown under shearing by means of a time-dependent structural parameter ( $\lambda$ , dimensionless):

$$\frac{d\lambda}{dt} = -k (\lambda - \lambda_e)^n \quad (3.2)$$

In the above equation, the rate constant  $k$  (s<sup>-1</sup>) is function of shear rate,  $\lambda_e$  is the structural parameter at the equilibrium state ( $t = \infty$ ), and  $n$  (dimensionless) is the reaction order. At a constant shear rate, Eq. 3.2 can be integrated and rearranged to yield:

$$(\lambda - \lambda_0)^{1-n} = (n-1) k t + (\lambda_0 - \lambda_e)^{1-n} \quad (3.3)$$

where  $\lambda_0$  is the structural parameter at the fully-structured state ( $t = 0$ ). Because  $\lambda$  cannot be obtained from experimental measurements, this structural parameter can be expressed in terms of the instantaneous apparent viscosity as follows,

$$\lambda(\dot{\gamma}, t) = \frac{(\eta - \eta_e)}{(\eta_0 - \eta_e)} \quad (3.4)$$

being  $\eta$  the apparent viscosity (Pa s) at time  $t$ ,  $\eta_0$  the initial apparent viscosity at the fully-structured state ( $t = 0$ ), and  $\eta_e$  the apparent viscosity at the equilibrium state ( $t = \infty$ ). Then, substituting Eq. 3.4 into Eq. 3.3 yields,

$$\left[ \frac{(\eta - \eta_e)}{(\eta_0 - \eta_e)} \right]^{1-n} = 1 + (n-1)k t \quad (3.5)$$

Although the above equation is only valid for constant shear rate conditions, this expression allows a simple way for the determination of the kinetic parameters ( $k$  and  $n$ ) using the experimental values of apparent viscosity obtained from the constant shear rate test. However, due to a constant value in the apparent viscosity was not found for some experimental tests at the end of the constant shearing time, the  $\eta_e$  values for all experiments were obtained by non-linear regression (Eq. 3.6) using the data from the constant shear rate test,

$$\eta = \eta_e \left( a - \exp^{-bt} \right) \quad (3.6)$$

where  $a$  and  $b$  are empirical parameters of the model proposed.

### 3.2.6. Microstructural characterization of the O/W emulsions

Microstructure of the emulsions was analyzed before and after the constant shear rate test. This microstructural characterization was carried out in terms of droplet size and droplet size distribution. Droplet diameter was determined from images of the O/W emulsions obtained with a light microscope (Olympus BX50, Optical Co. Ltd., Tokyo, Japan) and recorded with a digital CCD camera (CoolSnap-Pro Color, Photometrics Roper Division, Inc., Tucson, AZ, USA). Previous to this analysis, emulsion samples were diluted with emulsifier solution at a ratio 1:10 (v/v) to avoid the overlapping and agglomeration of oil droplets, which it can affect the further image analysis and processing. Dilution was made using the same protein concentration present in the continuous phase (Nandi et al., 2001).

Image processing for droplet size analysis was carried out automatically using a segmentation algorithm developed under Matlab environment (Matlab 7.6, R2009a, The MathWorks Inc, MA, USA), mainly based on mathematical morphology. Briefly, the data processing of the digitalized images consisted of different steps, including contrast enhancement, different filter operations followed by an automatic segmentation. This

procedure allowed considerable reduction of the data analysis time without losing accuracy. A substantial number of droplets ( $N > 2500$ ) were counted in order to obtain oil droplet diameters ( $D$ ) and oil droplet size distributions in each sample. Droplet size distributions were generated by grouping the droplets into classes belonging to a common interval. Droplet size frequency distributions were computed using MS-Excel (Microsoft<sup>TM</sup> Excel 2007). Volume frequency of any class interval was calculated as the number of oil droplets in that class (class frequency) divided by the total number of oil droplets, and expressed as a percentage. In order to characterize the cumulative droplet size distributions, the cut-off diameters at 10% ( $D_{10}$ ), 50% ( $D_{50}$ ), and 90% ( $D_{90}$ ) on the cumulative frequency distribution curve were determined.

### **3.2.7. Statistical analysis**

Analysis of variance (ANOVA) tests were used to analyze the data at a confidence level of 95%. The Kolmogorov–Smirnov test (confidence level of 95%) was used to compare the particle size distributions obtained before and after the constant shear rate test. The significance level for all findings reported as statistically significant was that all pairs of curves the distance between them (distance K–S) must not be statistically different ( $p > 0.05$ ) (Ramírez and Aguilera, 2011). In both statistical tests, Statgraphics Plus version 5.1 (Manugistics Inc., Statistical Graphics Corporation, Rockville, USA) was used.

## **3.3. Results and discussion**

### **3.3.1. Rheological behavior of WPI-stabilized O/W emulsions**

The composition of food emulsions has marked effects on their rheological properties. In order to better understand this point, this work focused on the impact of oil content in WPI-stabilized O/W emulsions on their susceptibility to rheological properties changes. This type of emulsion can be used as model system to enhance the understanding of the structural stability of food emulsions subjected to shear stresses.

As it was expected, the oil content affected the rheological behavior of O/W emulsions when subjected to shear forces (Figure 3.1). Emulsions containing 50 and 55 g oil/100g presented a Newtonian behavior, whereas emulsions containing 60 g oil/100g showed a non-Newtonian behavior. Over the range of shear rates studied rheological properties of the emulsions were described by a Power Law model (Equation 3.1), with regression coefficients ( $R^2$ ) > 0.99 (see Table 3.1). The rheological parameters obtained from the Power Law model are also presented in Table 3.1.

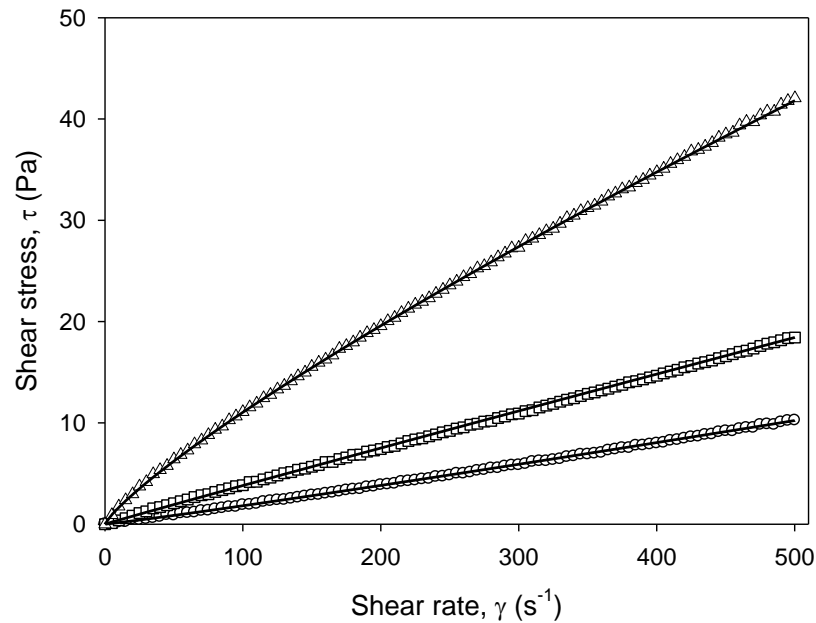


Figure 3.1. Rheogram for O/W emulsions containing different oil contents: (○) 50 g oil/100 g; (□) 55 g oil/100 g; and (Δ) 60 g oil/100g. Lines refer to the data generated by the Power Law model.

Table 3.1. Rheological parameters obtained from the Power Law model.

Oil content (g oil/100 g)	Consistency index, K (Pa s <sup>m</sup> )	Flow behavior index, <i>m</i> (dimensionless)	Correlation coefficient, $R^2$
50	0.013 [± 0.001] <sup>a</sup>	1.073 [± 0.006] <sup>a</sup>	0.9996
55	0.042 [± 0.001] <sup>b</sup>	0.979 [± 0.005] <sup>b</sup>	0.9996
60	0.245 [± 0.003] <sup>c</sup>	0.827 [± 0.002] <sup>c</sup>	0.9999

- Values in brackets are the 95% confidence intervals of the regression parameters  
- Columns with different letters indicate significant differences ( $p < 0.05$ )

The parameter  $m$  had a value of  $\sim 1$  at oil contents of 50 and 55 g oil/100g, and had a minimum of 0.83 for emulsions containing 60 g oil/100g. These findings indicated that the emulsions with the highest oil content presented a degree of shear-thinning behavior due to disruption of the spatial organization of the oil droplets in the emulsions in the shear field. For Newtonian liquids, at constant temperature and pressure, the viscosity does not vary with the shear rate. However, for most non-Newtonian liquids, the viscosity decreases with an increase in shear rate, giving rise to what is known as shear-thinning behavior or pseudoplasticity (Rao, 1977). Pseudoplasticity represents an irreversible structural breakdown that may occur as a result of the spatial redistribution of the particles under a shear field, alignment of non-spherical particles with the flow field, or deformation and disruption of flocs (McClements, 2005). In turn, it was determined that the consistency index ( $K$ ) was significantly increased ( $p < 0.05$ ) with increasing oil content. In emulsions with lower oil contents, the particles are far apart and the inter-particle interactions are relatively weaker. This structural conformation explains the low viscosity of these systems and their Newtonian behavior. As oil content increases, the particles are closer which leads to packing of the oil droplets and the inter-particle interactions are stronger, giving a non-Newtonian behavior. The attractive forces between droplets drive the formation of flocs which normally could evolve into a space-filling particulate network (Mewis and Wagner, 2009). According to the above explanation, the apparent viscosity of emulsions may be influenced by their oil content. Other studies have also evaluated the rheological behavior of O/W emulsions. In the work reported by Nikovska (2010), olive oil-in-water emulsions stabilized by WPI showed a typical non-Newtonian behavior. When the shear rate increased, the values of the apparent viscosity decreased, and this tendency was more strongly exhibited in the emulsions with higher dispersed-phase volume (70% v/v). In turn, Lizarraga et al. (2008) demonstrated that corn oil-in-water emulsions (50 g oil/100g) stabilized by whey protein concentrate presented a Newtonian behavior. These results in conjunction with our observations confirm the influence of the composition of the emulsions on their rheological properties. Undoubtedly, the strength and range of the colloidal interactions

between the droplets in emulsions are determined by the bulk physicochemical properties of the oily phase (e.g., density, viscosity, and surface tension). Hence, differences in these properties can cause appreciable changes in the rheology, stability and overall properties of food emulsions. Further, it is proper to mention that surfactants may also play an important role in the rheological behavior of emulsions at any concentration. Aggregation stability of droplets is determined mainly by the nature and concentration of a surfactant in the system creating and stabilizing the emulsion (Derkach, 2009).

As previously mentioned, the apparent viscosity of O/W emulsions may be related to their oil content. Particularly, the increase in apparent viscosity is produced because the effective volume fraction of a floc is greater than the sum of the volume fractions of the individual droplets due to the presence of the continuous phase trapped between the droplets in the flocs. This fact could be of particular relevance in the transition from a state called *partially crystalline* to another called *glassy* in the system. A partially crystalline state is found for O/W emulsions with oil fractions ranging from 0.49 to 0.54. This state is conformed by closely packed particles and mobile loosely packed particles. However, in the glassy state found for oil fractions between 0.58 and 0.64, the movement of the particles is severely restricted because of the close proximity of their neighbors. This last type of emulsion can exhibit both solid-like and fluid-like behaviors, acting like a solid at low shear stresses and a fluid once a critical yield stress has been exceeded and the particles can move past one another decreasing their apparent viscosity (McClements, 2005). On the other hand, one of the major factors influencing the rheological behavior of the O/W emulsions is the continuous breakdown or structural reorganization induced by mechanical stresses that occur during flow, causing a decrease in the flow resistance.

In order to establish in more detail the existence of structural changes in the system during flow, the emulsions were subjected to a constant shear rate test (see Figure 3.2). From our findings it could be argued that all emulsions presented a clear shear- and

time-dependent behavior because the apparent viscosity of the emulsions decreased with shearing time. This performance is characteristic of thixotropic fluids.

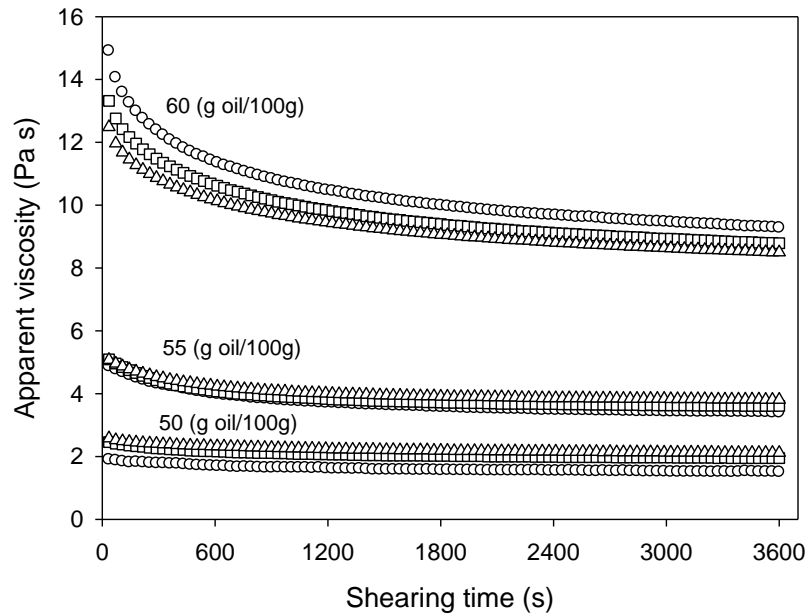


Figure 3.2. Effect of oil content on the thixotropic behavior of O/W emulsions for different constant shear rates: ( $\circ$ )  $100\text{ s}^{-1}$ ; ( $\square$ )  $300\text{ s}^{-1}$ ; and ( $\triangle$ )  $500\text{ s}^{-1}$ .

As can be seen from Figure 3.2, the time-dependent behavior was more pronounced during the first 20 minutes of shearing, reaching an almost constant value thereafter. Further, the shear- and time-dependent behavior was more clearly observed at higher oil contents. Concentrated emulsions that contain flocculated droplets tend to exhibit pronounced shear-thinning behavior. When constant shear is applied the flocs first breaks down, leading to the destruction of the structure and thus the reduction in the apparent viscosity with time (Mallik et al., 2010). To estimate the degree of thixotropy of all emulsions a hysteresis test was applied. Additionally, possible structural changes induced by shearing were assessed by using quantitative microscopic analysis before and after the constant shear rate test. The characterization of emulsion structure was performed in terms of droplet diameter and droplet diameter distribution.

Different hysteresis loops were observed among the samples (Figure 3.3). The area between the upward and downward curves of a hysteresis loop was used to evaluate the degree of thixotropy. The magnitudes of the loop areas were 87, 233 and 1149 Pa/s for emulsions with 50, 55 and 60 g oil/100g, respectively. These results indicate that increasing oil content increases the degree of thixotropy of the emulsions. This is explained by variation in the structuration level of the emulsions according to the oil content, which is controlled by weak colloidal interactions between WPI-coated droplets and/or flocs (Mewis and Wagner, 2009; Tadros, 2004). Thus, it is expected that concentrated emulsions possess a higher degree of structuration.

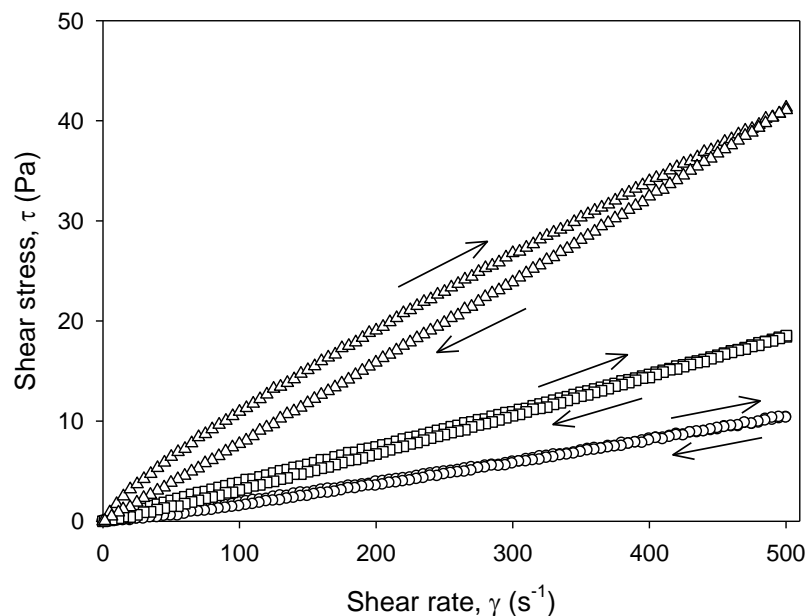


Figure 3.3. Hysteresis loops for O/W emulsions containing different oil contents: (○) 50 g oil/100 g; (□) 55 g oil/100 g; and (Δ) 60 g oil/100g.

As mentioned above, possible changes in the structural organization of the emulsions induced by shearing were evaluated. These structural changes were analyzed in order to determine oil droplet coalescence, which was described in terms of oil droplet diameter and oil droplet diameter distributions. No differences in droplet sizes can be observed both qualitatively from photomicrographs in Figure 3.4 and quantitatively from the size

distribution curves (Figure 3.5). In addition, for all experimental conditions, similar values for  $D_{10}$ ,  $D_{50}$  and  $D_{90}$  were found (Table 3.2). Confirming these observations, the Kolmogorov-Smirnov test demonstrated that there were no significant differences ( $p > 0.05$ ) between the oil droplet size distributions before and after the constant shear rate test. From these results, it is possible to establish that flow-induced coalescence in the O/W emulsions stabilized by WPI was not generated, which was probably due to the small size of the oil droplets in the emulsions. As it can be seen in Table 3.2, the cut-off diameters at 90% ( $D_{90}$ ) on the cumulative frequency distribution curve were always  $< 1 \mu\text{m}$ . In general, O/W emulsions containing small oil droplets are very stable to coalescence. Nevertheless, when proteins are used to stabilize these emulsions, they tend to create very stable interfaces. Both factors could be expected to decrease the interface rupture and coalescence (Walstra, 2003). Hence, O/W emulsions with small droplet size ( $< 1 \mu\text{m}$ ) could have a great technological potential for emulsion design in terms of stability during flow.

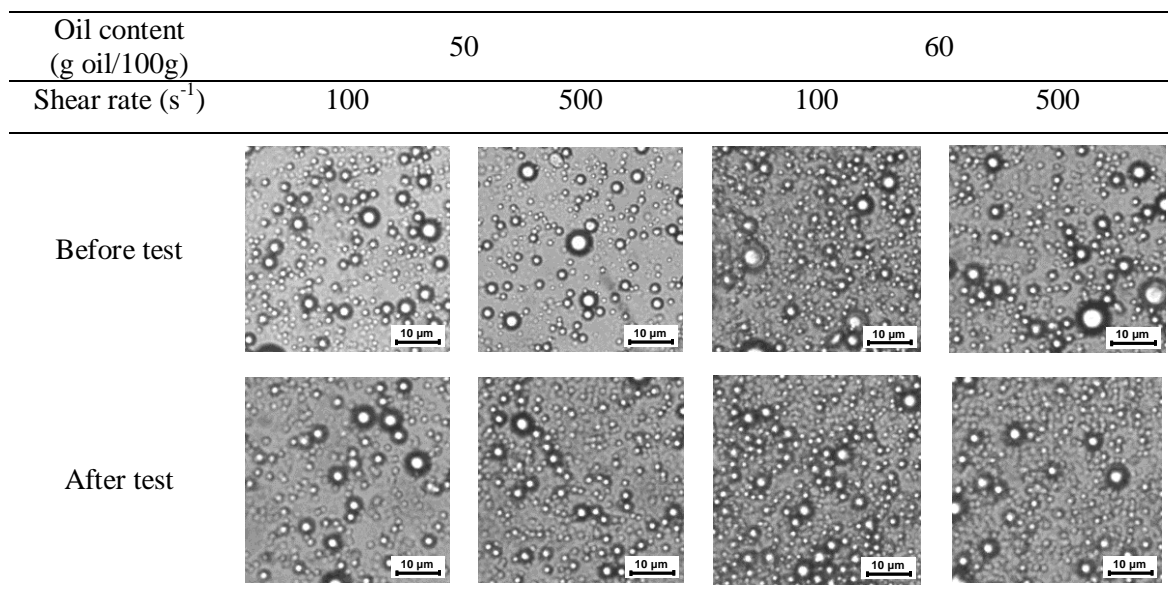


Figure 3.4. Photomicrographies of O/W emulsions before and after the constant shear rate test. Figure shows the extreme conditions of oil content and shear rate analyzed for this test.

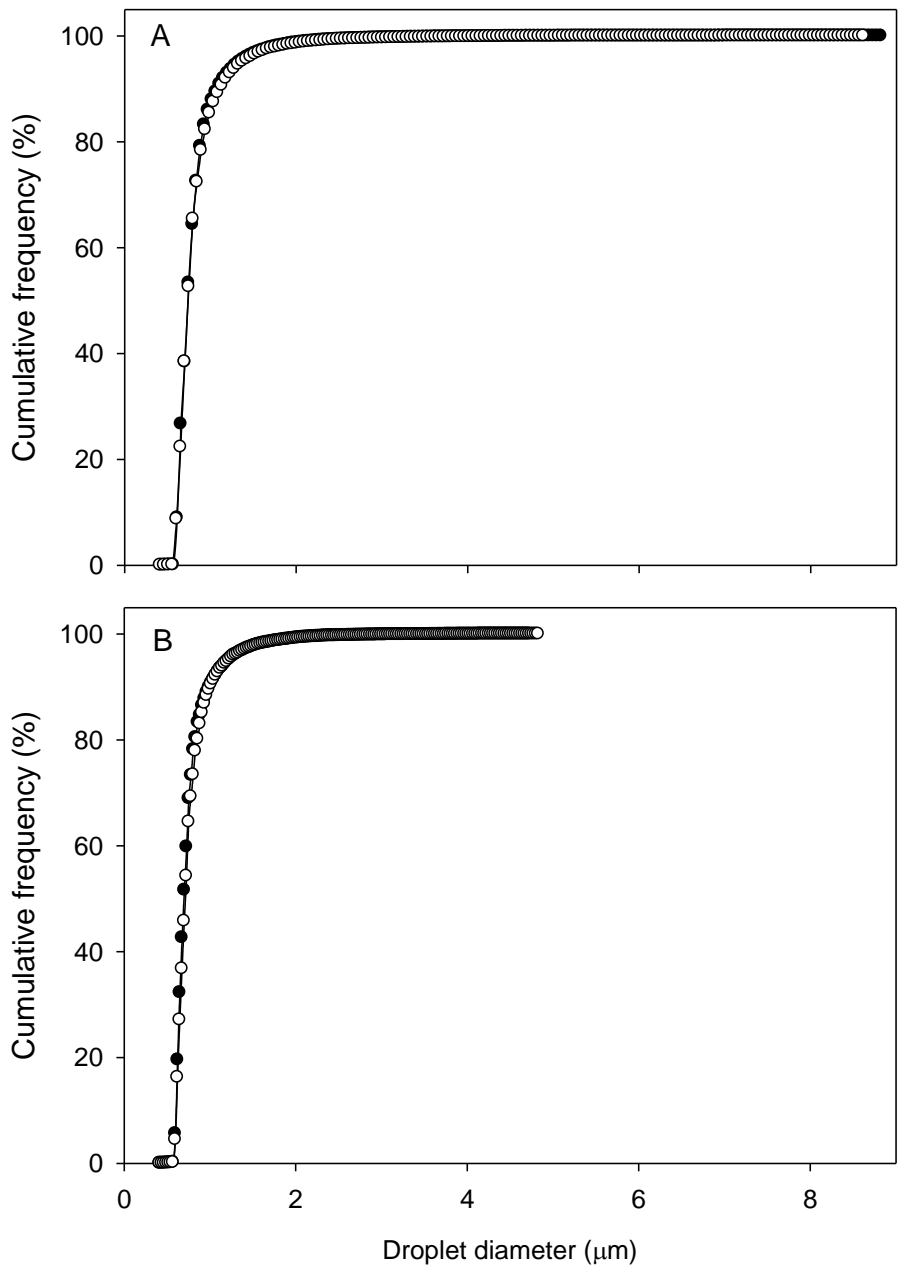


Figure 3.5. Cumulative frequency distribution curves for droplet diameter of O/W emulsions before (●) and after (○) the constant shear rate test. (A) Oil content of 50 g oil/100g and constant shear rate of 100 s<sup>-1</sup>, (B) Oil content of 60 g oil/100g and constant shear rate of 500 s<sup>-1</sup>.

Table 3.2. Oil droplet diameters of O/W emulsions before and after the constant shear rate test.

Oil content (g oil/100 g)	Time (min)	Shear rate (s <sup>-1</sup> )								
		100			300			500		
		<i>D</i> <sub>10</sub> (μm)	<i>D</i> <sub>50</sub> (μm)	<i>D</i> <sub>90</sub> (μm)	<i>D</i> <sub>10</sub> (μm)	<i>D</i> <sub>50</sub> (μm)	<i>D</i> <sub>90</sub> (μm)	<i>D</i> <sub>10</sub> (μm)	<i>D</i> <sub>50</sub> (μm)	<i>D</i> <sub>90</sub> (μm)
50	0	0.611	0.729	0.999	0.611	0.729	0.999	0.611	0.729	0.999
	60	0.606	0.744	1.074	0.603	0.723	1.020	0.598	0.735	1.046
55	0	0.600	0.715	0.987	0.600	0.715	0.987	0.600	0.715	0.987
	60	0.602	0.718	0.976	0.607	0.734	1.039	0.605	0.722	1.008
60	0	0.593	0.699	0.955	0.593	0.699	0.955	0.593	0.699	0.955
	60	0.602	0.722	0.996	0.594	0.713	1.000	0.602	0.715	0.977

### 3.3.2. Modeling of the constant shear rate test by the SK model

In order to obtain kinetic parameters related to the structural breakdown of the O/W emulsions, the SK model was fitted to the experimental data obtained from the constant shear stress test. This model has been widely used for modeling the time-dependent viscosity of food products (Abu-Jdayil and Mohameed, 2002; Abu-Jdayil, 2003; O'Donnell and Butler, 2002), hydrocolloids dispersions (Koocheki and Razavi, 2009; Razavi and Karazhiyan, 2009), and also non-food materials (Mallik et al., 2010). In all these studies, the reaction order for the structural breakdown has been fixed to  $n = 2.0$ . Nevertheless, Nguyen et al. (1998) reported that transient viscosity data for maize and waxy maize starch pastes could be fitted to a third-order kinetic model, whereas Mohameed et al. (2004) used a fractional reaction order of  $n = 1.5$  when they applied the SK model to concentrated yogurt. In this work, a fractional reaction order ( $n = 1.5$ ) and a second-order reaction ( $n = 2.0$ ) were used to estimate the goodness of the fit. The best fit to the experimental data was obtained with a reaction order of 1.5 (Table 3.3, Figure 3.6), suggesting that the reaction order for the structural breakdown may be dependent on the type of binding interactions between structural components of the emulsion (i.e., colloidal particles, polymers or protein-coated droplets). Therefore, the reaction order  $n$  should not be previously defined but rather determined by the particular features of each product under study.

As can be seen in Table 3.3, the rate constant ( $k$ ) values showed no particular trend with increasing shear rate. Only at a shear rate of  $100 \text{ s}^{-1}$ , the  $k$  values increase with increasing oil content. The rate constant can be considered as a measure of the rate of thixotropic breakdown (Abu-Jdayil and Mohameed, 2002; Abu-Jdayil, 2003). It has been shown that  $k$  generally increases with increasing shear rate, as expected for thixotropic structured material like concentrated yogurt (Abu-Jdayil and Mohameed, 2002; Mohameed et al., 2004), model mayonnaise (Abu-Jdayil, 2003), and hydrocolloids dispersions (Koocheki and Razavi, 2009; Razavi and Karazhiyan, 2009). However,  $k$  values for hydrocolloids extracted from Balangu seeds (Razavi and Karazhiyan, 2009) and solder pastes (Mallik et al., 2010) were not dependent on shear rate.

Table 3.3. Rate constants ( $k$ ) calculated by fitting the SK model using different reaction orders ( $n$ ) for the O/W emulsions subjected to the constant shear rate test.

Oil content (g oil/100 g)	$n$	Shear rate ( $s^{-1}$ )								
		100			300			500		
		$k \times 10^3 (s^{-1})$	$R^2$	$\eta_o/\eta_e$	$k \times 10^3 (s^{-1})$	$R^2$	$\eta_o/\eta_e$	$k \times 10^3 (s^{-1})$	$R^2$	$\eta_o/\eta_e$
50	1.5	$1.92 \pm 1.25$	0.949	$1.36 \pm 0.11$	$2.15 \pm 0.24$	0.974	$1.26 \pm 0.02$	$1.76 \pm 0.39$	0.976	$1.22 \pm 0.01$
	2.0	$2.90 \pm 2.10$	0.885		$3.29 \pm 0.42$	0.911		$2.64 \pm 0.66$	0.928	
55	1.5	$2.15 \pm 0.13$	0.974	$1.42 \pm 0.06$	$2.85 \pm 0.87$	0.971	$1.40 \pm 0.07$	$2.73 \pm 0.38$	0.972	$1.32 \pm 0.02$
	2.0	$3.26 \pm 0.22$	0.907		$4.46 \pm 0.64$	0.893		$4.25 \pm 0.65$	0.895	
60	1.5	$2.42 \pm 0.20$	0.977	$1.58 \pm 0.09$	$2.03 \pm 0.35$	0.980	$1.50 \pm 0.06$	$2.05 \pm 0.07$	0.978	$1.45 \pm 0.06$
	2.0	$3.77 \pm 0.35$	0.925		$3.25 \pm 0.65$	0.924		$3.13 \pm 0.13$	0.927	

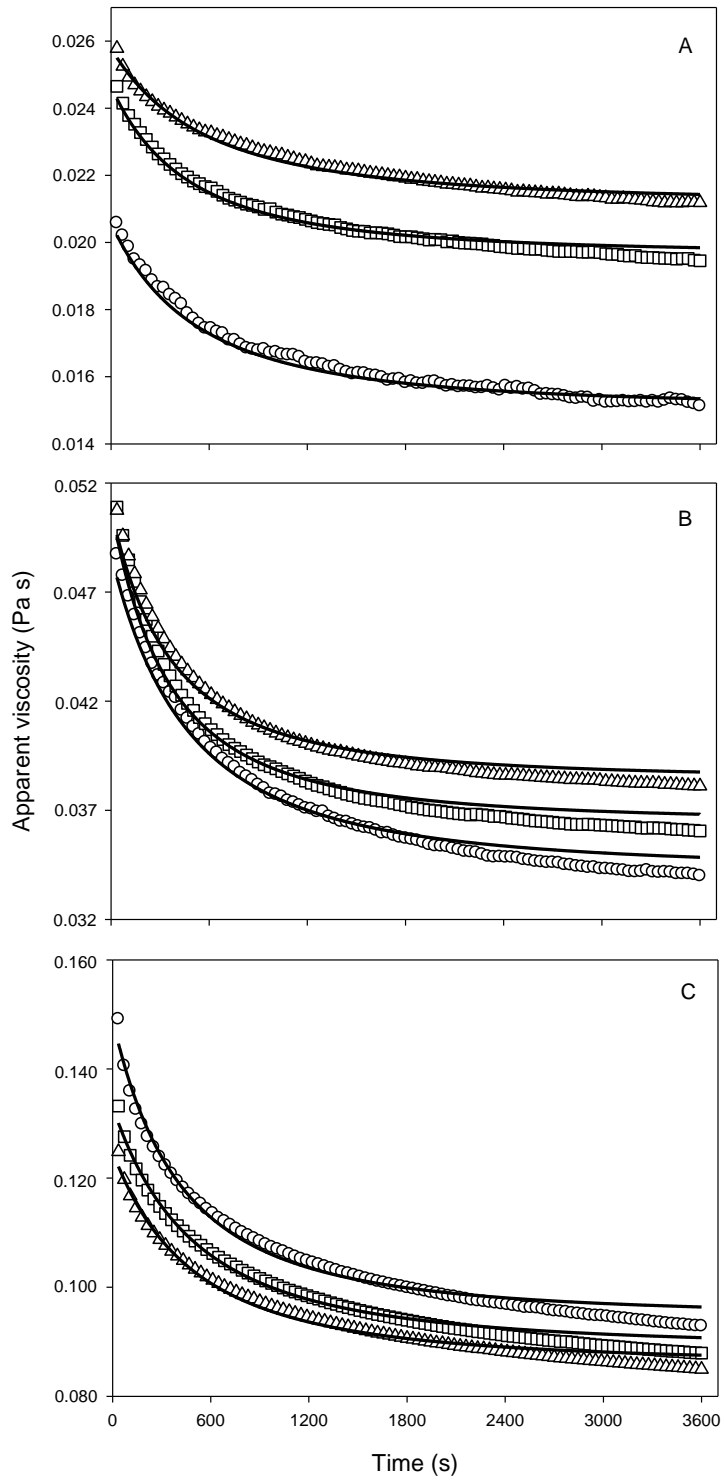


Figure 3.6. Apparent viscosity of O/W emulsions at shear rates of ( $\circ$ ) 100 ( $s^{-1}$ ), ( $\square$ ) 300 ( $s^{-1}$ ) and ( $\Delta$ ) 500 ( $s^{-1}$ ) for different oil contents: (A) 50 g oil/100g, (B) 55 g oil/100g, and (C) 60 g oil/100g. Lines correspond to the data fitted by the SK model with  $n = 1.5$ .

It is normally assumed that the liquid in contact with the surface of the measuring bob of the rheometer moves with it at the same speed. This assumption may not hold for emulsions. In fact, it is generally accepted that upon shearing of a concentrated suspension in a Couette geometry, particles within the suspension will tend to migrate to regions of lower shear stress (Goshawk et al., 1998). Under these conditions, phase separation occurs at the inner cylinder surface (i.e., radial particle migration within the bulk material), and a thin layer of continuous phase acts as a lubricant. Consequently, most of the deformation occurs within the depleted layer generating wall slip. Thus, the instrument response is mainly determined by the properties of this thin layer of liquid rather than by the bulk of the material being assayed (McClements, 2005). The rheometrical study performed by Goshawk et al. (1998) revealed that mayonnaise exhibits apparent wall slip in both small amplitude oscillatory shear flow and torsional flow. This behavior was explained by the formation of a boundary layer of only a few tens of nanometers thick. Then, it is highly probable that at high shear rates and high oil contents wall slip occurred for the WPI-stabilized O/W emulsions, leading to the results presented in Table 3.3 for  $k$  values.

Finally, the ratio of the initial to equilibrium apparent viscosity ( $\eta_0/\eta_e$ ) increased with oil content, but decreased with shear rate (Table 3.3). This ratio can be considered as a relative measure of the amount of structural breakdown or, in other words, as a relative measure of the extent of thixotropy (Abu-Jdayil, 2003). It has been shown for model mayonnaise that the  $\eta_0/\eta_e$  ratio increased with shear rate and oil content (Abu-Jdayil, 2003). Then, by increasing the oil content one would expect to enhance the “amount” of structure that can be broken down by shear forces at constant shear rate. In addition, and as explained above, wall slip could lead to a decrease in the  $\eta_0/\eta_e$  ratio with increasing shear rate.

### **3.4. Conclusions**

Our experimental results suggested that the decrease in the apparent viscosity of WPI-stabilized O/W emulsions is due to shear-induced structural changes when a constant

shear rate was applied. This behavior could be related to the disruption of the emulsion flocs and the rearrangement of the oil droplets promoted by the flow field. However, these structural changes were not caused by coalescence of the oil droplets, because there were no significant differences in the oil droplet size distributions before and after the application of constant shear rate. These results will eventually lead to a better understanding of the colloidal basis of emulsion rheology, thus having important implications for the design and production of food emulsions.

## References

Abu-Jdayil, B., and Mohameed, H. (2002). Experimental and modeling studies of the flow properties of concentrated yogurt as affected by the storage time. *Journal of Food Engineering*, 52, 359-365.

Abu-Jdayil, B. (2003). Modelling the time-dependent rheological behavior of semisolid foodstuffs. *Journal of Food Engineering*, 57, 97-102.

Aguilera, J. M., and Stanley, D. W. (1999). *Microstructural Principles of Food Processing and Engineering*. 2<sup>nd</sup> ed. Aspen Publishers Inc, Gaithersburg, MD.

Aguilera, J. M. (2005). Why food microstructure?. *Journal of Food Engineering*, 67, 3-11.

Bower, C., Gallegos, C., Mackley, M. R., and Madiedo, J. J. (1999). The rheological and microstructural characterisation of the non-linear flow behaviour of concentrated oil-in-water emulsions. *Rheologica Acta*, 38, 145-159.

Cheng, D. C. H., and Evans, F. (1965). Phenomenological characterization of the rheological behavior of inelastic reversible thixotropic and antithixotropic fluids. *British Journal of Applied Physics*, 16, 1599-1617.

Dalgleish, D. G. (2006). Food emulsions - their structures and structure-forming properties. *Food Hydrocolloids*, 20, 415-422.

Derkach, S. R. (2009). Rheology of emulsions. *Advances in Colloid and Interface Science*, 151, 1-23.

German, J. B., and Watzke, H. J. (2004). Personalizing food for health and delight. *Comprehensive Reviews in Food Science and Food Safety*, 3, 145-151.

- Goshawk, J. A., Binding, D. M., Kell, D. B., and Goodacre, R. (1998). Rheological phenomena occurring during the shearing flow of mayonnaise. *Rheologica Acta*, 42, 1537-1553.
- Koocheki, A., and Razavi, S. M. A. (2009). Effect of concentration and temperature on flow properties of Alyssum homolocarpum seed gum solutions: assessment of time dependency and thixotropy. *Food Biophysics*, 4, 353-364.
- Lizarraga, M. S., Panb, L. G., Añon, M. C., and Santiago, L. G. (2008). Stability of concentrated emulsions measured by optical and rheological methods. Effect of processing conditions - I. Whey protein concentrate. *Food Hydrocolloids*, 22, 868-878.
- Mallik, S., Ekere, N. N., Marks, A. E., Seman, A., and Durairaj, R. (2010). Modeling the structural breakdown of solder paste using the structural kinetic model. *Journal of Material Engineering and Performance*, 19, 40-45.
- McClements, D. J. (2005). *Food Emulsions: Principles, Practices, and Techniques*. 2<sup>nd</sup> ed. CRC Press, Boca Raton, FL.
- Mewis, J., and Wagner, N. J. (2009). Thixotropy. *Advances in Colloid and Interface Science*, 147-148, 214-227.
- Mohameed, H. A., Abu-Jdayil, B., and Al-Shawabkeh, A. (2004). Effect of solids concentration on the rheology of labneh (concentrated yogurt) produced from sheep milk. *Journal of Food Engineering*, 61, 347-352.
- Nandi, A., Khakhar, D. V., and Mehra, A. (2001). Coalescence in surfactant-stabilized emulsions subjected to shear flow. *Langmuir*, 17, 2647-2655.
- Nguyen, Q. D., Jensen, C. T. B., and Kristensen, P. G. (1998). Experimental and modeling studies of the flow properties of maize and waxy starch pastes. *Chemical Engineering Journal*. 70, 165-171.
- Nikovska, K. (2010). Oxidative stability and rheological properties of oil-in-water emulsions with walnut oil. *Advance Journal of Food Science and Technology*, 2, 172-177.
- O'Donnell, H. J., and Butler, F. (2002). Time-dependent viscosity of stirred yogurt. Part I: coquette flow. *Journal of Food Engineering*, 51, 249-254.
- Ramírez, C., and Aguilera, J. M. (2011). Determination of a representative area element (RAE) based on nonparametric statistics in bread. *Journal of Food Engineering*, 102, 197-201.

Rao, M. A. (1977). Rheology of liquid foods - A review. *Journal of Texture Studies*, 8, 135-168.

Razavi, S. M. A., and Karazhiyan, H. (2009). Flow properties and thixotropy of selected hydrocolloids: experimental and modeling studies. *Food Hydrocolloids*, 23, 908-912.

Tadros, T. F. (2004). Application of rheology for assessment and prediction of the long-term physical stability of emulsions. *Advances in Colloid and Interface Science*, 108-109, 227-258.

Walstra, P. (2003). *Physical Chemistry of Foods*. Marcel Dekker Inc. New York, NY.

## 4. FABRICATION, CHARACTERIZATION AND LIPASE DIGESTIBILITY OF FOOD-GRADE NANOEMULSIONS

### Abstract

The behavior of nanoemulsion-based delivery systems within the gastrointestinal tract determines their functional performance. In this study, the influence of oil droplet diameter (60-172 nm) on the *in vitro* digestion of nanoemulsions containing non-ionic surfactant stabilized lipid (corn oil) droplets was examined using simulated small intestine conditions. Nanoemulsions were prepared by a combination of high-pressure homogenization and solvent (hexane) displacement. Lipid droplets with different sizes were prepared by varying the oil-to-solvent ratio in the disperse phase prior to homogenization. The fraction of free fatty acids (FFA) released from emulsified triacylglycerols during digestion was measured by an *in vitro* model (pH-Stat titration). Nanoemulsions exhibited a lag-period before any FFA were released, which was explained by inhibition of lipase adsorption to the oil-water interface by free surfactant. After the *lag*-period, the digestion rate increased with decreasing oil droplet diameter (increasing specific surface area). The total amount of FFA released from the emulsions increased from 61% to 71% as the mean droplet diameter decreased from 172 nm to 60 nm. The incomplete digestion of the emulsified lipids could be explained by inhibition of lipase activity by the release of fatty acids and/or by interactions between lipase and surfactants molecules.

### 4.1. Introduction

There is considerable interest in developing delivery systems to encapsulate, protect, and release lipophilic bioactive components (Lee and McClements, 2010; Li and McClements, 2010; Parada and Aguilera, 2007). For certain applications, these delivery systems must be formulated so that they are suitable for oral ingestion, e.g., functional foods and some pharmaceutical preparations. Emulsion-based delivery systems are

particularly suitable for oral applications because they can be fabricated from edible components (e.g., oil, water, surfactants, and proteins) using economic processing operations (e.g., mixing and homogenization). A variety of emulsion-based delivery systems are available, including conventional emulsions, nanoemulsions, solid lipid nanoparticles, multiple emulsions, and multilayer emulsions (McClements and Li, 2010).

Oil-in-water nanoemulsions consist of small oil droplets (*diameter* < 200 nm) dispersed within a watery continuous phase, with each droplet being surrounded by a protective coating of emulsifier molecules (Acosta, 2009; Anton et al., 2008; Gutiérrez et al., 2008; Lee et al., 2011; Qian and McClements, 2011). Like conventional emulsions, nanoemulsions are non-equilibrium systems having characteristics and properties that depend not only on their composition but also on the preparation method used (Mason et al., 2006). Nevertheless, nanoemulsions do have a number of advantages over conventional emulsions for certain applications due to their relatively small particle size: (i) they scatter light weakly and so tend to be transparent or translucent; (ii) they have high stability to particle aggregation and gravitational separation; (iii) they have unique rheological characteristics; and, (iv) they can greatly increase the bioavailability of encapsulated lipophilic components (Anton et al., 2008; Huang et al., 2010; Mason et al., 2006; McClements, 2005; Velikov and Pelan, 2008). For these reasons, edible nanoemulsions are finding increasing utilization as oral delivery systems within the food and pharmaceutical industries.

The design of delivery systems for oral ingestion requires an understanding of their behavior within the complex environment of the GIT, where variations in pH, ionic strength, enzyme activity, surface active molecules, and motility occur. The composition and microstructure of delivery systems are the major factors determining their biological fate (Golding and Wooster, 2010; Golding et al., 2011; Lundin and Golding, 2009; Singh et al., 2009; Wickham et al., 2009). In principle, nanoemulsion-based delivery systems can be designed to control the extent, rate and site of release of encapsulated components within the GIT. However, there is currently a poor understanding of the

influence of specific nanoparticle characteristics (such as size, charge, composition, and interfacial properties) on the behavior of nanoemulsions within the GIT. The objective of this research was therefore to start building our understanding of the behavior of orally-ingested nanoemulsions. In particular, we focus on the influence of particle size on the rate and extent of lipid digestion using simulated small intestinal conditions.

In this study, a range of nanoemulsions with different particle sizes was produced using a combined high pressure homogenization/solvent displacement method. The droplet size can be controlled using this method by varying the homogenization conditions, emulsifier concentration, and ratio of oil-to-solvent present in the system prior to homogenization (Chu et al., 2007a; Chu et al., 2007b; Lee et al., 2011; Silva et al., 2011; Tan and Nakajima, 2005). For example, protein-stabilized  $\beta$ -carotene nanodispersions with particle diameters ranging from 10 to 300 nm have been prepared using this method (Chu et al., 2007a; Chu et al., 2007b; Silva et al., 2011; Tan and Nakajima, 2005). In addition, we recently used this approach to produce protein-stabilized nanoemulsions (*diameter* = 70 nm) using high-pressure homogenization (microfluidization) and organic solvent (ethyl acetate) displacement (Lee and McClements, 2010; Lee et al., 2011).

In the current study, we initially examine the effect of the organic phase composition (oil-to-solvent ratio) on the particle size distribution, electrical characteristics, microstructure, and appearance of nanoemulsions stabilized by a small molecule non-ionic surfactant (Tween 20). Subsequently, the influence of particle size on the *in vitro* digestibility under simulated small intestinal conditions of the nanoemulsions was assessed. Ultimately, the information obtained from this study should facilitate the rational design of oral delivery systems for utilization within the pharmaceutical, food, and other industries.

## **4.2. Materials and methods**

### **4.2.1. Raw materials**

Corn oil was purchased from a local supermarket and was used without further purification. Tween 20 (polyoxyethylene sorbitan monolaurate) was purchased from

Acros Organics (Lot # B0518680, Fair Lawn, NJ). Hexane was acquired from Fisher Scientific (Lot # 103567, Fair Lawn, NJ). Monobasic sodium phosphate, dibasic sodium phosphate, and sodium azide were obtained from Sigma-Aldrich (St. Louis, MO). Analytical grade hydrochloric acid (HCl) and sodium hydroxide (NaOH) were purchased from Sigma-Aldrich (St. Louis, MO). Purified water from a Nanopure water system (Nanopure Infinity, Barnstead International, Dubuque, IA) was used for the preparation of all solutions.

Bile extract (porcine, B8631, Batch # 058K0066) and lipase from porcine pancreas (activity  $\geq 2.0$  USP units/mg, Type II, L3126, Batch # 096K0747) were obtained from Sigma-Aldrich (St. Louis, MO). The composition of the bile extract (BS) was: total bile salt content = 49 wt%; with 10-15% glycodeoxycholic acid, 3-9% taurodeoxycholic acid, 0.5-7% deoxycholic acid, 1-5% hyodeoxycholic acid, and 0.5-2% cholic acid; 5 wt% phosphatidyl choline (PC);  $\text{Ca}^{2+} < 0.06$  wt%; CMC of bile extract  $0.07 \pm 0.04$  mM; the mole ratio of BS to PC being around 15 to 1. Type II lipase contains amylase and protease, as well as lipases. Lipase activity is 100–400 units/mg protein (using olive oil) and 30–90 units/mg protein (using triacetin) for 30 minutes incubation. Calcium chloride ( $\text{CaCl}_2 \cdot 2\text{H}_2\text{O}$ ) was obtained from Sigma-Aldrich (St. Louis, MO).

#### **4.2.2. Solution preparation**

Emulsions were prepared from an aqueous and an organic phase. The aqueous phase corresponded to emulsifier solutions prepared by stirring for at least 2 hours 1.0 wt% of Tween 20 into 5 mM phosphate buffer solution (pH 7.0) containing 0.02 wt% sodium azide. The dispersions were kept overnight at 4°C to ensure complete hydration. Organic phases consisting of corn oil and hexane with different ratios (100:0, 90:10, 75:25, 50:50, 25:75, 10:90, 5:95 w/w) were prepared using a magnetic stirrer during 60 min at room temperature. Bile extract (4.5% w/w) and  $\text{CaCl}_2$  (9.9% w/w) solutions in 5 mM phosphate buffer (pH 7) were prepared by stirring for 1 h at room temperature.

### 4.2.3. Nanoemulsion preparation

Initial emulsions were made by mixing 10% organic phase with 90% aqueous phase. For the organic phase, different corn oil/hexane ratios were used, while the aqueous phase consisted of an emulsifier solution containing 1.0 wt% Tween 20. O/W emulsions were prepared using a two-step homogenization process. First, a coarse O/W emulsion was prepared by homogenizing the organic and aqueous phases with a high-speed blender for 2 min (M133/1281-0, Biospec Products, Inc., ESGC, Switzerland). Then the coarse emulsions were immediately passed 5 times through a high-pressure homogenizer (Microfluidics M-110Y, F20Y 75  $\mu\text{m}$  interaction chamber, Newton, MA) at 15,000 psi to produce fine emulsions. The mean particle size of the microfluidized emulsion decreased upon recirculation; however, this effect diminished with the number of passes and became negligible after five passes. To avoid hexane evaporation during high-pressure homogenization, the homogenization chamber was cooled by ice. After the fine O/W emulsions were obtained, the hexane was evaporated using a rotary evaporator (Büchi Rotavapor, RE111, Switzerland) at 55°C under reduced pressure. The evaporation system included a water bath (Büchi, 461, Switzerland) and a vacuum pump (Fisher Scientific, Maxima Dry PU 1319, Pittsburgh, PA). Different evaporation times were used according to the hexane amount in the samples that were previously determined by carrying out mass balances during preliminary runs. Initially, a preliminary experiment was carried out to confirm that all of the organic solvent (hexane) was removed from the nanoemulsions after evaporation (Table 4.1). The amount of hexane removed from the samples was in close agreement to the total amount of hexane originally present, which indicated that all of the hexane was removed by evaporation. However, it is important to highlight that some of the water may have been removed from the samples during the evaporation process. A schematic illustration of the methodology used to prepare the nanoemulsions is shown in Figure 4.1.

Table 4.1. Percentage of error between the expected final mass (without hexane) of nanoemulsions obtained using mass balances and its experimental value.

Oil in organic phase (%)	Error (%) *
100	-
90	0.12
75	0.15
50	0.35
25	0.08
10	0.05
5	0.32

\* Value defined as the ratio of the difference between the estimated and experimental values and the estimated value obtained by a mass balance of hexane.

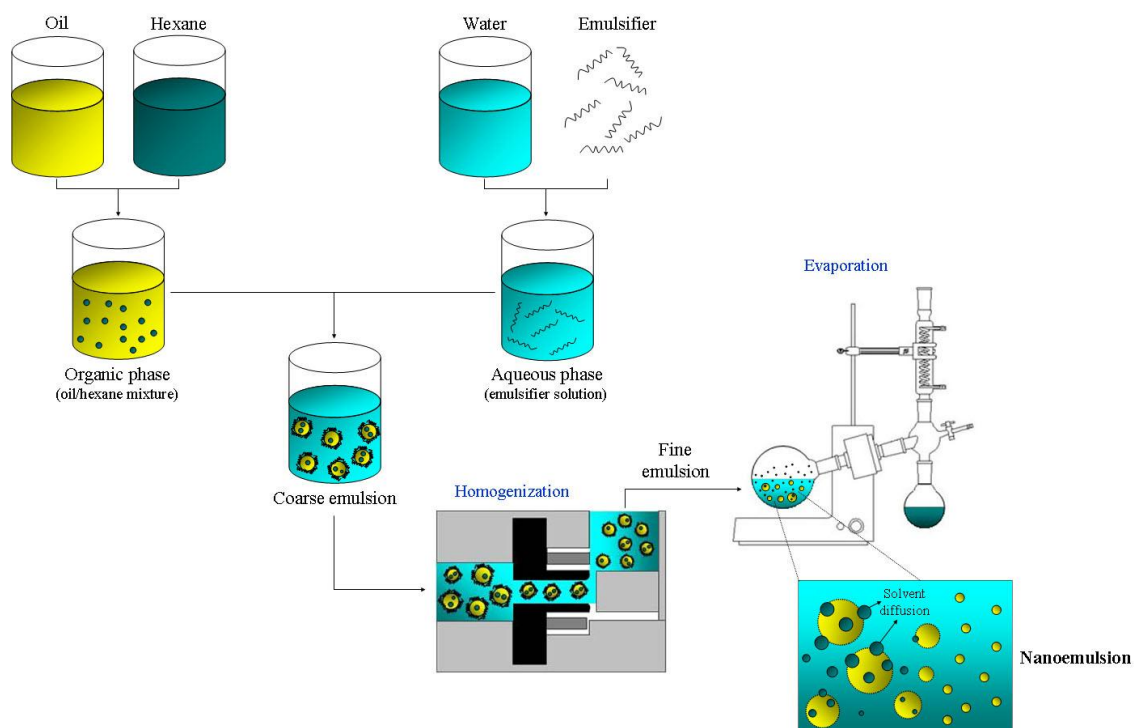


Figure 4.1. Schematic representation of the nanoemulsion preparation using high-pressure homogenization and solvent evaporation stages.

#### **4.2.4. Characterization of nanoemulsions properties**

##### **4.2.4.1. Particle size measurements**

The influence of the initial hexane content in the organic phase on particle size distribution, mean particle size, and polydispersity index (PDI) was determined using a dynamic laser light scattering instrument (Nano-ZS, Malvern Instruments, Worcestershire, UK) equipped with a 4mW helium/neon laser (wavelength 633 nm). To avoid multiple scattering effects, the emulsion samples were diluted with 5 mM phosphate buffer (pH 7) at a ratio 1:500 (v/v) and then placed in a measurement cell that was loaded into the instrument. Samples were equilibrated for 1 min inside the instrument before dynamic light backscattering (detection angle =  $173^\circ$ ) data were collected. The Z-average particle diameter was calculated by the instrument using the Stokes-Einstein equation, assuming that the nanoemulsion droplets were spherical. The PDI was  $\leq 0.1$ , which indicated that the nanoemulsions had a narrow particle size distribution (Anton et al., 2007). The measurements were done at least in triplicate. It was assumed that the refractive index of the disperse phase was that of corn oil ( $n = 1.47$ ). This may have caused errors in the reported particle sizes for samples containing appreciable amounts of hexane measured before solvent evaporation since hexane has a lower refractive index ( $n = 1.37$ ) than corn oil.

##### **4.2.4.2. Particle electrical charge measurements**

Particle electrical charge ( $\zeta$ -potential) in the nanoemulsions was determined using particle electrophoresis (Nano-ZS, Malvern Instruments, Worcestershire, UK). Samples were diluted (if necessary) with 5 mM phosphate buffer (pH 7) to avoid multiple scattering and then equilibrated for 1 min inside the instrument. The  $\zeta$ -potential of the particles was calculated by the instrument using the Smoluchowski model through electrophoretic mobility measurements.

#### **4.2.4.3. Appearance of nanoemulsions**

The appearance of nanoemulsions was evaluated using a laser-profiling instrument (Turbiscan Classic MA 2000, Formulacion, Wynnewood, PA). An emulsion sample was transferred to a cylindrical glass cell (internal diameter: 15 mm; height: 150 mm), and then carefully mixed to ensure that it remained homogeneous without introducing air bubbles. The sample was analyzed by a light beam emitted in the near infrared wavelength (850 nm) that scanned the sample cell from the bottom to the top. Two synchronous optical sensors received the light transmitted through the sample and the light backscattered by the sample, respectively. By scanning the sample at preset height intervals, a pattern of the light flux as a function of the sample height was obtained. The sample in the cell was scanned every 400  $\mu\text{m}$  at room temperature while moving along the entire height of the cell (65 mm), and transmission and backscattering profiles as a function of sample height were collected and analyzed using a software program (Turbisoft version 1.21). To quantify differences in the appearance among samples, the area under the backscattering curve (AUCbs) was calculated by integration using the trapezoidal rule included as a tool in mathematical software (SigmaPlot 10.0, Systat Software, San Jose, CA). The general appearance of the samples was also recorded using a digital camera (PowerShot SD 1000, Canon, USA).

#### **4.2.4.4. Microscopic analysis**

The microstructure of the nanoemulsions was observed by transmission electron microscopy (TEM). A drop of nanoemulsion diluted by a factor of 200 was deposited onto a carbon support film on a copper grid. Excess sample was removed using filter paper. After drying the sample at room temperature for 5 min, micrographs were taken by a transmission electron microscope (Philips Tecnai 12 Bio Twin, Eindhoven, The Netherlands) operating at 80 kV. Images were registered on Kodak film SO163 and the negative scanned (Canon, Canoscan 9950F) at a resolution of 300 dpi.

#### 4.2.5. *In vitro* digestion model

*In vitro* digestion behavior of O/W nanoemulsions stabilized by Tween 20 was determined by measuring the rate of lipid hydrolysis occurring under simulated intestinal fluid conditions using the pH-Stat method. To evaluate only the effect of the oil droplet size on *in vitro* digestion, nanoemulsions were diluted with different emulsifier solutions to obtain samples with the same oil/emulsifier ratio and oil concentration as those obtained for emulsions with the lowest oil-to-emulsifier ratio and oil concentration after hexane evaporation (~0.56 corn oil-to-emulsifier ratio and 0.55 wt% corn oil), corresponding to the emulsions with 95 wt% of hexane in the initial organic phase. The basic procedure to carry out the *in vitro* digestion was: (i) 30 ml of sample were placed in a glass beaker and incubated in a water bath at 37°C for 10 min and then the system was adjusted to pH 7 using HCl or NaOH solutions; (ii) 4.0 mL of bile extract solution and 1.0 mL of CaCl<sub>2</sub> solution were added into the sample under continuous stirring and the system was adjusted back to pH 7 if required; (iii) 2.5 mL of freshly prepared lipase suspension (60 mg of lipase powder dispersed in phosphate buffer pH 7, 37 °C) was added to the above mixture; (iv) immediately after, the pH of the mixture under digestion was monitored by a pH-Stat automatic titration unit (835 Titrando, Metrohm, Riverview, FL) and maintained at pH 7.0 by titrating the FFA hydrolyzed with an appropriate volume of 0.28 M NaOH solution at 2 min intervals for the whole period of incubation (60 min). The volume of NaOH solution added to the digested mixture was recorded and used to calculate the concentration of FFA generated by lipolysis. Since each TAG molecule generates two FFA molecules when fully digested, it is possible to calculate the fraction of FFA released from the sample during digestion as the total amount of TAG originally present in the sample is known. Finally, the percentage of FFA released can be calculated as follows (Li and McClements, 2010):

$$\% FFA = \left( \frac{V_{NaOH}(t) \cdot M_{NaOH} \cdot MW_{TAG}}{m_{TAG} \cdot 2} \right) \times 100 \% \quad (4.1)$$

where  $V_{NaOH}(t)$  is the volume of NaOH solution required to neutralize the FFA generated at digestion time  $t$  (L),  $M_{NaOH}$  is the molarity of the NaOH solution used to

titrate the sample ( $\text{mol L}^{-1}$ ),  $MW_{TAG}$  is the molecular weight of the triacylglycerol oil ( $\text{g mol}^{-1}$ ), and  $m_{TAG}$  is the total mass of triacylglycerol oil initially present in the digestion cell (g). Blanks were carried out in the absence of oil in the samples and subtracted from the reported values.

It should be noted that we did not include a mouth or stomach stage to our *in vitro* digestion model and that passage of nanoemulsions through these regions of the GIT could influence the composition, size, and interfacial characteristics of lipid droplets. In future studies it would be useful to use a more sophisticated *in vitro* digestion model to examine the effects of these additional digestive stages on nanoemulsion performance.

#### **4.2.6. Statistical analysis**

All experiments were carried out in triplicate using freshly prepared samples. The results were then reported as averages and standard deviations of these measurements. Analysis of variance was carried out when required using Statgraphic Statistical Package (Statistical Graphics Corporation, version 4.0, Rockville, USA), including multiple range tests ( $p > 0.05$ ) for separation of least square means.

### **4.3. Results and discussion**

The purpose of our study was to fabricate O/W nanoemulsions by a combination of high-pressure homogenization and solvent displacement, analyzing the influence of disperse phase composition on the physicochemical properties and *in vitro* digestion of Tween 20-stabilized O/W nanoemulsions. This information is essential for determining the design and production of edible delivery systems based on nanoemulsions and the control of lipid digestion.

#### **4.3.1. Effect of disperse phase composition and solvent evaporation on particle size**

The influence of the initial organic phase composition on the mean particle diameter of the nanoemulsions was evaluated by dynamic light scattering (Figure 4.2). The size of

the oil droplets decreased with increasing hexane content, both before and after hexane removal from the emulsions. In the absence of hexane, the mean particle diameter was ~ 170 nm after homogenization, and the evaporation step had little impact on this size, which would be expected since there would be no droplet shrinkage due to hexane removal. The decrease in particle size with increasing hexane levels observed after homogenization (but before evaporation) can be attributed to the influence of hexane on the bulk physicochemical properties of the dispersed phase. Hexane will decrease the viscosity of the dispersed phase, which will facilitate the formation of small droplets during homogenization (see next section). The decrease in particle size with increasing hexane content after evaporation can be attributed to droplet shrinkage due to removal of hexane from the dispersed phase.

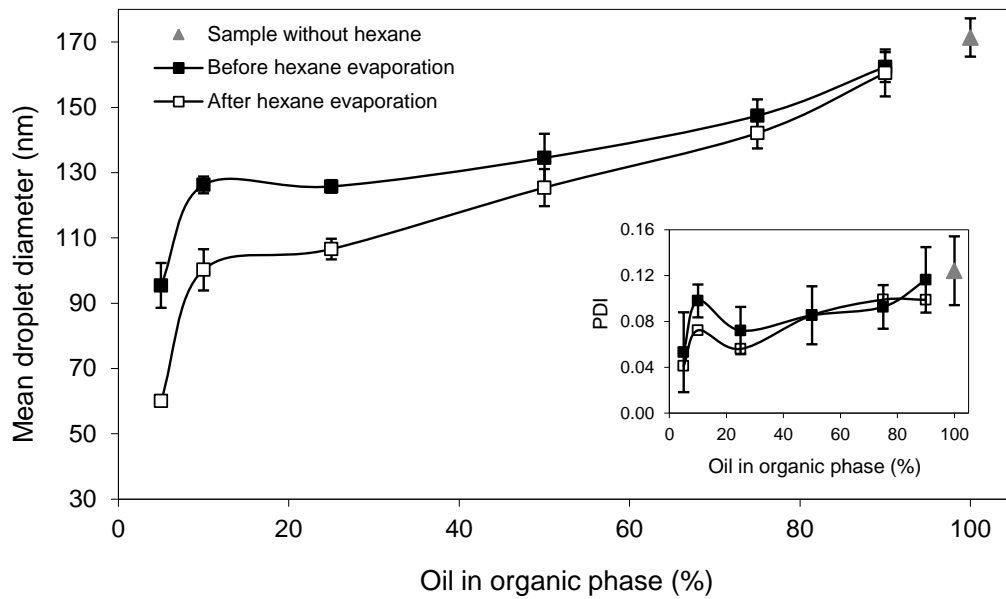


Figure 4.2. Dependence of the oil content in the initial organic phase of emulsions on mean droplet diameter and PDI of oil droplets. The concentration of hexane in the organic phase was 100% - % oil.

Decreasing the corn oil:hexane ratio in the initial organic phase from 100:0 to 5:95 w/w produced a reduction in the mean particle diameter by around 44% after homogenization

and 64% after evaporation (Figure 4.2). For the maximum hexane content used (95% w/w hexane, 5% w/w corn oil in the dispersed phase), the mean droplet diameters were around 96 and 60 nm before and after hexane evaporation, respectively. For all conditions studied, the particle size distributions of the nanoemulsions were monomodal, but the width of the distributions decreased with increasing hexane content and with evaporation (Figure 4.3).

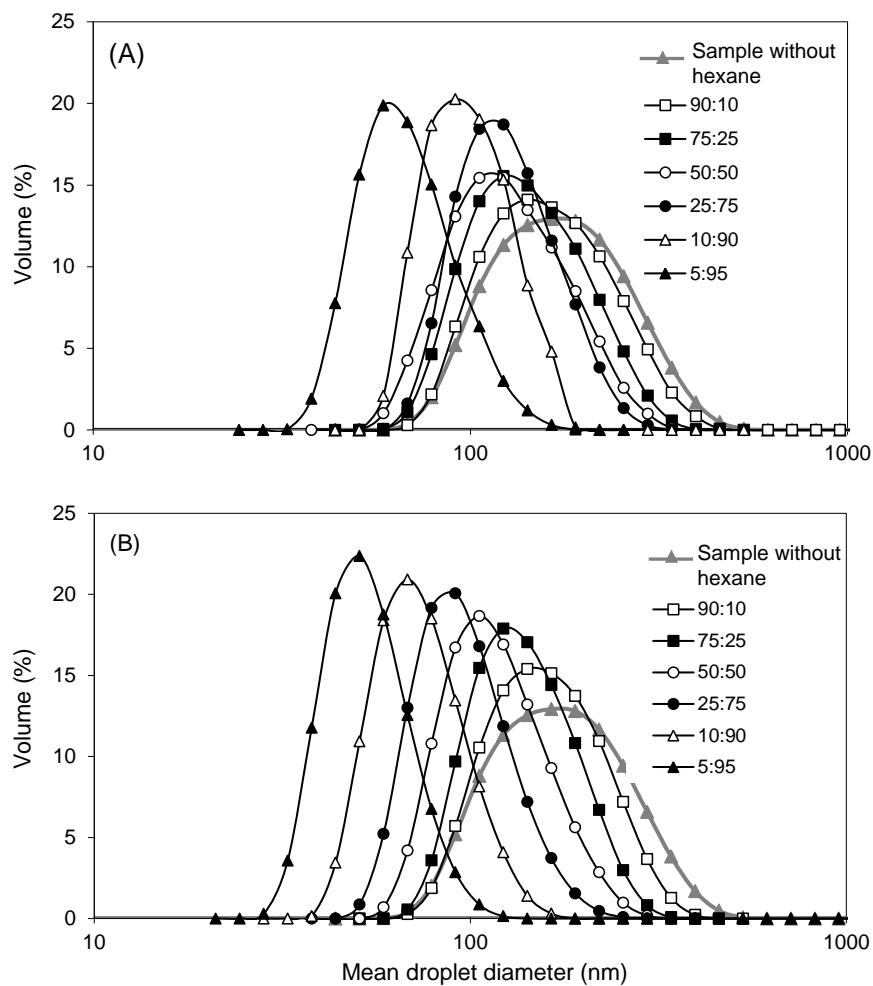


Figure 4.3. Particle size distributions of nanoemulsions containing different corn oil/hexane ratios in the initial dispersed phase. (A) Before hexane evaporation, and (B) after hexane evaporation.

The quality of a colloidal dispersion can be quantified in terms of its PDI. The nanoemulsions had PDI ranging from 0.04 to 0.12, which indicates a good monodispersity of the samples (insert in Figure 4.2). Representative TEM images of the Tween 20-stabilized O/W nanoemulsions are shown in Figure 4.4. Figure 4.4(A) shows oil droplets in a nanoemulsion without hexane in the initial dispersed phase, while Figure 4.4(B) presents oil droplets in a nanoemulsion originally containing a corn oil:hexane ratio of 5:95 w/w after hexane evaporation. The TEM images clearly show that most of the oil droplets had a spherical morphology, and that there was an appreciable decrease in particle size after hexane evaporation. These results confirm the important role of the organic phase composition, on both favoring the formation of nanoemulsions and improving the quality of the dispersion.

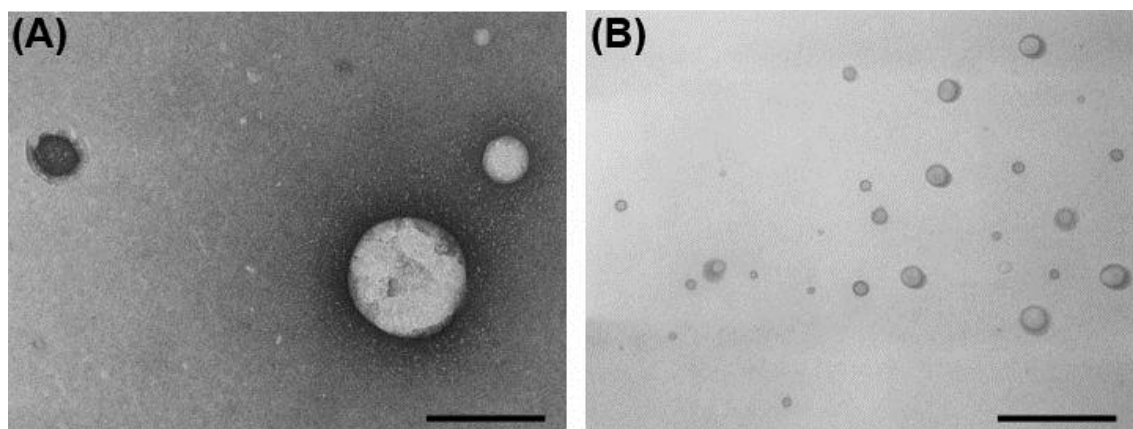


Figure 4.4. TEM micrographs of Tween 20-stabilized nanoemulsions. (A) nanoemulsion without hexane in initial the organic phase, (B) nanoemulsion obtained after hexane evaporation, initially containing 95 wt% hexane in the organic phase. Bars correspond to 200 nm.

#### **4.3.2. Interpretation of droplet size changes induced by the emulsification process and physicochemical properties of the phases**

The results presented in the previous section indicate that the mean particle size produced by the homogenization/solvent removal method depend on two factors: (i) the size of the droplets produced by the homogenizer; (ii) the reduction in droplet size due to

solvent removal. Within the homogenizer, the large oil droplets present in the emulsion pre-mix are broken down to smaller ones due to turbulent, cavitation and shear stresses in the homogenizer (Walstra, 2003). Under these conditions, the Tween 20 molecules rapidly adsorb to the surfaces of the newly formed small droplets and prevent them from coalescing (Jafari et al., 2008). After homogenization, droplet size reduction was induced by removal of the organic solvent through evaporation, which depends on the fraction of solvent within the dispersed phase. The volume of a spherical particle is proportional to the radius cubed ( $V \propto r^3$ ), hence halving the particle radius requires a  $1/8^{\text{th}}$  reduction in the particle volume.

The efficiency of oil droplet disruption during homogenization may vary considerably according to the processing conditions (e.g., temperature, pressure and number of passes), composition of organic and aqueous phases (e.g., organic phase, aqueous phase, and emulsifier ratios), emulsifier properties (e.g., adsorption kinetics, interfacial tension depression, and stabilizing properties), and the physicochemical properties of the different phases (e.g., viscosity and interfacial tension) (Lee and McClements, 2010). In the present study, the homogenization conditions, emulsifier type and concentration, and the total water content were kept constant. However, the ratio of corn oil-to-hexane in the initial disperse phase was varied, thus altering the physicochemical properties of the dispersed phase. The composition of the organic phase affects droplet disruption within a high-pressure homogenizer, and smaller droplet sizes are to be expected by decreasing the disperse phase viscosity and/or lowering the interfacial tension (Walstra, 1993; Wooster et al., 2008). For example, droplets in nanoemulsions made with high viscosity oils, such as those with long chain triglycerides (e.g. corn oil), were considerably larger (mean diameter = 120 nm) than those prepared with low viscosity liquids such as hexadecane (mean diameter = 80 nm), using the same emulsifier (Wooster et al., 2008). Also, flavor oils tend to have much lower viscosities than triglyceride oils, making them good candidates for nanoemulsion formation (Jafari et al., 2006). Since the viscosity of corn oil (52.3 mPa s) (Saravacos and Maroulis, 2001) at ambient temperature is considerably higher than that of hexane (~ 0.30 mPa s) (Poling et al., 2008), the

viscosity of the dispersed phase decreases with increasing hexane concentration, which in turn decreases the dispersed-to-continuous phase viscosity ratio ( $\eta_D/\eta_C$ ). A lower  $\eta_D/\eta_C$  is known to facilitate droplet break-up within a high-pressure homogenizer (Wooster et al., 2008).

On the other hand, the interfacial tension at ambient temperature has been reported to be  $\sim 31.5 \text{ mN m}^{-1}$  for a corn oil/water interface (Chaiyasit et al., 2008) and  $\sim 50.5 \text{ mN m}^{-1}$  for a hexane/water interface (Aratono et al., 1982; Liggieri et al., 1995). Hence, the interfacial tension between the dispersed and continuous phases would be expected to increase as the hexane content in the organic phase increased. The formation of small droplets during homogenization would therefore be expected to get harder with increasing hexane content due to this effect, since droplet disruption would be less favourable due to the increase in Laplace pressure (McClements, 2005). Experimentally, we actually observed a decrease in mean droplet size with increasing hexane content after homogenization (Figure 4.2), which suggests that the impact of hexane on the viscosity ratio was more important than its impact on the interfacial tension. This would be expected since the difference in the viscosities of the oil and organic solvent is much greater than the difference in their interfacial tensions. In addition, when the oil-water interface is saturated with Tween 20 the interfacial tensions have been reported to be  $\sim 5 \text{ mN m}^{-1}$  for both the corn oil/water interface (Vladisavljević et al., 2006) and hexane/water interface (Wang et al., 2009), which would mean that the effect of oil type on interfacial tension is less important during homogenization.

Another important factor in determining the size of the droplets produced by homogenization is the type and amount of emulsifier used. In this study, we used a small molecule non-ionic surfactant (Tween 20), which is known to adsorb rapidly to oil-water interfaces during homogenization (Mao et al., 2009; Qian and McClements, 2011). Nevertheless, it is also important to have sufficient emulsifier present to entirely cover the surfaces of the droplets formed during homogenization. The minimum oil droplet radius that can be produced during homogenization is governed by the type and concentration of emulsifier present (McClements, 2005):

$$r_{min} = \frac{3 \cdot \Gamma \cdot \varphi}{c_s} = \frac{3 \cdot \Gamma \cdot \varphi}{c'_s (1 - \varphi)} \quad (4.2)$$

where  $\Gamma$  is the surface load of the emulsifier at saturation ( $\text{kg m}^{-2}$ ),  $\varphi$  is the disperse phase volume fraction (dimensionless),  $c_s$  is the concentration of emulsifier in the emulsion ( $\text{kg m}^{-3}$ ), and  $c'_s$  is the concentration of emulsifier in the continuous phase ( $\text{kg m}^{-3}$ ). In this work, the emulsions contained 1 wt% of emulsifier in the continuous phase ( $c'_s = 10 \text{ kg m}^{-3}$ ) and had  $\varphi$  values of 0.1 during homogenization. If we assume that  $\Gamma$  is  $\sim 1.5 \times 10^{-6} \text{ kg m}^{-2}$ , value reported for Tween 20 adsorbed to water-hydrophobic interfaces (Tcholakova et al., 2003), the minimum oil droplet radius that could theoretically have been reached is  $\sim 51 \text{ nm}$  (*diameter* = 102 nm). Our experimental measurements were close to this value for the system containing high hexane contents (*diameter* = 96 nm at 95% hexane), but were appreciably higher in the absence of hexane (*diameter* = 170 nm). These results suggest that the homogenizer was incapable of generating sufficiently intense disruptive forces at the pressure used for the more viscous corn oil (Qian and McClements, 2011).

#### 4.3.3. The appearance of nanoemulsions

The optical properties of nanoemulsions are one of their most important functional characteristics. As expected, the appearance of the nanoemulsions changed when the mean droplet size decreased (Figure 4.5). The nanoemulsions were more turbid or opaque prior to hexane evaporation, which can be attributed to their larger particle sizes. After evaporation, the nanoemulsions became more translucent and bluish in appearance as the initial hexane content increased, which can be attributed to the decrease in mean particle size due to greater droplet shrinkage after evaporation. The effect of particle size on the optical properties of the nanoemulsions was quantified by plotting the area under the curve ( $\text{AUC}_{bs}$ ) for backscattered light using an optical profiling method (Figure 4.6). The overall extent of light scattering decreased after evaporation due to droplet shrinkage caused by hexane removal (with the exception of the nanoemulsion containing no hexane), and decreased with increasing hexane concentration in the disperse phase.

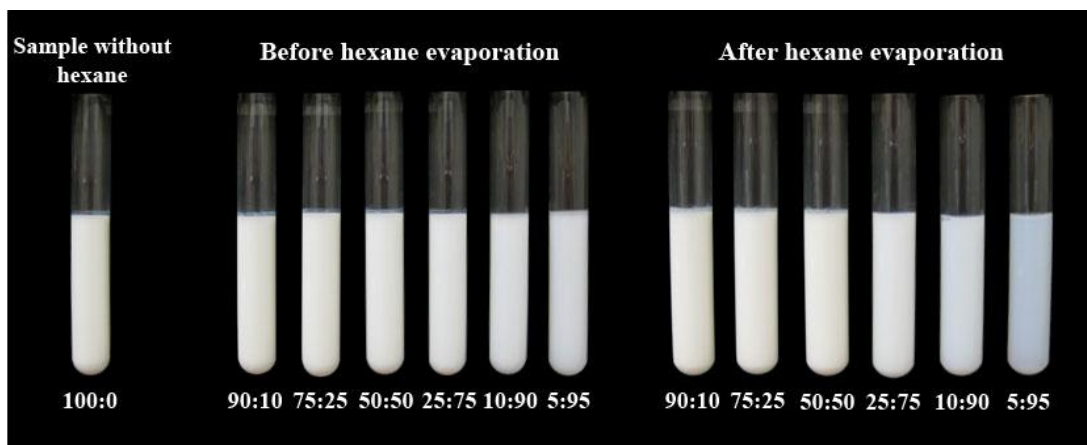


Figure 4.5. Photographs of nanoemulsions containing different corn oil/hexane ratios in the initial dispersed phase.

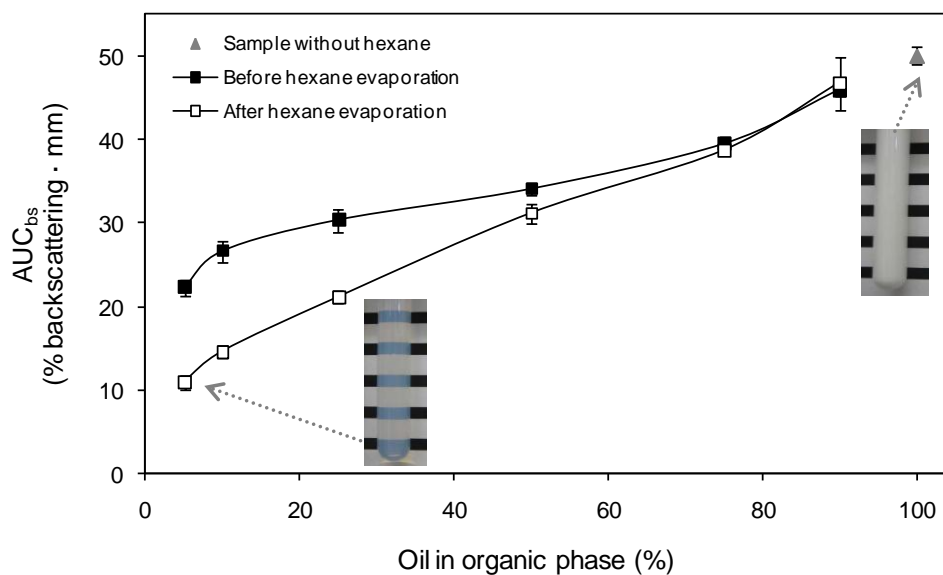


Figure 4.6. Effect of the initial oil concentration in the organic phase of nanoemulsions on the area under the backscattering curve.

#### 4.3.4. The electrical charge on oil droplets surface in the nanoemulsions

The electrical potential at the surface of oil droplets obtained after hexane evaporation is shown in Figure 4.7. The  $\zeta$ -potential decreased from -5 to -20 mV when the corn

oil:hexane ratio in the initial disperse phase increased from 5:95 to 100:0 w/w. The fact that droplets stabilized by Tween 20 had a net negative charge is well established in the literature and has been attributed to the ability of oil-water interfaces to preferentially adsorb  $\text{OH}^-$  species from water or due to the presence of anionic impurities in the oil or surfactant phases (such as free fatty acids) (McClements, 2005). The fact that the  $\zeta$ -potential of the droplets depended on initial dispersed phase composition suggests that droplet charge may be influenced by particle size and/or oil properties. The influence of particle size on droplet charge was recently reported for WPI-stabilized emulsions, where systems with mean particle diameters of 66 nm and 326 nm had  $\zeta$ -potentials of -31 mV and -62 mV, respectively (Lee et al., 2011). In principle, the  $\zeta$ -potential should be independent of particle size (Hiemenz and Rajagopalan, 1997), nevertheless there are a number of physicochemical mechanisms that might explain the observed dependence. First, the Von Smoluchowski theory is used to determine the  $\zeta$ -potential of oil droplets from their electrophoretic potential. This theory assumes that the particle radius  $r$  is much larger than the Debye screening length  $k^{-1}$  (i.e.  $k^{-1} \ll r$ ) (Tadros, 2005). This condition holds for the oil droplets with large particle sizes ( $r \sim 85$  nm, *diameter*  $\sim 170$  nm) but not for those with small particle size ( $r \sim 30$  nm, *diameter*  $\sim 60$  nm). Thus, although the measurement of particle mobility is fairly straightforward, interpretation of the results is not always simple. Second, the ionic strength of the continuous phase surrounding the oil droplets may differ among the samples studied. When the hexane is evaporated from the samples, the surfactant concentration increases, and so more electrical charges are present in the continuous phase of the emulsions. Alternatively, some impurities (such as fatty acids) from the different oils used to prepare the disperse phase could have affected the electrical charge on the oil droplets.

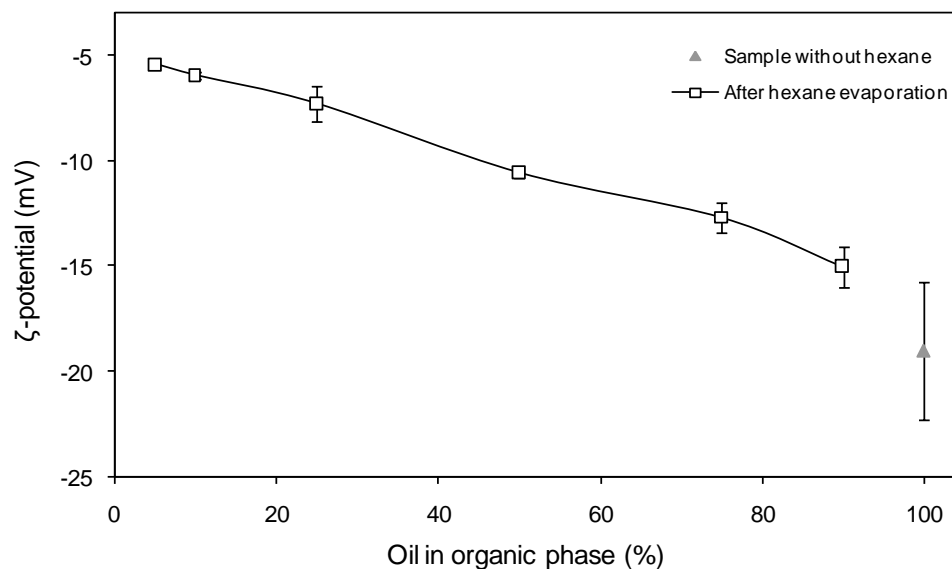


Figure 4.7. Influence of the oil content in the initial organic phase on  $\zeta$ -potential of nanoemulsions without hexane and those obtained after hexane evaporation.

#### 4.3.5. *In vitro* digestibility of nanoemulsions

Finally, we examined the *in vitro* digestibility of the nanoemulsions by lipase to obtain a better understanding of their potential behavior under gastrointestinal conditions. The particle size distribution of nanoemulsions may be an important parameter in determining their behavior because the activity of lipolytic enzymes is highly dependent on the properties of the substrate-water interface. Lipid digestion is an interfacial phenomenon that involves adsorption of lipase molecules to lipid droplet surfaces so that the enzyme can come into close proximity with its substrate (triacylglycerols) (McClements and Li, 2010). Previous studies suggest that the specific interfacial area ( $\text{m}^2/\text{g}$ ) of an emulsion, which increases when the particle size decreases, governs the activity of lipases on emulsified triacylglycerols (Armand et al., 1992; Armand et al., 1999; Golding et al., 2011).

The effect of oil droplet size on the *in vitro* digestibility under simulated small intestinal conditions monitored using pH-Stat titration is shown in Figure 4.8. In general, the FFA-digestion time profiles could be divided into three regions: (i) a *lag period* in which no

FFAs were observed; (ii) a *digestion period* in which the FFAs increased rapidly with time; (iii) a *plateau period* in which the FFAs released remained relatively constant. The length of the lag period, the rate of FFAs formation in the digestion period, and the final amount of FFA produced in the plateau period depended on the initial composition of the dispersed phase of the nanoemulsions (Table 4.2).

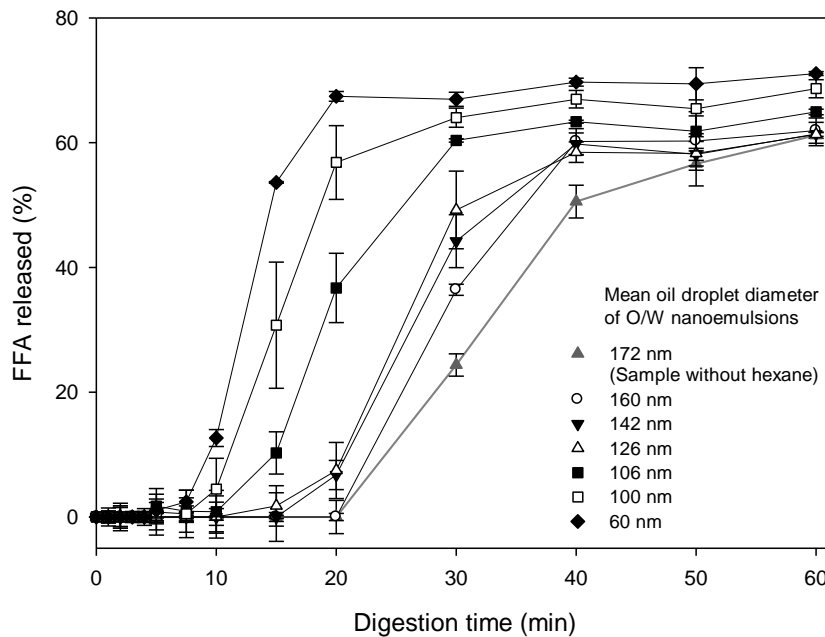


Figure 4.8. Free fatty acids released from corn oil-in-water nanoemulsions stabilized by Tween 20 as a function of digestion time. The nanoemulsions digested were those obtained after hexane evaporation and the samples without hexane.

Table 4.2. Summary of the digestion data for nanoemulsions with different initial compositions and particle sizes.

Oil in the initial dispersed phase (%)	Mean particle diameter (nm)	Lag time (min)	Digestion rate (FFA% min <sup>-1</sup> )	Final extent (FFA released %)
100	172	22.52	1.96	61.20
90	160	18.41	2.05	61.94
75	142	13.23	2.65	61.40
50	126	12.43	3.31	61.33
25	106	4.68	3.20	64.94
10	100	4.39	5.24	68.65
5	60	4.09	7.02	71.09

The duration of the lag-period increased from around 5 to 20 min as the mean droplet diameter increased from around 60 to 172 nm. The presence of a lag-period has also been reported for Tween 20-stabilized emulsions during their *in vitro* digestion by pancreatic lipase in the presence of bile extract (Mun et al., 2007). These findings could be explained by the time taken for surface-active components from the bile extract to displace the small-molecule surfactant from the surface of the oil droplet and thereby facilitate lipase adsorption and activity. Small molecule surfactants are more surface-active than lipase, so that the interfacial layer of Tween 20 may delay the contact of the enzyme with the emulsified lipids (Reis et al., 2009). As the droplet size decreases, the interfacial area increases, and therefore there will be less free Tween 20 present in the aqueous phase to compete with bile salt or lipase adsorption. We do not anticipate that Tween 20 directly interfered with lipase activity since previous studies have demonstrated that similar surfactants do not cause irreversible denaturation of pancreatic lipase (Gargouri et al., 1983).

The rate of FFA released per unit time ( $\text{FFA}\% \text{ min}^{-1}$ ) in the digestion period increased with decreasing oil droplet diameter (Table 4.2), which would be expected because nanoemulsions with smaller oil droplets have larger specific surface areas (i.e., higher surface area-to-volume ratios). A number of workers have reported similar results for lipid digestion (Armand et al., 1992; Armand et al., 1999; Pafumi et al., 2002). Recently, the effect of lipid droplet diameter (196 nm vs. 14,700 nm) on the pH-Stat digestion profiles of medium-chain triglyceride oil-in-water emulsions stabilized by  $\beta$ -lactoglobulin was examined. It was found that the rate of FFA released per unit time increased as the lipid droplet diameter decreased (Li and McClements, 2010). On the other hand, the rate and extent of FFA production from WPI-stabilized nanoemulsions (*diameter* = 66 nm) produced using the homogenization/solvent displacement method was found to be less than WPI-stabilized conventional emulsions (*diameter* = 326 nm), which was attributed to changes in interfacial structure and composition during the evaporation process (Lee and McClements, 2010).

At the end of the digestion period, the total amount of FFAs released increased with decreasing mean particle diameter (Table 4.2). The total FFAs released increased from about 61% to 71% as the oil droplets diameter decreased from around 172 nm to 60 nm. The reason that a fairly constant value in the amount of FFAs released from the emulsions after a certain time was reached, may be due to the inhibition of lipase activity by the progressive release of protonated FFAs that might accumulate at the lipid droplet surface (Borel et al., 1994; Golding et al., 2011). Fatty acids are surface active molecules that will tend to adsorb onto the surface of the oil droplets and, at a sufficiently high concentration, they could displace lipase from the oil-water interface, thereby preventing it from coming into close contact with the emulsified lipids. Thus, lipolysis of triacylglycerols generates products that can probably compete with the enzyme for the interface and/or modify the protein via molecular interactions (Reis et al., 2009). Both of these potential mechanisms can have an impact on lipase catalysis. In addition, the nanoemulsions with the smallest droplet sizes will have the largest specific surface areas, and so it is possible for more FFAs to accumulate at the oil-water interface before the reaction is inhibited.

These results suggest that the digestibility of emulsified lipids may be controlled by manipulating the particle size of nanoemulsions. An increased understanding of the behavior of nanoemulsion-based delivery systems under gastrointestinal conditions would allow the food industry to design healthier foods and the pharmaceutical industry to create more effective drugs. Nevertheless, one must be careful in extrapolating results from a simple *in vitro* digestion model to complex real-life situations. For instance, the *in vitro* digestion model is a closed system where competitive adsorption between surface active substances and lipase may occur. In reality, some of the fatty acids and surfactants may be adsorbed by the human body and therefore their effects of lipid digestion through competitive adsorption may be less pronounced.

#### 4.4. Conclusions

A combination of high-pressure homogenization and a solvent displacement technique led to the formation of emulsions with oil droplets in the nanometer range (*diameter* < 200 nm). By varying the solvent (hexane) content in the dispersed phase of the initial emulsion and its subsequent removal, oil droplets with diameters from 60 to 170 nm with a low polydispersity were fabricated. Nanoemulsions containing droplets of small sizes appear to be translucent and a bit bluish. The lipid digestion profile depended strongly on the particle size of the nanoemulsions. As the lipid droplet size was decreased, the lag time was decreased, the digestion rate was increased, and the total amount of free fatty acids released was increased. Controlling the composition of the initial dispersed phase and type of homogenization procedure used appear to be key parameters in the formation, appearance, microstructure, and digestibility of nanoemulsions. These results have important implications for the design and production of edible delivery systems based on nanoemulsions and the control of lipid digestion. Nevertheless, there is clearly a need for further research to establish the key physicochemical factors (e.g., interfacial properties) that impact the performance of nanoemulsion-based delivery systems under gastrointestinal conditions.

#### References

- Acosta, E. (2009). Bioavailability of nanoparticles in nutrient and nutraceutical delivery. *Current Opinion in Colloid & Interface Science*, 14(1), 3-15.
- Anton, N., Gayet, P., Benoit, J. P., and Saulnier, P. (2007). Nano-emulsions and nanocapsules by the PIT method: An investigation on the role of the temperature cycling on the emulsion phase inversion. *International Journal of Pharmaceutics*, 344(1-2), 44-52.
- Anton, N., Benoit, J. -P., and Saulnier, P. (2008). Design and production of nanoparticles formulated from nano-emulsion templates - A review. *Journal of Controlled Release*, 128(3), 185-199.

Aratono, M., Yamanaka, M., Motomura, K., and Matuura, R. (1982). Adsorption of dioctyldimethylammonium chloride at water/hexane interface. *Colloid & Polymer Science*, 260(6), 632-637.

Armand, M., Borel, P., Ythier, P., Dutot, G., Melin, C., Senft, M., Lafont, H., and Lairon, D. (1992). Effects of droplet size, triacylglycerol composition, and calcium on the hydrolysis of complex emulsions by pancreatic lipase: An in vitro study. *The Journal of Nutritional Biochemistry*, 3(7), 333-341.

Armand, M., Pasquier, B., André, M., Borel, P., Senft, M., Peyrot, J., Salducci, J., Portugal, H., Jaussan, V., and Lairon, D. (1999). Digestion and absorption of 2 fat emulsions with different droplet sizes in the human digestive tract. *American Journal of Clinical Nutrition*, 70, 1096-1106.

Borel, P., Armand, M., Ythier, P., Dutot, G., Melin, C., Senft, M., Lafont, H., and Lairon, D. (1994). Hydrolysis of emulsions with different triglycerides and droplet sizes by gastric lipase in vitro. Effect on pancreatic lipase activity. *Journal of Nutritional Biochemistry*, 5(3), 124-133.

Chaiyasit, W., McClements, D. J., Weiss, J., and Decker, E.A. (2008). Impact of surface-active compounds on physicochemical and oxidative properties of edible oil. *Journal of Agricultural and Food Chemistry*, 56(2), 550-556.

Chu, B. S., Ichikawa, S., Kanafusa, S., and Nakajima, M. (2007a). Preparation and characterization of  $\beta$ -carotene nanodispersions prepared by solvent displacement technique. *Journal of Agricultural and Food Chemistry*, 55(16), 6754-6760.

Chu, B. S., Ichikawa, S., Kanafusa, S., and Nakajima, M. (2007b). Preparation of protein-stabilized  $\beta$ -carotene nanodispersions by emulsification-evaporation method. *Journal of the American Oil Chemists' Society*, 84(11), 1053-1062.

Gargouri, Y., Julien, R., Bois, A. G., Verger, R., and Sarda, L. (1983). Studies on the detergent inhibition of pancreatic lipase activity. *Journal of Lipid Research*, 24(10), 1336-1342.

Golding, M., and Wooster, T. J. (2010). The influence of emulsion structure and stability on lipid digestion. *Current Opinion in Colloid & Interface Science*, 15(1-2), 90-101.

Golding, M., Wooster, T. J., Day, L., Xu, M., Lundin, L., Keogh, J., and Clifton, P. (2011). Impact of gastric structuring on the lipolysis of emulsified lipids. *Soft Matter*, 7, 3513-3523.

Gutiérrez, J. M., González, C., Maestro, A., Solè, I., Pey, C. M., and Nolla, J. (2008). Nano-emulsions: New applications and optimization of their preparation. *Current Opinion in Colloid & Interface Science*, 13(4), 245-251.

Hiemenz, P. C., and Rajagopalan, R. (1997). *Principles of Colloid and Surface Chemistry* (3<sup>rd</sup> ed.). Marcel Dekker, New York, NY.

Huang, Q., Yu, H., and Ru, Q. (2010). Bioavailability and delivery of nutraceuticals using nanotechnology. *Journal of Food Science*, 75(1), R50-R57.

Jafari, S. M., He, Y., and Bhandari, B. (2006). Nano-emulsion production by sonication and microfluidization – A comparison. *International Journal of Food Properties*, 9(3), 475-485.

Jafari, S. M., Assadpoor, E., He, Y., and Bhandari, B. (2008). Re-coalescence of emulsion droplets during high-energy emulsification. *Food Hydrocolloids*, 22(7), 1191-1202.

Lee, S. J., and McClements, D. J. (2010). Fabrication of protein-stabilized nanoemulsions using a combined homogenization and amphiphilic solvent dissolution/evaporation approach. *Food Hydrocolloids*, 24(6-7), 560–569.

Lee, S. J., Choi, S. J., Li, Y., Decker, A., and McClements, D. J. (2011). Protein-stabilized nanoemulsions and emulsions: Comparison of physicochemical stability, lipid oxidation, and lipase digestibility. *Journal of Agricultural and Food Chemistry*, 59(1), 415-427.

Li, Y., and McClements, D. J. (2010). New mathematical model for interpreting pH-Stat digestion profiles: Impact of lipid droplet characteristics on in vitro digestibility. *Journal of Agricultural and Food Chemistry*, 58(13), 8085-8092.

Liggieri, L., Ravera, F., and Passerone, A. (1995). Equilibrium interfacial tension of hexane/water plus Triton X-100. *Journal of Colloid and Interface Science*, 169(1), 238-240.

Lundin, L., and Golding, M. (2009). Structure design for healthy food. *Australian Journal of Dairy Technology*, 64(1), 68-74.

Mao, L., Xu, D., Yang, J., Yuan, F., Gao, Y., and Zhao, J. (2009). Effect of small and large molecules emulsifiers on the characteristics of  $\beta$ -carotene nanoemulsions prepared by high pressure homogenization. *Food Technology and Biotechnology*, 47(3), 336-342.

- Mason, T. G., Wilking, J. N., Meleson, K., Chang, C. B., and Graves, S. M. (2006). Nanoemulsions: formation, structure, and physical properties. *Journal of Physics: Condensed Matter*, 18(41), R635–R666.
- McClements, D. J. (2005). *Food emulsions: Principles, Practice, and Techniques*. CRC Press, Boca Raton, FL.
- McClements, D. J., and Li, Y. (2010). Structured emulsion-based delivery systems: Controlling the digestion and release of lipophilic food components. *Advances in Colloid and Interface Science*, 159(2), 213-228.
- Mun, S., Decker, E. A., and McClements, D. J. (2007). Influence of emulsifier type on in vitro digestibility of lipid droplets by pancreatic lipase. *Food Research International*, 40(6), 770-781.
- Pafumi, Y., Lairon, D., Lechene de la Porte, P., Juhel, C., Storch, J., Hamosh, M., and Armand, M. (2002). Mechanisms of inhibition of triacylglycerol hydrolysis by human gastric lipase. *The Journal of Biological Chemistry*, 277(31), 28070-28079.
- Parada, J., and Aguilera, J. M. (2007). Food microstructure affects the bioavailability of food several nutrients. *Journal of Food Science*, 72(2), R21-R32.
- Poling, B. E., Thomson, G. H., Friend, D. G., Rowley, R. L., and Wilding, W. V. (2008). Physical and chemical data. In D. Green, and R. Perry (Eds.), *Perry's Chemical Engineers' Handbook* (Section 2, pp. 2-429). New York, NY: McGraw-Hill Companies, Inc.
- Qian, C., and McClements, D. J. (2011). Formation of nanoemulsions stabilized by model food-grade emulsifiers using high-pressure homogenization: Factors affecting particle size. *Food Hydrocolloids*, 25(5), 1000-1008.
- Reis, P., Holmberg, K., Watzke, H., Leser, M. E., and Miller, R. (2009). Lipases at interfaces: A review. *Advances in Colloid and Interface Science*, 147-148, 237-250.
- Saravacos, G. D., and Maroulis, Z. B. (2001). *Transport Properties of Foods*. Marcel Decker, New York, NY.
- Silva, H. D., Cerqueira, M. A., Souza, B. W. S., Ribeiro, C., Avides, M. C., Quintas, M. A. C., Coimbra, J. S. R., Carneiro-da-Cunha, M. G., and Vicente, A. A. (2011). Nanoemulsions of  $\beta$ -carotene using a high-energy emulsification–evaporation technique. *Journal of Food Engineering*, 102(2), 130-135.

- Singh, H., Ye, A., and Horne, D. (2009). Structuring food emulsions in the gastrointestinal tract to modify lipid digestion. *Progress in Lipid Research*, 48(2), 92-100.
- Tadros, T. F. (2005). *Applied surfactants: Principles and Applications*. Wiley-VCH Verlag GmbH & Co., Weinheim.
- Tan, C. P., and Nakajima, M. (2005).  $\beta$ -carotene nanodispersions: preparation, characterization and stability evaluation. *Food Chemistry*, 92(4), 661-671.
- Tcholakova, S., Denkov, N. D., Sidzhakova, D., Ivanov, I. B., and Campbell, B. (2003). Interrelation between drop size and protein adsorption at various emulsification conditions. *Langmuir*, 19(14), 5640-5649.
- Velikov, K. P., and Pelan, E. (2008). Colloidal delivery systems for micronutrients and nutraceuticals. *Soft Matter*, 4, 1964-1980.
- Vladislavljević, G. T., Surh, J., and McClements, D. J. (2006). Effect of emulsifier type on droplet disruption in repeated Shirasu porous glass membrane homogenization. *Langmuir*, 22(10), 4526-4533.
- Walstra, P. (1993). Principles of emulsion formation. *Chemical Engineering Science*, 48(2), 333-349.
- Walstra, P. (2003). *Physical Chemistry of Foods*. Marcel Decker, New York, NY.
- Wang, K., Lu, Y. C., Xu, J. H., and Luo, G. S. (2009). Determination of dynamic interfacial tension and its effect on droplet formation in the T-shaped microdispersion process. *Langmuir*, 25(4), 2153-2158.
- Wickham, M., Faulks, R., and Mills, C. (2009). *In vitro* digestion methods for assessing the effect of food structure on allergen breakdown. *Molecular Nutrition & Food Research*, 53(8), 952-958.
- Wooster, T. J., Golding, M., and Sanguansri, P. (2008). Impact of oil type on nanoemulsion formation and Ostwald ripening stability. *Langmuir*, 24(22), 12758-12765.

## 5. INFLUENCE OF PARTICLE SIZE ON THE *IN VITRO* DIGESTIBILITY OF PROTEIN-COATED LIPID NANOPARTICLES

### Abstract

The influence of particle size on the *in vitro* digestion of BLG-coated lipid nanoparticles was examined using simulated small intestine conditions. Nanoemulsions were prepared by high-pressure homogenization and organic solvent (hexane) evaporation. The effect of the initial organic phase composition on the size, microstructure, electrical properties, and digestion of the lipid nanoparticles was evaluated. The diameter of the nanoparticles decreased (from 170 to 96 nm) as the solvent concentration in the initial organic phase increased (from 0% to 95%). The lipid digestion rate initially decreased with decreasing particle diameter (for *diameter* = 170-118 nm), but then it increased (for *diameter* = 118-96 nm). This dependence is contrary to the usual assumption that lipid digestion increases with increasing lipid surface area. Our results suggest that the structure of the protein layer coating the lipid nanoparticles has an important effect on lipid digestion.

### 5.1. Introduction

Delivery systems designed to encapsulate, protect and release bioactive components at controlled rates to specific locations within the human body are finding growing interest in the food and pharmaceutical industries (McClements and Li, 2010; Pouton, 2006). A wide variety of emulsion-based delivery systems have been developed for food applications, including conventional emulsions, nanoemulsions, multilayer emulsions, solid lipid nanoparticles, filled hydrogel particles, and others (McClements and Li, 2010). These systems are suitable for oral application in pharmaceuticals and functional foods because they can be fabricated from edible components (e.g., oil, water, surfactants, and proteins) using economic processing operations (e.g., mixing and homogenization).

Oil-in-water nanoemulsions consist of small emulsifier-coated lipid droplets (*diameter* < 200 nm) dispersed within an aqueous medium (Mason et al., 2006; McClements, 2011;

McClements, 2012; Tadros et al., 2004). These systems have a number of potential advantages over conventional emulsions for encapsulation of bioactive components in the pharmaceutical, food, and beverage industries: (i) they scatter light weakly and so can be incorporated into optically transparent products; (ii) they have unique rheological characteristics; (iii) they usually have better stability to particle aggregation and gravitational separation; and (iv) they have been reported to increase the bioavailability of hydrophobic substances (Acosta, 2009; Mason et al., 2006; Tadros et al., 2004; Wooster et al., 2008). The very small particle size in nanoemulsions increases their specific interfacial area ( $\text{m}^2/\text{g}$ ) so that any chemical reactions that occur at the oil–water interface (e.g., hydrolysis by lipases) should be accelerated (Li and McClements, 2010; Li et al., 2011; Troncoso et al., 2012). The ability to increase the rate and extent of lipid digestion may be of interest for the development of dietary lipid formulations for humans with disorders that inhibit efficient lipid digestion or absorption e.g., cystic fibrosis or pancreatitis (Fave et al., 2004). On the other hand, enzymatic hydrolysis of lipids has also been shown to depend on the properties of the substrate-water interface (Armand et al., 1992; Armand et al., 1999; Golding et al., 2011). The interfacial properties of lipid particles may affect the ability of lipases (as well as co-lipases, phospholipids, and bile salts) to adsorb to their surfaces and act upon the non-polar substrates contained within the droplets (Reis et al., 2009; Sonesson et al., 2006). The efficient design of nanoemulsion-based delivery systems for oral administration therefore requires an understanding of their behavior within the complex environment of the gastrointestinal tract.

The purpose of this study was to systematically investigate the influence of particle size on lipid digestion in protein-stabilized nanoemulsions. Nanoemulsions were fabricated using a combined high pressure homogenization/solvent evaporation method. The droplet size can be controlled using this method by varying the homogenization conditions and the oil-to-solvent ratio in the organic phase prior to homogenization. We recently used high-pressure homogenization (microfluidization) and organic solvent (ethyl acetate and hexane) evaporation to produce protein-stabilized nanoemulsions

(*diameter* = 70 nm) (Lee and McClements, 2010; Lee et al., 2011) and surfactant-stabilized nanoemulsions (*diameter* = 60-170 nm) (Troncoso et al., 2012). Other researchers have used a similar approach to prepare  $\beta$ -carotene nanodispersions stabilized by proteins (*diameter* = 10-300 nm) (Chu et al., 2008; Silva et al., 2011; Tan and Nakajima, 2005). In the present study, we focus on the influence of particle size on the *in vitro* digestibility of protein-coated lipid nanoparticles. The information gained from this study should facilitate the rational design of oral delivery systems with targeted health and nutritional benefits.

## **5.2. Materials and methods**

### **5.2.1. Materials**

Powdered BLG was obtained from Davisco Foods International (lot JE 002-8-415, Le Sueur, MN). Corn oil was purchased from a local grocery and used without further purification. Hexane was acquired from Fisher Scientific (Lot # 103567, Fair Lawn, NJ). Monobasic sodium phosphate, dibasic sodium phosphate, and sodium azide were obtained from Sigma-Aldrich (St. Louis, MO). Analytical grade hydrochloric acid (HCl) and sodium hydroxide (NaOH) were purchased from Sigma-Aldrich (St. Louis, MO). Purified water from a Nanopure water system (Nanopure Infinity, Barnstead International, Dubuque, IA) was used for the preparation of all solutions. Lipase from porcine pancreas, type II (L3126, Batch # 096K0747), bile extract (porcine, B8631, Batch # 058K0066), and calcium chloride ( $\text{CaCl}_2 \cdot 2\text{H}_2\text{O}$ ) were obtained from Sigma-Aldrich (St. Louis, MO).

### **5.2.2. Solution preparation**

Emulsions were prepared from an aqueous and an organic phase. The aqueous phase corresponded to emulsifier solutions prepared by dispersing 1.0 wt.% of BLG into 5 mM phosphate buffer solution (pH 7.0) containing 0.02 wt.% sodium azide and stirring for at least 2 h. The dispersions were kept overnight at 4 °C to ensure complete hydration of

the protein. Organic phases consisting of corn oil and hexane with different ratios (100:0, 90:10, 75:25, 50:50, 25:75, 10:90, 5:95 w/w) were prepared by mixing them in a closed flask to avoid solvent evaporation. Bile extract (4.5% w/w) and CaCl<sub>2</sub> (9.9% w/w) solutions were prepared by dissolving a certain amount of powder into 5 mM phosphate buffer solution (pH 7.0) and stirring for 1 h at room temperature.

### **5.2.3. Nanoemulsion preparation**

Initial emulsions were prepared by mixing 10% organic phase (with different corn oil:hexane ratios) and 90% aqueous phase (1.0 wt.% BLG, pH 7.0). Emulsions were prepared using a two-step homogenization process. First, coarse O/W emulsions were made by homogenizing the organic and aqueous phases with a high-speed blender for 2 min (M133/1281-0, Biospec Products, Inc., ESGC, Basle, Switzerland) followed by passage five times through a high-pressure homogenizer (Microfluidics M-110Y, F20Y 75 µm interaction chamber, Newton, MA) at 15,000 psi to produce fine emulsions. The homogenizer was cooled using ice during homogenization to avoid hexane evaporation. After the fine emulsions were obtained, the hexane was evaporated using a rotary evaporator (Büchi Rotavapor, RE111, Switzerland) operated at 55 °C under reduced pressure. The amount of hexane removed from the samples was in close agreement to the total amount of hexane originally present (within ± 0.4%), which indicated that all of the hexane was removed by evaporation.

### **5.2.4. Characterization of nanoemulsions properties**

#### **5.2.4.1. Particle characteristics**

Mean particle size, particle size distribution, polydispersity index, and ζ-potential were measured using a dynamic laser light scattering/particle electrophoresis instrument (Nano-ZS, Malvern Instruments, Worcestershire, UK). Nanoemulsions were diluted with phosphate buffer (pH 7.0) at a ratio 1:500 (v/v) before measurement to avoid multiple scattering. A refractive index of 1.47 for corn oil was used in the calculations of particle size.

#### **5.2.4.2. Microstructure analysis**

The microstructure of nanoemulsions was observed by transmission electron microscopy. A drop of nanoemulsion diluted by a factor of 200 was deposited onto a carbon support film on a copper grid. Excess sample was removed using filter paper. After drying the sample at room temperature for 5 min, micrographs were taken by a transmission electron microscope (Philips Tecnai 12 Bio Twin, Eindhoven, The Netherlands) operating at 80 kV. Images were registered on Kodak film SO163 and the negative scanned (Canon, Canoscan 9950F) at a resolution of 300 dpi.

#### **5.2.5. *In vitro* digestion model**

The *in vitro* digestion model (pH-stat method) used in this study was similar to that described in a previous work (Troncoso et al., 2012). The homogenization/evaporation method used to prepare the nanoemulsions produced systems with different total oil contents and oil-to-emulsifier ratios. We therefore diluted the nanoemulsions with emulsifier solutions containing different amounts of protein to obtain final samples that had the same total oil content (0.55 wt.% corn oil) and oil-to-emulsifier ratio (~0.56). This allowed us to distinguish the effects of particle size on lipid digestion from the effects of system composition.

The basic procedure to carry out the *in vitro* digestion was: (i) 30 mL of emulsion were placed into a glass beaker and incubated in a water bath at 37 °C for 10 min and then adjusted to pH 7.0 using HCl or NaOH solutions; (ii) 4.0 mL of bile extract solution and 1.0 mL of CaCl<sub>2</sub> solution were added into the emulsion under stirring, and the system was adjusted back to pH 7.0 if required; (iii) 2.5 mL of freshly prepared lipase suspension (2.3% w/w of lipase powder dispersed in phosphate buffer pH 7.0, 37 °C) was added to the mixture; (iv) immediately after, the pH of the mixture was monitored by a pH-stat automatic titration unit (835 Titrando, Metrohm, Riverview, FL) and maintained at pH 7.0 by titrating appropriate volumes of 0.28 M NaOH solution for the whole period of incubation (60 min). The volume of NaOH solution added to the digested mixture was recorded and used to calculate the concentration of FFAs

generated by lipolysis. Since each TAG molecule generates two FFA molecules when fully digested, it is possible to calculate the fraction of FFAs released during digestion as the total amount of TAGs originally present in the sample is known. Hence, the percentage of FFAs released can be calculated as (Li et al., 2011):

$$\% FFA = \left( \frac{V_{NaOH}(t) \cdot M_{NaOH} \cdot MW_{oil}}{m_{oil} \cdot 2} \right) \times 100 \% \quad (5.1)$$

where  $V_{NaOH}(t)$  is the volume of NaOH solution required to neutralize the FFAs produced at digestion time  $t$  (L),  $M_{NaOH}$  is the molarity of the NaOH solution used to titrate the sample ( $\text{mol L}^{-1}$ ),  $MW_{oil}$  is the molecular weight of the oil ( $\text{g mol}^{-1}$ ), and  $m_{oil}$  is the total weight of oil initially present in the incubation cell (g). Blanks were carried out in the absence of oil in the samples and subtracted from the reported values.

The percentage of total FFAs released ( $\Phi$ ) as a function of digestion time ( $t$ ) measured by the pH-stat method can be determined by the following expression (Li and McClements, 2010):

$$\Phi = \phi_{\max} \left( 1 - \left( 1 + \frac{3 k MW_{oil} t}{4 r_0 \rho_{oil}} \right)^{-2} \right) \quad (5.2)$$

Here,  $\phi_{\max}$  provides a measure of the extent of digestion (i.e., the maximum percentage of FFAs released at the end of digestion time),  $k$  is a measure of the rate of digestion (i.e., number of moles of FFAs released per unit oil droplet surface area per unit time),  $r_0$  is the initial mean droplet radius, and  $\rho_{oil}$  is the density of the oil. For corn oil, we used  $MW_{oil} = 0.8 \text{ kg mol}^{-1}$  and  $\rho_{oil} = 910 \text{ kg m}^3$ . The values of  $\phi_{\max}$  and  $k$  were determined from the FFAs vs. digestion time profiles by non-linear regression analysis by fitting Eq. (5.2) to the experimental data and finding the values that minimize the difference between the experimental and predicted values. It should be noted that the above equation was derived assuming that the lipid droplets in an emulsion shrink in size during digestion, but the total number of droplets remains constant (Li and McClements, 2010). In other words, the total oil-water interfacial area in an emulsion decreases over time during lipid digestion, which will change the ratio of enzyme to substrate available for digestion at the interface. A detailed analysis of this effect was not carried out in this

study due to the difficulties of accurately measuring the surface area of the lipid droplets in the chemically and structurally complex digestion medium.

#### **5.2.6. Data analysis**

All experiments were performed in triplicate using freshly prepared samples. The results were then reported as averages and standard deviations of these measurements. Analysis of variance was carried out when required using a statistical package (Statistical Graphics Corporation, version 4.0, Rockville, USA), including multiple range tests ( $p > 0.05$ ) for separation of least square means.

### **5.3. Results and discussion**

#### **5.3.1. Influence of organic phase composition on particle size**

The size of the droplets produced by the homogenization/evaporation method depended on the initial composition of the organic phase (Figure 5.1). When the organic phase was composed of only corn oil (no hexane), the mean particle diameter was ~170 nm after homogenization, and the evaporation step had little impact on particle size. When the initial organic phase contained both corn oil and hexane the droplet size decreased with decreasing corn oil content, both before and after hexane evaporation. The appearance of the nanoemulsions also depended on organic phase composition and evaporation: the systems became more translucent and bluish in color as the particle decreased (data not shown).

After hexane evaporation, we observed a further reduction in particle size, which can be attributed to removal of the organic solvent from the droplets. Decreasing the oil:hexane ratio in the initial organic phase from 100:0 to 5:95 w/w led to a reduction in the mean particle diameter by around 26% after homogenization and 43% after evaporation (Fig. 5.1). In turn, for the maximum hexane content used (95% w/w), the mean droplet diameters were around 124 and 96 nm before and after hexane evaporation, respectively. The particle size distributions of all the nanoemulsions contained a single peak, with the

width of the peak decreasing with increasing hexane content and with evaporation (Fig. 5.2). The polydispersity index ranged from 0.08 to 0.13, which suggested a high degree of monodispersity of the nanoemulsions (insert in Fig. 5.1). The appearance of the nanoemulsions also depended on organic phase composition and evaporation: the systems became more translucent and bluish in color as the particle decreased (data not shown). Representative TEM images of the lipid nanoparticles in the protein-stabilized nanoemulsions are shown in Figure 5.3. The TEM images indicate that most of the oil droplets had a spherical morphology (Fig. 5.3A and B), and that there was a considerable decrease in particle size after hexane evaporation (Fig. 5.3B).

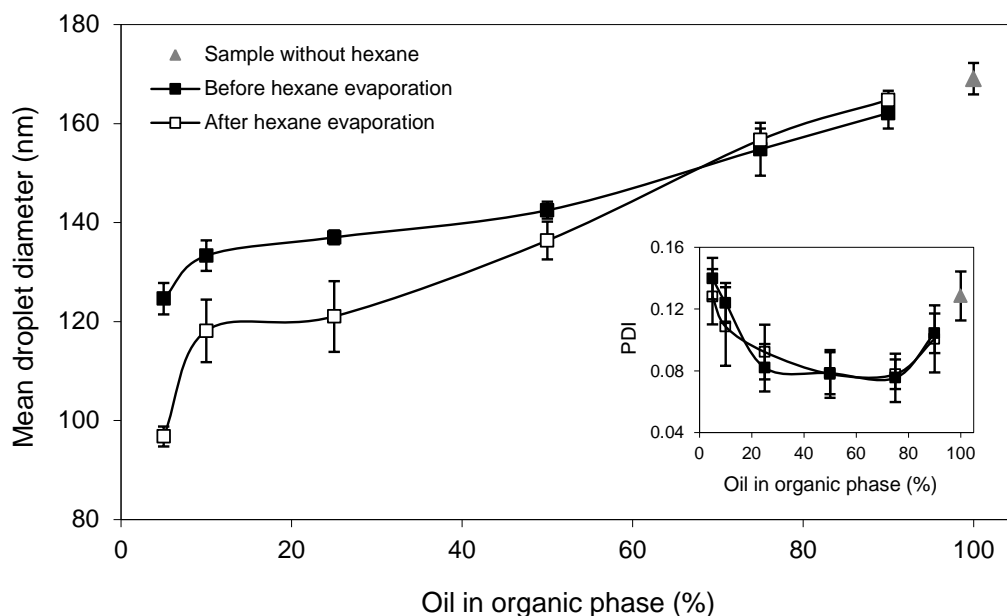


Figure 5.1. Influence of the oil content in the initial organic phase of emulsions on mean droplet diameter and polydispersity index (PDI). The concentration of hexane in the organic phase was 100% - % oil.

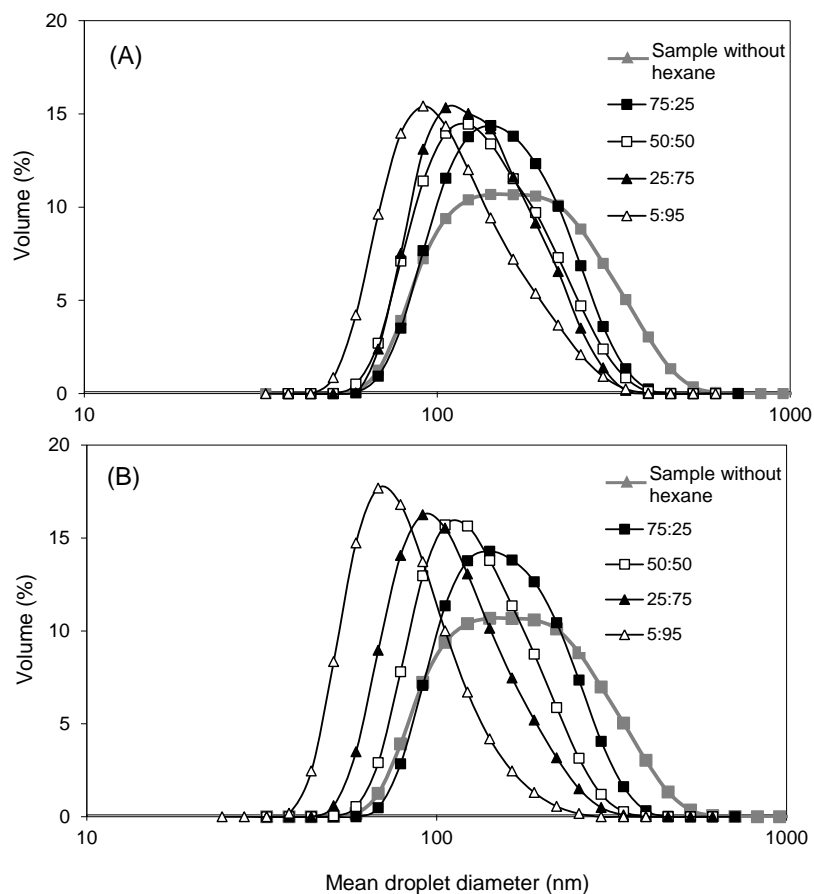


Figure 5.2. Particle size distributions of nanoemulsions containing different corn oil-to-hexane ratios in the initial dispersed phase. (A) Before hexane evaporation, and (B) after hexane evaporation.

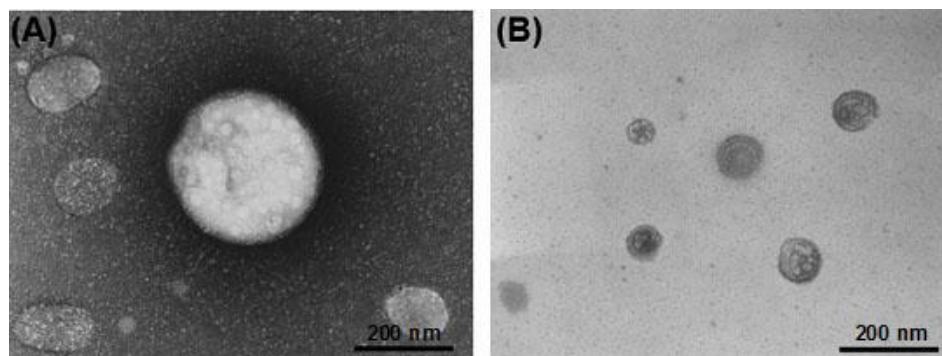


Figure 5.3. TEM micrographs of O/W nanoemulsions stabilized with BLG. (A) Nanoemulsion containing 100 wt.% corn oil in the initial disperse phase after homogenization, (B) nanoemulsion with 95 wt.% hexane in the initial disperse phase obtained after hexane evaporation.

The reduction in particle size observed before evaporation (Figs. 5.1-5.3) can be attributed to the influence of hexane on the bulk physicochemical properties of the organic phase. The particle size produced by high pressure homogenization has been shown to decrease with decreasing disperse phase viscosity and/or interfacial tension since this facilitates droplet disruption within the homogenizer (Qian and McClements, 2011; Walstra, 1993; Wooster et al., 2008). Since the viscosity of corn oil (~52 mPa s) at ambient temperature (Saravacos and Maroulis, 2001) is considerably higher than that of hexane (~0.30 mPa s) (Poling et al., 2008), the viscosity of the dispersed phase should decrease with increasing hexane content thereby leading to smaller droplets. Other studies have also shown that the droplet size in nanoemulsions can be reduced by using low viscosity oils, such as d-limonene, lemon oil, and hexadecane (Jafari et al., 2007; Wooster et al., 2008). The interfacial tension for corn oil/water and hexane/water interfaces have been reported to be ~32 mN m<sup>-1</sup> (Chaiyasit et al., 2008) and ~51 mN m<sup>-1</sup> (Goebel and Lunkenheimer, 1997) at ambient temperature, respectively. Thus, the interfacial tension between the dispersed and continuous phases would be expected to increase as the hexane concentration in the organic phase increased. The formation of small droplets during homogenization would therefore be expected to become more difficult with increasing hexane content according to this effect (Walstra, 1993). In our experiments we actually observed a decrease in mean droplet size with increasing hexane content after homogenization (Fig. 5.1), which indicated that the impact of hexane on the viscosity ratio was more important than its impact on the interfacial tension. This would be expected since the difference in the viscosities of the oil and organic solvent was much greater than the difference in their interfacial tensions.

In a recent study using nanoemulsions stabilized by a non-ionic surfactant (Tween 20) we also found that the particle size decreased with increasing solvent concentration after homogenization (*diameter* = 96-172 nm) and after hexane evaporation (*diameter* = 60-172 nm) (Troncoso et al., 2012). However, smaller droplets were produced using the non-ionic surfactant than with the protein used in this study. This effect can be attributed to the fact that small-molecule surfactants are able to adsorb to the freshly formed

droplet surfaces within the homogenizer more rapidly than polymeric surfactants (Qian and McClements, 2011; Schubert et al., 2003).

The minimum size of stable droplets that can theoretically be produced during homogenization given a certain amount of emulsifier can be estimated by using Equation 4.2. (McClements, 2005). Thus, the minimum oil droplet radius can be estimated by using Equation 4.2. In this study, the nanoemulsions contained 1 wt.% emulsifier in the continuous phase ( $c'_s = 10 \text{ kg m}^{-3}$ ) and had  $\phi$  values of  $\sim 0.1$  during homogenization. In turn, the surface load of globular proteins at oil droplets surfaces has been reported to be  $\sim 2 \text{ mg m}^{-2}$  ( $\Gamma = 2 \times 10^{-6} \text{ kg m}^{-2}$ ) (Tcholakova et al., 2003). Hence, the minimum oil droplet radius that could theoretically have been achieved assuming that all the protein adsorbed to the droplet surfaces during homogenization is  $\sim 67 \text{ nm}$  (*diameter* = 134 nm). The experimental mean droplet diameters obtained in this work were close to this value for those systems containing 50, 75, 90 and 95 wt.% of hexane in the disperse phase (*diameter* = 142, 137, 133 and 125 nm, respectively), which suggested that there was enough emulsifier initially present to cover all of the droplets formed by the homogenizer. But, our experimental droplet diameters were significantly higher at low hexane contents (*diameter* = 155-162 nm) and in the absence of hexane (*diameter* = 170 nm). These findings suggest that the homogenizer was incapable of generating sufficiently intense disruptive forces at the pressure used for the more viscous organic phases. Overall these results highlight the importance of the initial organic phase composition on the formation of nanoemulsions.

### **5.3.2. Electrical characteristics of lipid nanoparticles**

The electrical charge ( $\zeta$ -potential) of the particles in the nanoemulsions changed from -32 to -57 mV when the hexane content in the initial organic phase decreased from 95 to 0 wt.% (Figure 5.4). The sign and magnitude of the electrical charge on lipid droplets determines their functional performance e.g., aggregation stability, interaction with other charged components, and binding to charged surfaces. We therefore measured the

electrical charge at the surface of the lipid nanoparticles obtained after hexane evaporation (Figure 5.4).

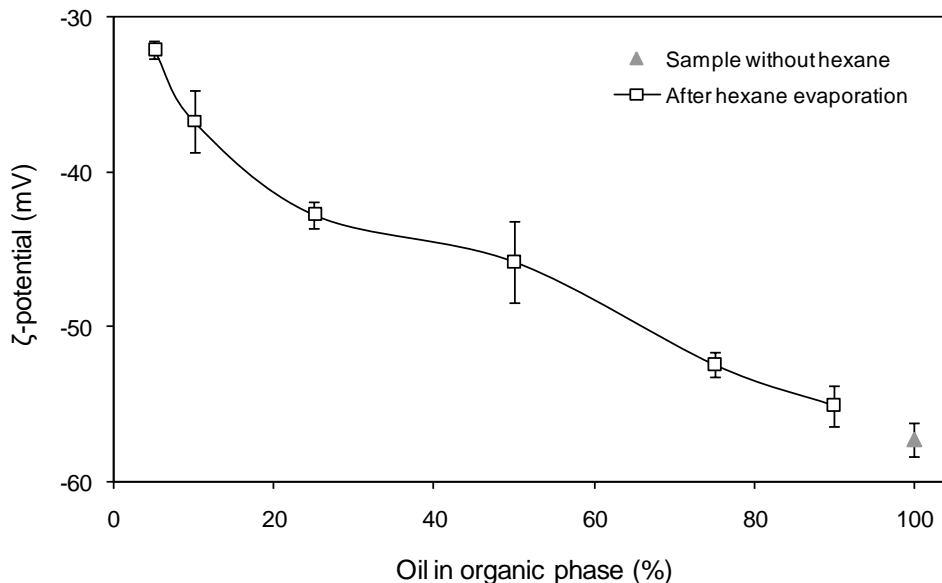


Figure 5.4. Dependence of droplet  $\zeta$ -potential of nanoemulsions after hexane removal on the initial corn oil content in the organic phase (corn oil + hexane).

The fact that droplets stabilized by BLG have a net negative charge at neutral pH is well established in the literature, since the protein is above its isoelectric point (Gu et al., 2005). On the other hand, the fact that the  $\zeta$ -potential depended on the initial organic phase composition indicated that the electrical characteristics of the lipid nanoparticles was influenced by differences in particle size, interfacial properties, and/or oil composition. Similar tendencies have been reported for corn oil-in-water emulsions stabilized by whey protein isolate (Lee et al., 2011) or Tween 20 (Troncoso et al., 2012). In principle, the  $\zeta$ -potential should be independent of particle size (Hiemenz and Rajagopalan, 1997), nevertheless there are a number of physicochemical mechanisms that might explain the observed behavior. First, the change in  $\zeta$ -potential with particle size could be due to limitations in the theory used by the electrophoresis instrument to interpret the data (Doane et al., 2012; Hiemenz and Rajagopalan, 1997). In this study, we used an instrument that utilized the Smoluchowski theory to convert the measured

particle electrophoretic mobility into a  $\zeta$ -potential. This theory assumes that the particle radius  $r$  is much larger than the Debye screening length  $k^{-1}$  (Tadros et al., 2004), which may be true for the oil droplets with large particle sizes (*diameter*  $\sim$  170 nm) but not for those with small particle size (*diameter*  $\sim$  96 nm). Accordingly, the interpretation of the particle mobility measurements could have been inaccurate (Doane et al., 2012). Second, the electrical charge of the lipid nanoparticles could have been affected by the presence of ionic impurities (such as fatty acids) arising from either the corn oil or the hexane. Third, the nature of the protein layer surrounding the oil droplets may have changed when hexane was evaporated. After adsorption to an oil–water interface globular proteins undergo surface denaturation, which can lead to covalent cross-linking through disulfide bond formation (Kim et al., 2002; Monahan et al., 1996). During the evaporation step the droplets shrink, but the cross-linked protein molecules should remain attached to the droplet surfaces, leading to the formation of a thicker protein layer around smaller droplets. This change in interfacial composition and structure would be expected to alter the electrical characteristics of the particles (Hiemenz and Rajagopalan, 1997).

### **5.3.3. *In vitro* digestibility of the nanoemulsions**

The influence of lipid nanoparticle size on the *in vitro* digestion of the BLG-stabilized nanoemulsions under simulated small intestinal conditions is shown in Figure 5.5. The activity of lipase was quantified in terms of the percentage of FFAs released from the emulsions during hydrolysis using a pH-stat method. A mathematical digestion model (Eq. 5.2) was used to fit the experimental FFA-digestion time profiles and estimate the rate ( $k$ ), and extent ( $\phi_{\max}$ ) of lipid digestion for each sample (Table 5.1). As a general trend, there was a good fit between the mathematical model and the experimental data for the systems studied (RMS average value of  $\sim$ 8%), indicating that the model was suitable for describing the pH-stat digestion profiles.

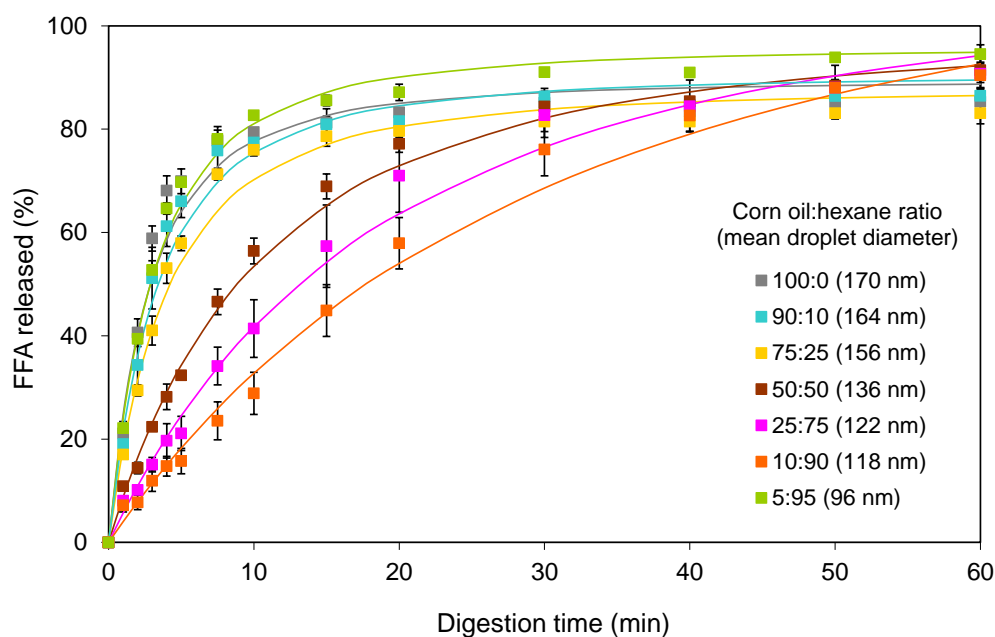


Figure 5.5. Free fatty acids released from O/W nanoemulsions stabilized with BLG as a function of digestion time. The nanoemulsions digested were those obtained after hexane evaporation. Lines represent the mathematical model fit using Eq. (5.2).

Table 5.1. Summary of the kinetics parameters describing the rate ( $k$ ) and extent ( $\phi_{\max}$ ) of digestion of BLG-stabilized O/W nanoemulsions with different initial compositions and particle sizes

Oil in the initial dispersed phase (%)	Mean particle diameter (nm)	$k$ ( $\mu\text{mol s}^{-1} \text{m}^{-2}$ )	$\phi_{\max}$ (%)	RMS* (%)
100	170	$22.5 \pm 1.6$	$89.4 \pm 4.8$	7.8
90	164	$18.1 \pm 0.9$	$90.5 \pm 3.4$	6.6
75	156	$14.7 \pm 0.4$	$87.7 \pm 2.3$	5.6
50	136	$4.9 \pm 0.3$	$99.0 \pm 4.2$	7.3
25	122	$2.5 \pm 0.1$	$107.6 \pm 4.3$	10.2
10	118	$1.5 \pm 0.1$	$103.6 \pm 6.4$	13.7
5	96	$11.4 \pm 0.7$	$95.8 \pm 4.1$	4.1

\* RMS means root mean square. RMS values less than 10% indicate a good agreement between experimental and fitted data.

In general, the FFA-digestion time profiles had a steep initial increase in the percentage of FFAs released (*digestion period*) after which the FFAs released remained relatively

constant (*plateau period*). The rate of FFA formation in the digestion period and the final amount of FFAs produced in the plateau period depended on the initial organic phase composition of the nanoemulsions, and therefore on particle size. The total amount of FFAs produced per unit time (Figure 5.5) and the FFA release rate per unit surface area (Table 5.1) both decreased when the mean droplet diameter decreased, i.e.,  $k$  went from  $\sim 23$  to  $2 \mu\text{mol s}^{-1} \text{m}^{-2}$  when the droplet diameter decreased from 170 to 118 nm. On the other hand, the overall amount of FFAs released at the end of the digestion period increased when the droplet diameter decreased, i.e.,  $\phi_{\text{max}}$  went from around 89% to 104% when diameter decreased from 170 to 118 nm. Surprisingly, the nanoemulsion containing the smallest droplets did not follow the same trend as the other systems. We actually observed an increase in the digestion rate ( $k$  from  $\sim 2$  to  $11 \mu\text{mol s}^{-1} \text{m}^{-2}$ ) when the droplet diameter was decreased from 118 to 96 nm (Table 5.1, Figure 6).

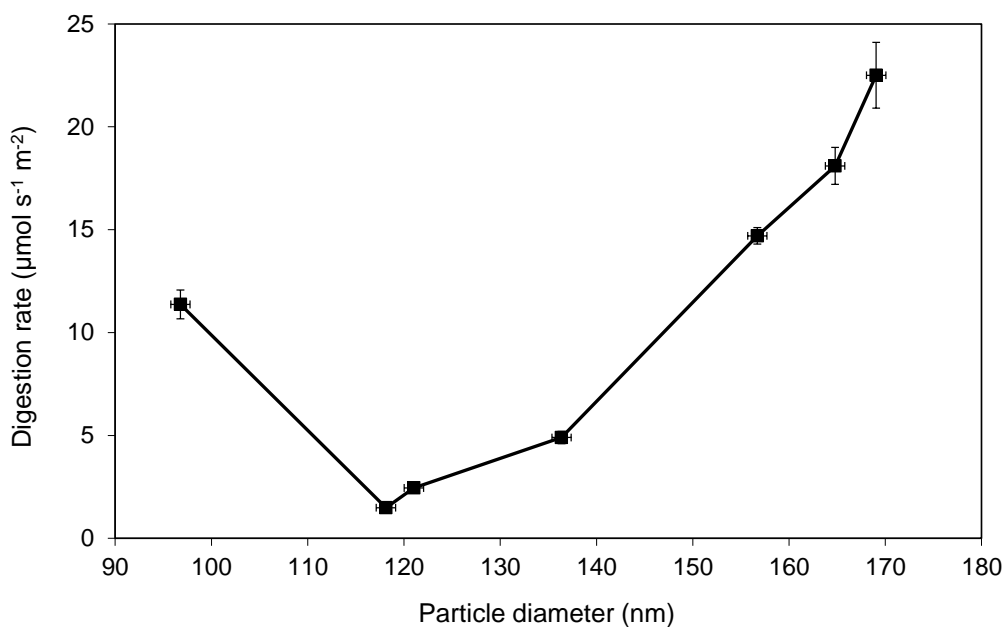


Figure 5.6. Influence of mean particle diameter on digestion rate for corn oil-in-water nanoemulsions.

The purpose of these experiments was to characterize the influence of particle size in protein-stabilized nanoemulsions on the rate and extent of lipid digestion using a

simulated intestinal model. We hypothesized that lipid nanoparticles with different interfacial areas or structures would be digested differently as these factors would impact the ability of lipase to come into contact with the lipid substrate.

Other researchers have reported that the lipid digestion rate (FFAs released per unit time) increased with decreasing droplet size, which was attributed to the increase in the surface area of lipid substrate exposed to lipase (Armand et al., 1992; Armand et al, 1999; Golding et al, 2011). The fact that we observed a more complex dependence of lipid digestion rate on particle size (Fig. 5.5 and 5.6) suggests that some other phenomenon must also be important.

The digestion rates ( $k$ ) derived from Eq. (5.2) are proportional to the amount of free fatty acids produced per unit surface area, and therefore they should be independent of particle size provided that other factors remain constant, such as lipid substrate concentration, enzyme-substrate ratio, and interfacial structure (Li and McClements, 2010; Li et al, 2011). In this study, we used the same *in vitro* digestion conditions for all of the samples studied, and all the nanoemulsions had the same overall composition (total oil and protein content). Any differences in the digestion behavior of the nanoemulsions can therefore be attributed to differences in the structural organization of the components in the system. The differences in the rate of lipid digestion observed in this study may therefore be related to changes in the interfacial structure. As mentioned earlier, the lipid droplets shrink when solvent is evaporated from the emulsions, but the protein layer would be expected to remain attached to the lipid droplet surfaces. Consequently, the thickness of the protein layer surrounding the lipid droplets would be expected to increase as the droplet size decreased. In addition, the structural organization (packing) of the protein molecules in the interfacial layer may have changed when the droplets shrank. Indeed, our electron microscopy images indicate some evidence of structure on the droplet surfaces after solvent evaporation. Changes in the thickness and structural organization of the protein layer surrounding the lipid droplets may have influenced their digestion in a number of ways. First, it may have been more difficult for bile salts and other surface active substances to displace the protein layer from the lipid

droplet surfaces. Second, it may have been more difficult for reactants (e.g., lipase) and products (e.g., free fatty acids and monoacylglycerols) to penetrate through a thicker and denser interfacial layer, thereby slowing the lipolysis reaction.

These phenomena may explain the difference in the impact of droplet size on lipid digestion in nanoemulsions produced using the homogenization/evaporation method compared to nanoemulsions produced using homogenization only. For example, in a recent study it was found that the rate of lipid digestion (FFAs released per unit time) in BLG-stabilized nanoemulsions increased as the lipid droplet diameter decreased (Li and McClements, 2010). The nanoemulsions used in that study were prepared by homogenization only, and therefore the interfacial structure should have been relatively independent of droplet size. Thus, the rate of lipid digestion was mainly determined by differences in interfacial surface area, rather than differences in interfacial structure (thickness and packing).

Recently, we examined the influence of oil droplet diameter (60-170 nm) on the *in vitro* digestion of nanoemulsions containing non-ionic surfactant (Tween 20) stabilized lipid (corn oil) droplets using simulated small intestine conditions (Troncoso et al., 2012). The nanoemulsions were prepared using the same homogenization/evaporation method used in the current study. We found that the nanoemulsions exhibited a lag-period before any FFAs were released, which was explained by the time taken for surface-active substances from the bile extract to displace the small-molecule surfactant from the surface of the oil droplets and thereby facilitate lipase adsorption and activity. After the lag-period, the rate of lipid digestion increased as the oil droplet diameter decreased (increasing specific surface area). In addition, the total amount of FFAs released from the nanoemulsions increased from 61% to 71% as the mean droplet diameter decreased from 172 nm to 60 nm. The incomplete lipid digestion was attributed to the fact that small molecule surfactants are more surface-active than lipase, so that the interfacial layer of Tween 20 may delay the contact of the enzyme with the emulsified lipids (Reis et al., 2009). In consequence, the difference in behavior of surfactant-coated and globular protein-coated lipid droplets can be attributed to the fact that surfactants can

move from the droplet surface to the continuous phase when the lipid droplets shrink during the solvent evaporation step, whereas globular proteins tend to remain attached to the lipid droplet surfaces thereby changing the interfacial structure.

#### **5.4. Conclusions**

The results obtained in this study suggest that particle characteristics, such as size and interfacial properties, modulate the digestibility of emulsified lipids in nanoemulsions. A deeper understanding of the phenomena underlying lipid digestion is crucial to designing food-grade delivery systems based on nanoemulsions for controlled or targeted release applications. Nevertheless, one must be careful in extrapolating results from a simple *in vitro* digestion model to complex real-life situations. In particular, this study did not consider the influence of oral and gastric conditions on the properties of the nanoemulsions prior to lipid digestion. Previous studies have shown that passage through these regions of the GIT may cause appreciable changes in particle size and interfacial composition that could alter their subsequent digestibility in the small intestine (Singh and Sarkar, 2011). In addition, globular proteins may undergo hydrolysis in the stomach, with the hydrolysis rate depending on their molecular conformation. Differences in the susceptibility of protein coatings to hydrolysis due to differences in structure could alter the subsequent digestion rate of emulsified lipids in the small intestine. It would therefore be useful in future studies to use a more realistic *in vitro* digestion model that included oral, gastric and small intestinal stages, as well as to carry out additional *in vivo* digestion studies using animals to provide a more comprehensive understanding of the biological fate of nanoparticles.

#### **References**

- Acosta, E. (2009). Bioavailability of nanoparticles in nutrient and nutraceutical delivery. *Current Opinion in Colloid & Interface Science*, 14(1), 3-15.
- Armand, M., Borel, P., Ythier, P., Dutot, G., Melin, C., Senft, M., Lafont, H., and Lairon, D. (1992). Effects of droplet size, triacylglycerol composition, and calcium on

the hydrolysis of complex emulsions by pancreatic lipase: An in vitro study. *The Journal of Nutritional Biochemistry*, 3(7), 333-341.

Armand, M., Pasquier, B., André, M., Borel, P., Senft, M., Peyrot, J., Salducci, J., Portugal, H., Jaussan, V., and Lairon, D. (1999). Digestion and absorption of 2 fat emulsions with different droplet sizes in the human digestive tract. *American Journal of Clinical Nutrition*, 70, 1096-1106.

Chaiyasit, W., McClements, D. J., Weiss, J., and Decker, E.A. (2008). Impact of surface-active compounds on physicochemical and oxidative properties of edible oil. *Journal of Agricultural and Food Chemistry*, 56(2), 550–556.

Chu, B. S., Ichikawa, S., Kanafusa, S., and Nakajima, M. (2008). Stability of protein-stabilised  $\beta$ -carotene nanodispersions against heating, salts and pH. *Journal of the Science of Food and Agriculture*, 88(10), 1764-1769.

Doane, T. L., Chuang, C. H., Hill, R. J., and Burda, C. (2012). Nanoparticle  $\zeta$ -potentials. *Accounts of Chemical Research*, 45(3), 317-326.

Fave, G., Coste, T. C., and Armand, M. (2004). Physicochemical properties of lipids: New strategies to manage fatty acid bioavailability. *Cellular and Molecular Biology*, 50(7), 815-831.

Goebel, A., and Lunkenheimer, K. (1997). Interfacial tension of the water/*n*-alkane interface. *Langmuir*, 13(2), 369-372.

Golding, M., Wooster, T. J., Day, L., Xu, M., Lundin, L., Keogh, J., and Clifton, P. (2011). Impact of gastric structuring on the lipolysis of emulsified lipids. *Soft Matter*, 7, 3513-3523.

Gu, Y. S., Decker, E.A., and McClements, D. J. (2005). Influence of pH and carrageenan type on properties of  $\beta$ -lactoglobulin stabilized oil-in-water emulsions. *Food Hydrocolloids*, 19(1), 83-91.

Hiemenz, P. C., and Rajagopalan, R. (1997). *Principles of Colloid and Surface Chemistry* (3<sup>rd</sup> ed.). Marcel Dekker, New York, NY.

Jafari, S. M., He, Y., and Bhandari, B. (2007). Optimization of nano-emulsions production by microfluidization. *European Food Research and Technology*, 225(5-6), 733-741.

Kim, H. J., Decker, E. A., and McClements, D. J. (2002). Role of postadsorption conformation changes of  $\beta$ -lactoglobulin on its ability to stabilize oil droplets against flocculation during heating at neutral pH. *Langmuir*, 18(20), 7577-7583.

Lee, S. J., and McClements, D. J. (2010). Fabrication of protein-stabilized nanoemulsions using a combined homogenization and amphiphilic solvent dissolution/evaporation approach. *Food Hydrocolloids*, 24(6-7), 560–569.

Lee, S. J., Choi, S. J., Li, Y., Decker, A., and McClements, D. J. (2011). Protein-stabilized nanoemulsions and emulsions: Comparison of physicochemical stability, lipid oxidation, and lipase digestibility. *Journal of Agricultural and Food Chemistry*, 59(1), 415-427.

Li, Y., and McClements, D. J. (2010). New mathematical model for interpreting pH-Stat digestion profiles: Impact of lipid droplet characteristics on *in vitro* digestibility. *Journal of Agricultural and Food Chemistry*, 58(13), 8085-8092.

Li, Y., Hu, M., and McClements, D. J. (2011). Factors affecting lipase digestibility of emulsified lipids using an *in vitro* digestion model: Proposal for a standardised pH-stat method. *Food Chemistry*, 126(2), 498-505.

Mason, T. G., Wilking, J. N., Meleson, K., Chang, C. B., and Graves, S. M. (2006). Nanoemulsions: formation, structure, and physical properties. *Journal of Physics: Condensed Matter*, 18(41), R635–R666.

McClements, D. J. (2005). *Food emulsions: Principles, Practice, and Techniques*. CRC Press, Boca Raton, FL.

McClements, D. J. and Li, Y. (2010). Structured emulsion-based delivery systems: Controlling the digestion and release of lipophilic food components. *Advances in Colloid and Interface Science*, 159,213-228.

McClements, D. J. (2011). Edible nanoemulsions: fabrication, properties, and functional performance. *Soft Matter*, 7(6), 2297-2316.

McClements, D. J. (2012). Nanoemulsions versus microemulsions: terminology, differences, and similarities. *Soft Matter*, 8(6), 1719-1729.

Monahan, F. J., McClements, D. J., and German, J. B. (1996). Disulfide mediated polymerization reactions and physical properties of heated WPI-stabilized emulsions. *Journal of Food Science*, 61(3), 504-509.

Poling, B. E., Thomson, G. H., Friend, D. G., Rowley, R. L., and Wilding, W. V. (2008). Physical and chemical data. In D. Green, and R. Perry (Eds.), *Perry's Chemical Engineers' Handbook* (Section 2, pp. 2-429). New York, NY: McGraw-Hill Companies, Inc.

- Pouton, C. W. (2006). Formulation of poorly water-soluble drugs for oral administration: Physicochemical and physiological issues and the lipid formulation classification system. *European Journal of Pharmaceutical Sciences*, 29(3-4), 278-287.
- Qian, C., and McClements, D. J. (2011). Formation of nanoemulsions stabilized by model food-grade emulsifiers using high-pressure homogenization: Factors affecting particle size. *Food Hydrocolloids*, 25(5), 1000-1008.
- Reis, P., Holmberg, K., Watzke, H., Leser, M. E., and Miller, R. (2009). Lipases at interfaces: A review. *Advances in Colloid and Interface Science*, 147-148, 237-250.
- Saravacos, G. D., and Maroulis, Z. B. (2001). *Transport Properties of Foods*. Marcel Dekker, New York, NY.
- Schubert, H., Ax, K., and Behrend, O. (2003). Product engineering of dispersed systems. *Trends in Food Science & Technology*, 14(1-2), 9-16.
- Silva, H. D., Cerqueira, M. A., Souza, B. W. S., Ribeiro, C., Avides, M. C., Quintas, M. A. C., Coimbra, J. S. R., Carneiro-da-Cunha, M. G., and Vicente, A. A. (2011). Nanoemulsions of  $\beta$ -carotene using a high-energy emulsification–evaporation technique. *Journal of Food Engineering*, 102(2), 130-135.
- Singh, H., and Sarkar, A. (2011). Behaviour of protein-stabilised emulsions under various physiological conditions. *Advances in Colloid and Interface Science*, 165(1), 47-57.
- Sonesson, A. W., Elofsson, U. M., Brismar, H., and Callisen, T. H. (2006). Adsorption and mobility of a lipase at a hydrophobic surface in the presence of surfactants. *Langmuir*, 22(13), 5810-5817.
- Tadros, T., Izquierdo, P., Esquena, J., and Solans, C. (2004). Formation and stability of nano-emulsions. *Advances in Colloid and Interface Science*, 108-109, 303-318.
- Tan, C. P., and Nakajima, M. (2005).  $\beta$ -carotene nanodispersions: preparation, characterization and stability evaluation. *Food Chemistry*, 92(4), 661-671.
- Tcholakova, S., Denkov, N. D., Sidzhakova, D., Ivanov, I. B., and Campbell, B. (2003). Interrelation between drop size and protein adsorption at various emulsification conditions. *Langmuir*, 19(14), 5640-5649.
- Troncoso, E., Aguilera, J. M., and McClements, D. J. (2012). Fabrication, characterization and lipase digestibility of food-grade nanoemulsions. *Food Hydrocolloids*, 27(2), 355-363.

Walstra, P. (1993). Principles of emulsion formation. *Chemical Engineering Science*, 48(2), 333-349.

Wooster, T. J., Golding, M., and Sanguansri, P. (2008). Impact of oil type on nanoemulsion formation and Ostwald ripening stability. *Langmuir*, 24(22), 12758-12765.

## 6. GENERAL CONCLUSIONS AND FUTURE PROSPECTS

### 6.1. General conclusions

In principle, rational design of lipid structures may be a useful tool for food processors to control lipid digestibility and bioavailability. Nevertheless, there is clearly a need for further research to establish the key physicochemical factors that impact on the performance of food lipids within the gastrointestinal tract. All of these issues have limited the capacity of the industry to create lipid-based products with tailored nutritional properties.

In order to increase our knowledge about the impact of different factors controlling the digestion of lipids in emulsion-based food systems, this doctoral thesis attempted to study the time-dependent rheological properties of whey protein isolate-stabilized O/W emulsions to establish relationships between structure and shear rates as found in the gastrointestinal tract. Also, we studied the influence of particle size and interfacial properties on the *in vitro* digestibility of the emulsions under simulated small intestinal conditions.

The composition of O/W emulsions stabilized by whey protein isolate had marked effects on their rheological properties. The decrease in the apparent viscosity of O/W emulsions could be due to shear-induced structural changes when a constant shear rate was applied. This behavior could be related to the disruption of emulsion flocs and the rearrangement of the oil droplets promoted by the flow field. However, these structural changes were not caused by coalescence of the oil droplets, because there were no significant differences in the oil droplet size distributions before and after the application of a constant shear rate. Under these observations, a better understanding of the colloidal basis of emulsion rheology has important implications for the design of food emulsions.

On the other hand, a combination of high-pressure homogenization and a solvent displacement technique led to the formation of nanoemulsions with oil droplets in the nanometer range ( $r < 100$  nm). The influence of the organic phase composition (oil-to-

solvent ratio) on the particle size distribution, microstructure, and appearance of nanoemulsions stabilized by Tween 20 was examined. This kind of emulsion-based food system was chosen because they are nowadays widely used as delivery systems for oral ingestion and present results would allow the food industry to design healthier foods and the pharmaceutical industry to create more effective drugs. Also, the influence of particle size on the *in vitro* digestibility under simulated small intestinal conditions of the nanoemulsions was assessed. By varying the solvent (hexane) content in the dispersed phase of the initial emulsion and its subsequent removal, O/W nanoemulsions stabilized by Tween 20 containing oil droplets with diameters from 60 to 170 nm with a low polydispersity were fabricated. These nanoemulsions appear translucent and a bit bluish. It was found that the *in vitro* lipid digestion profile depended strongly on the particle size of the nanoemulsions. The nanoemulsions exhibited a lag-period before any free fatty acids were released, which was explained by the time taken for surface-active substances from the bile extract to displace the small-molecule surfactant from the surface of the oil droplets and thereby facilitate lipase adsorption and activity. After the lag-period, the rate of lipid digestion increased as the oil droplet diameter decreased (i.e., increasing specific surface area). In addition, the total amount of free fatty acids released from the nanoemulsions increased from 61% to 71% as the mean droplet diameter decreased from 170 nm to 60 nm. These results suggest that controlling the composition of the initial dispersed phase and type of homogenization procedure appear to be key parameters in the formation, appearance, microstructure, and digestibility of nanoemulsions. Nevertheless, there is clearly a need for further research to establish the key physicochemical factors (e.g., interfacial properties) that impact the performance of nanoemulsion-based delivery systems under gastrointestinal conditions. For the above reason, O/W nanoemulsions stabilized by  $\beta$ -lactoglobulin were also fabricated in order to study the effect of particle size and interfacial properties on *in vitro* digestibility of emulsified lipids. The diameter of the nanoparticles stabilized by  $\beta$ -lactoglobulin decreased from 170 to 96 nm as the solvent concentration in the initial organic phase increased (from 0% to 95%). Thus, smaller droplets were produced using the non-ionic surfactant than with the protein. This effect can be attributed to the fact that small-molecule surfactants are able to adsorb to the freshly formed droplet surfaces within the homogenizer more rapidly than polymeric

surfactants. The lipid digestion rate initially decreased with decreasing particle diameter (for *diameter* = 170-118 nm), but then it increased (for *diameter* = 118-96 nm). This dependence is contrary to the usual assumption that lipid digestion increases with increasing lipid surface area. Thus, these results suggest that the structure of the protein layer coating the lipid nanoparticles has an important effect on lipid digestion. Consequently, the difference in behavior of surfactant-coated and globular protein-coated lipid droplets can be attributed to the fact that surfactants can move from the droplet surface to the continuous phase when the lipid droplets shrink during the solvent evaporation step, whereas globular proteins tend to remain attached to the lipid droplet surfaces thereby changing the interfacial structure. Finally, it is concluded that the digestibility of emulsified lipids may be controlled by manipulating the particle size and interfacial properties of emulsions. Nevertheless, one must be careful in extrapolating results from a simple *in vitro* digestion model to complex real-life situations.

## **6.2. Future prospects**

At the end and through the development of this thesis, some interesting possibilities for further studies were raised. Recommendations for future work can be divided in two categories:

(i) The first one is related with the deeper exploration of lipid structures and the interaction of other nutrients contained in them (e.g., protein and starch) that could eventually affect the digestibility of emulsified lipids. All the components conforming the food matrix should be considered when the impact of food microstructure is studied. It would be quite interesting to assess the effect of different food matrices and nutrient interactions on digestion of lipid foods, with the aim of optimizing their performance in the gastrointestinal tract.

(ii) The second one is focused on the development of new *in vitro* studies that incorporate the oral and gastric steps since the passage of nanoemulsions through these regions of the gastrointestinal tract could influence the composition, size, and interfacial characteristics

of lipid droplets. In future studies it would be useful to use a more sophisticated *in vitro* digestion model to examine the effects of these additional digestive stages on emulsion performance. An increased understanding of the behavior of emulsion-based delivery systems under gastrointestinal conditions would allow the food industry to design healthier foods and the pharmaceutical industry to create more effective drugs.

All of these possibilities for further studies will help in our future understanding of the kinetics of microstructure breakdown under conditions approaching those in the gastrointestinal tract. This valuable information may then be used to plan experiments in larger scale laboratory digestion systems and in human studies that attempt to assess the impact of food microstructure on health related phenomena.

